M-Pos236

Thermodynamic Evaluation of the Tissue Factor-Factor VII(a) Binding Interaction.

E. Waxman[1], J.B.A. Ross[1], & Y. Nemerson[1,2],
Departments of Biochemistry[1] and Medicine[2],
Mount Sinai School of Medicine, New York, NY 10029

The formation of a complex between the serine protease apoenzyme Factor VII(a) and its integral membrane cofactor Tissue Factor (TF) at the site of damaged tissue is the trigger event in the extrinsic pathway of coagulation. We are interested in studying this event at the molecular level. Previous studies (Bach *et al.*, Biochemistry 1986; Broze, J. Clin. Invest. 1982; Fair and MacDonald, J. Biol. Chem. 1987) have shown that complex formation involves a tremendous change in free energy (K_d = 0.1 nM to 10 nM). Positive cooperativity was observed in some situations. These studies were performed under a variety of conditions and as a result are not directly comparable. In addition, these studies employed techniques with which it is difficult to verify equilibrium. We have examined the binding interaction of TF, reconstituted into phospholipid vesicles, with VII(a) by fluorescence spectroscopic techniques using hydrostatic pressure as the perturbant. The degree of dissociation was evaluated by measuring either a decrease in the steady-state fluorescence anisotropy of a chromophore attached at VIIa's active site, or by following the decrease in energy transfer from a donor chromophore randomly attached to VIIa to an acceptor chromophore attached randomly to TF. Preliminary data using TF incorporated into pure phosphatidylcholine vesicles are consistent with a K_d of approximately 0.1 nM. The thermodynamic surface obtained provides fundamental information regarding this important interaction.

Supported by NIH Grants GM39750 and HL29019.

M-Pos237

UNASSISTED REFOLDING OF UREA DENATURED RHODANESE. Jose Mendoza+, George H. Lorimer*, and Paul M. Horowitz+, *E.I. du Pont & Co. and +The University of Texas Health Science Center, San Antonio, Texas 78284.

In vitro refolding after urea denaturation of the enzyme rhodanese (EC2.8.1.1) normally requires the assistance of detergents or chaperonin proteins. These procedures have been suggested to stabilize intermediates that can aggregate and that kinetically limit folding. Based on this hypothesis, we have developed a protocol for refolding without assistants that gives a highly reversible unfolding transition and leads to >80% recovery of native enzyme. In addition to low protein concentration (10ug/ml), low temperatures are required to maximize refolding. Otherwise optimal conditions give <10% refolding at 37C, while at 10C the recovery approaches 80%. When two electrophoretic variants of rhodanese are tested separately, the more electronegative species refolds significantly better than the other. Both forms refold equally well in the presence of detergents or chaperonins. The unfolding/refolding phases of the transition curves are most similar in the region of the transition, and refolding yields are significantly reduced at low urea concentrations. This result indicates that productive paths are preferentially stabilized in the transition region. Apparently, non-native structures can form rapidly at low denaturant concentrations while the interconversion of conformers to give the native structure is slow under these conditions. (Supported by Welch grant AQ723 to PMH).

M-Pos238

THE QUATERNARY STRUCTURE OF THE BOVINE α-CRYSTALLIN. A. C. Sen and B. Chakrabarti, Eye Research Institute, Dept. of Ophthalmology, Harvard Medical School, Boston, MA. To resolve the controversial issue of the quaternary structure of α-crystallin, we recently proposed (Walsh et al., Biochemistry, submitted) a model for this oligomeric protein suggesting that its subunits are assembled in three layers, the innermost layer being a micelle. The model was based on the thermal behavior of the protein as monitored by circular dichroism and differential scanning calorimetry. The core (innermost) micellar layer in this structure has 12 subunits arranged in a cubooctahedral symmetry and accommodates only six more subunits to form the second layer. The second layer constitutes a similar but not identical micelle-like structure with octahedral symmetry. The third layer adds more subunits in a relatively loose manner, and the layer could be irreversibly dissociated by minor insults, namely pH, temperature, or chemical denaturant. To provide further support of this model, we report here the results of extrinsic fluorescence studies of α-crystallin. The protein was labeled with both the thiol-specific fluorescent probes N-1-pyrene-maleimide (PM) and 2-(4'-maleimidyl-anilino) naphthalene-6-sulfonic acid (MIANS) in the native as well as under denaturing conditions. PM-labeled protein exhibits an excimer fluorescence band, indicating a close proximity of -thiol groups. It was observed that the excimer band intensity of the PM-labeled protein was greatly enhanced with increasing concentrations of the urea. Distinct differences also were noted while titrating the protein with increasing concentrations of MIANS in the absence and presence of varied amounts of urea (1-8M). In the presence of 5M urea, a significant red shift in the emission maximum of the labeled protein was noted upon increasing the amount of the probe. These results clearly indicate the presence of more than one class of -thiol groups of the protein, supporting the multi-layer structure in our proposed model for the oligomeric α-crystallin.

Supported by NIH Grant EY 04161 (BC)

M-Pos239

A NEW APPROACH TO THE CALCULATION OF HYDRATION ENTROPIES. M.A.Bukatin & A.A.Rashin. Biosym Technologies, Inc., 1515 Rt 10, Suite 1000, Parsippany, NJ 07054.

We suggest a new statistical mechanical procedure which allows to compute entropies of the water reorganization around any solutes. To simplify the computations greatly we make three assumptions: 1) only water molecules in the immediate hydration shell whose energetics is significantly perturbed by the solute contribute to the entropy change relative to the bulk water; 2) correlations between positions of different water molecules can be neglected, so that the total entropy is the sum of entropies of individual water molecules; 3) the influence of other water molecules and of the solute on the energetics and mobility of a selected water molecule can be calculated representing other water molecules as a continuum dielectric. Our calculations reproduce well known experimental trends: with the increase of the size of a spherical solute total water entropy increases for nonpolar solutes, and decreases for ionic ones. For nonpolar solutes the entropy loss per water molecule increases with the solute size, and thus water reorganization entropy increases faster than the accessible surface area of the solute in agreement with the latest experimental data. The results depend somewhat on a complex interplay between the loss of hydration energy, and the polarization of the solute and the water molecule. A physically reasonable description of these factors should be included in the calculation.

M-Pos240

ELECTROSTATIC ANALYSIS OF DOCKED COMPLEXES OF CYTOCHROME c AND CYTOCHROME b_5 MUTANTS.

Cynthia M. Miller[1], Scott H. Northrup[1], Lindsay D. Eltis[2], Paul D. Barker[2], and A. Grant Mauk[2]
[1]Tennessee Technological University, Department of Chemistry, Cookeville, TN, 38505; [2]University of British Columbia, Department of Biochemistry, Vancouver, B.C., Canada V6T 1W5.

The diffusional association and electron transfer reaction of ferric horse cytochrome c or yeast iso-1-cytochrome c with ferrous bovine cytochrome b_5 has been studied theoretically by a combination of Brownian dynamics simulation and electrostatic analysis of complexes. A robust model of protein structures and their electrostatic interactions were used based on an atomic-level spatial description. Accurate residue charge assignments at the appropriate pH and ionic strength are computed by the Tanford-Kirkwood theory with surface accessibility modification. Accurate interaction potentials are computed by iterating solutions of the linearized Poisson-Boltzmann equation on a grid. An extensive analysis of the electrostatic binding energies of a large representative set of docked complexes has been performed using several electrostatic treatments. We examine the role of electrostatic charge distribution and solvent mediation in the facilitation of protein-protein docking prior to the electron transfer step. Effects of site-directed mutagenesis on the bimolecular rates are predicted.

M-Pos241

Ca^{2+}-DEPENDENT INTERACTION OF PROTEIN C WITH THROMBIN AND THE ELASTASE FRAGMENT OF THROMBOMODULIN. ANALYSIS BY ULTRACENTRIFUGATION (II).

[1]Olsen P.H., [2,3]Esmon C.T., [3]Esmon N.L., [1]Laue T.M.
[1]Dept. Biochemistry, UNH, Durham, NH 03824 and [2]Howard Hughes Medical Institute, Oklahoma City, OK 73104, and [3]Oklahoma Medical Research Foundation, Oklahoma City, OK 73104.

Thrombin (T), bound to the elastase proteolytic fragment of thrombomodulin (elTM), activates protein C (pC) in a calcium dependent manner. Activation rates increase from 0 to 0.3 mM Ca^{2+}, then decline rapidly with higher Ca^{2+} concentration. Sedimentation equilibrium has been used to examine the calcium ion dependence of the interactions between these three proteins. All experiments were carried out in Tris buffered saline (pH 7.65) that included 1 mM benzamidine and from about 0 mM to 5 mM $CaCl_2$. The T-elTM complex has 1:1 stoichiometry, and is characterized by a strong association that is relatively Ca^{2+} independent. On the other hand, the T-pC interaction, examined using two inhibited forms of thrombin and either the substrate (pC) or the product (activated pC), is very Ca^{2+} dependent. In low Ca^{2+} concentrations, T complexes with a single pC, but an additional macromolecular complex of greater than 1:1 stoichiometry of T to pC is also observed. At Ca^{2+} concentrations greater than 1.5 mM only the 1:1 T-pC complex remains, although its dissociation constant is approximately tripled. Thrombin was inactivated by a tripeptide chloromethyl ketone inhibitor (FPRCK) which may occupy some of the substrate recognition site, and by diisopropylfluorophosphate (DIP), which blocks only the catalytic site. Initial results suggest that pC "recognizes" FPRCK-T no differently from DIP-T, but that pC binds either inhibited form of T with higher affinity than activated pC. Further studies have shown that elTM, T and pC form a complex of 1:1:1 stoichiometry. As the Ca^{2+} concentration increases, pC appears to dissociate from the complex. Thus, it appears that the calcium ion inhibition of pC activation may be due to decreased affinity of the elTM-T complex for pC. Supported by NSF BBS 8615815, NSF DIR 9002027, AHA 871092, R37 HL 30340.

M-Pos242

Oligomerization and Stability of TrpR: An In-Depth Fluorescence Study

Teresa Fernando[a], Kathleen S. Matthews[b] and Catherine A. Royer[c]
a-University of Illinois (Biochemistry), b-Rice University (Biochemistry), and c-University of Wisconsin (Pharmacy)

Fluorescence spectroscopy has been employed to investigate the oligomeric properties, as well as the stablility of the *trp* repressor protein (TrpR). These studies of polarization of fluorescence of dansyl labeled TrpR and steady-state emission and the decay associated spectra (DAS) of the intrinsic tryptophan residues have revealed that TrpR in vitro exists as either a monomer, dimer or tetramer, depending upon its concentration. In addition, time-dependence of the dilution profiles has been observed. The dissociation of TrpR to its monomeric subunits appears both by steady-state and time-resolved methodologies to be a relatively concerted transition, and the dilution curves suggest that the TrpR monomer may be somewhat unfolded. A comparison of the fluorescence properties of the dilution dissociated and chemically denatured forms of TrpR demonstrates, however, that the dissociated TrpR is very different from the denatured TrpR. The denaturation appears to be two-state when the steady-state fluorescence energy is monitored. However, examination of the urea and guanidine dependence of the time-resolved fluorescence brings to light a more complex denaturation profile. Studies in presence of the co-repressor, tryptophan, using the dansyl labeled protein suggest that tryptophan binding stabilizes the dimer with respect both to the tetramer and to the denatured form. High pressure fluorescence studies carried out on TrpR demonstrate that the application of pressure results in either a dissociation or a denaturation of the protein, depending upon the state of the system at atmospheric pressure.

M-Pos243

EFFECTS OF PROTONS ON THE ENERGETICS OF COOPERATIVITY FOR THE INTERMEDIATE ALLOSTERIC SPECIES OF HUMAN HEMOGLOBIN

Margaret A. Daugherty, Madeline A. Shea and Gary K. Ackers
Department of Biochemistry and Molecular Biophysics, Washington University School of Medicine, St. Louis, MO 63108

The 10 ligation species of cyanomet human hemoglobin were previously found to distribute into three discrete cooperative free energy levels with the intermediate level occupied by the two singly-ligated species and one of the 4 doubly ligated species (Smith, F.R. and Ackers, G.K., 1985, P.N.A.S. USA 82, 5347). This distribution, subsequently found with other heme-site ligands, was shown to be incompatible with the classical two-state MWC mechanism and requires a minimum of three allosteric structures (G.K. Ackers, 1990, Biophys. Chem. 16, 371). To further characterize the intermediate allosteric state we studied the effects of pH on its free energy of quaternary assembly, in parallel with corresponding data on the deoxy (T) and fully-ligated (R) species. Results indicate that the intermediate allosteric tetramer has the deoxy (T) quaternary structure. This assignment is supported by studies on the effects of temperature and single-site mutations. This finding, together with the resolved energetic distributions, implies that: (a) ligand-induced tertiary energy alters binding affinity within the T structure by 170-fold prior to quaternary switching, and (b) the T-R switch follows a Symmetry Rule: switching occurs whenever a binding step creates a tetramer with one or more ligated subunits on each side of the $\alpha^1\beta^2$ interface.

M-Pos244

EVIDENCE FOR HYDROPHOBIC PROTEIN-PROTEIN INTERACTION IN THE THERMAL UNFOLDING OF γ-CRYSTALLINS.

M.T. Walsh[1], A.C. Sen[2] and B. Chakrabarti[2,3]
[1]Department of Biophysics & Biochemistry, Boston University School of Medicine, [2]Eye Research Institute, [3]Department of Ophthalmology, Harvard Medical School, Boston, MA.

Our recent high resolution differential scanning calorimetric studies (DSC) have demonstrated that γ-crystallin fractions II, IIIA, IIIB and IV exhibit major endothermic transitions at Tm of 71°, 70°, 67° and 78°C, respectively, with corresponding exothermic peaks ~3° above Tm and subsequent irreversible precipitation (Sen et al., 1990, Biochemistry, submitted). The calorimetric enthalpy change (ΔH) associated with the exotherm was very large for all fractions. The hydrophobic fluorescent probe, 1-anilinonaphthalene-8-sulfonic acid (ANS) was used to examine if this highly exothermic event could be the result of hydrophobic protein-protein interaction. At room temperature, ANS, when bound to γ-crystallins, does not show a significantly higher characteristic emission than that of the dye in water. However, at temperatures ≥60°C, the ANS-bound protein shows intense emission (blue shifted), suggesting that the aggregation associated with the large ΔH arises from protein-protein interaction as the hydrophobic regions of the proteins become exposed during heating and unfolding. The ionic detergent, tetradecyl trimethyl ammonium bromide stabilizes the protein from thermal denaturation, thus protecting the hydrophobic groups from being exposed, eliminating the potential for these protein-protein interactions and association of hydrophobic regions, and the subsequent exothermic transition observed by DSC. The possibility of thiol oxidation as a precursor of high temperature aggregation was ruled out since the DSC scan of γ's in the absence and presence of excess dithiothreitol (DTT) was almost identical. The mechanism of thermal aggregation is thus distinctly different from photoaggregation as we have demonstrated that the latter could be prevented in the presence of DTT (Kono et al., 1988, Photochem. Photobiol. 47:593).

Supported by NIH Grants EY-04161 (B.C.) and HL 26335 (M.T.W.)

M-Pos245

OSMOTIC PRESSURE MEASUREMENTS OF BETA-CRYSTALLINS FROM BOVINE LENS

A.K. Kenworthy and A.D. Magid, Department of Cell Biology, Duke University Medical Center, Durham, N.C. 27710

We have argued (*Biophys J* 55:21a) as have others (*Eur J Biophys* 17: 61) that, in the lens of the vertebrate eye, a constant colloid osmotic pressure is exerted by the crystallins despite their steep radial concentration gradient and that this constancy is enabled by differences in the osmotic properties of the constituent crystallins. A corresponding gradient in refractive index, which improves visual acuity by minimizing spherical aberration, is produced by these differences in protein concentration. Not only do total crystallin concentrations differ across the lens radius but so do the relative abundance of the various species of crystallins. Since we suppose that the differential distribution of crystallin species provides the basis for radial concentration differences, we have begun an effort to purify crystallin fractions from regions within the lens and to characterize their osmotic properties. Here we report osmotic pressure *vs* concentration isotherms for β-crystallins. A differential distribution of β-crystallins exists across the lens. In the nucleus, β_H (heterogeneous oligomers, 100–300 kDa) predominates. Its formation depends on the expression of a 31 kDa subunit. In the cortex, β_L (dimers and trimers, 42–80 kDa) predominates. In our study, β-crystallins were isolated by Sepharose 6B chromatography from nuclear (inner 50% by weight) and cortical (outer 50%) bovine lens extracts. β-crystallin peak fractions were pooled, based on analysis by SDS-PAGE, and concentrated by ultrafiltration. Osmotic pressure was measured by secondary membrane osmometry. Here, samples are exposed to known osmotic pressures by dialysis to equilibrium against dextran solutions (at room temperature) and protein concentration followed by refractive index measurements. For all work, the buffer comprised 50 mM NaCl, 50 mM Tris, 1 mM EDTA, and 5 mM azide, pH 7.6. We find large differences in osmotic pressure behavior between β-crystallin classes. Below about 0.1 g/ml both proteins gave approximately van't Hoff behavior but then pressure rose more steeply with concentration for both classes of β-crystallin. However, for a given protein concentration, β_H always exhibited a smaller osmotic pressure than β_L. These results suggest that the differential abundance of the β-crystallins contributes to the observed differences in both regional protein concentration and the osmotic behavior of isolated total crystallins: a higher concentration of β_H is required to maintain a given osmotic pressure than β_L. Additionally, as described for alpha-crystallin by others, both β-crystallins also showed an apparent limiting concentration, about 0.35 g/ml for β_L and about 0.45 g/ml for β_H where pressure rose asymptotically. Partial support from NIH grant GM27278 to T.J. McIntosh and the use of lab facilities of H.P. Erickson are gratefully acknowledged.

M-Pos246

INDEPENDENT DETERMINATION OF COOPERATIVE BINDING INTERACTIONS USING ISOTHERMAL TITRATION CALORIMETRY.

Gabrielle Bains and Ernesto Freire. Biocalorimetry Center. Department of Biology, The Johns Hopkins University, Baltimore, MD 21218

It is demonstrated that isothermal titration calorimetry can be used to determine cooperative interaction energetics even for extremely tight binding processes in which the binding affinity constants are beyond the limits of experimental determination. The approach is based on the capability of calorimetry to measure the apparent binding enthalpy at any degree of ligand saturation. When calorimetric measurements are performed under conditions of total association at partial saturation (TAPS), the dependence of the apparent binding enthalpy on the degree of saturation is a function only of the cooperative binding interactions. The method developed here allows an independent estimation of cooperative energetic parameters without the need to simultaneously estimate or precisely know the value of the association constants. Computer simulations using a two-site binding system indicate that cooperative free energies ranging from -4 to 4 kcal/mole can be accurately determined. Since total ligand association at partial saturation is achieved only at macromolecular concentrations much larger than the dissociation constants, (Kd), the method is especially suited for high and very high affinity processes. Biological associations in this category include fundamental cellular processes like cell surface receptor binding or protein-DNA interactions. (Supported by NIH grants RR-04328 and NS-24520.)

M-Pos247

SELF ASSOCIATION OF HUMAN AND PORCINE RELAXIN AS ASSESSED BY ANALYTICAL ULTRACENTRIFUGATION AND CIRCULAR DICHROISM.

Steven J. Shire*, Leslie A. Holladay† and Ernst Rinderknecht*
*Genentech, Inc. S. San Francisco, CA 94002
†Beckman Instruments, Inc., Palo Alto, CA 94303-0803

The self association properties of recombinant DNA derived human relaxin and porcine relaxin isolated from porcine ovaries have been studied by sedimentation equilibrium analytical ultracentrifugation and circular dichroism. The human relaxin centrifuge data were adequately defined by a monomer-dimer self association model with an association constant of ~6×10^5 M^{-1} whereas porcine relaxin was essentially monomeric in solution. An approximate 5 fold increase in weight fraction of human relaxin monomer elicited by dilution of the protein resulted in no change in the far UV CD spectrum at 220 nm. In contrast, after an approximate 5 fold increase in weight fraction of monomer, the near UV circular dichroism spectra for human relaxin exhibited significant decrease of the CD signal at 275 and 284 nm. These CD bands from the lone tyrosine in human relaxin are superimposed over a broad envelope which is probably due to the disulfide chromophores. Although both proteins have two tryptophan residues, the near UV circular dichroism spectra only show a broad shoulder near 291 nm rather than the strong CD bands often found for tryptophan. Moreover, there is little change in this broad band after dilution of human relaxin to concentrations which resulted in a 5 fold increase in monomer weight fraction. These data suggest that dissociation of the relaxin dimer to monomer is not accompanied by large overall changes in secondary structure or alteration of tryptophan environment, whereas there is a significant change in the tyrosine environment. This tyrosine is replaced by an arginine in porcine relaxin and this substitution may affect the self association properties of the latter protein.

M-Pos248

END-TO-END DIFFUSION OF FLEXIBLE BICHROMOPHORIC MOLECULES AND PROTEINS OBSERVED BY INTRAMOLECULAR ENERGY TRANSFER USING FREQUENCY-DOMAIN FLUOROMETRY.

J. Kuśba, I. Gryczynski, W. Wiczk and J.R. Lakowicz, University of Maryland School of Medicine, Department of Biological Chemistry and Center for Fluorescence Spectroscopy, Baltimore, MD 21201, and M.L. Johnson, University of Virginia, Department of Pharmacology, Charlottesville, VA 22908.

We used the phenomena of fluorescence resonance (non-radiative) energy transfer (FRET) to recover both the end-to-end distance distribution and diffusion coefficient of a flexible molecule (TUD), and of the protein melittin. This information was recovered using only the donor intensity decay (FRET occurs from the indole donor to the dansyl acceptor), as observed by the technique of frequency-domain fluorometry. The differential equation describing the donor population (*Biopolymers* 17:11-31, 1978) was solved numerically. The data were fit using least squares and the predicted frequency response for a model which includes end-to-end diffusion. Both the initial distance distribution at t = 0 and the diffusion coefficient could be recovered from the data.

The static and dynamic distance characteristics of melittin were also studied by diffusion dependent intramolecular energy transfer from the single tryptophan (residue 19) to the N-terminal α-amino group, which was labeled with a dansyl residue. The revealed donor to acceptor diffusion coefficients are 0.16 and 9.9 x 10^{-6} cm^2/s in the random coil and α-helical states, respectively. The larger donor to acceptor diffusion in the α-helical state may be a consequence of the limited range of motion ≤ 9 Å in the α-helix as compared with ≤ 27 Å in the random coil state.

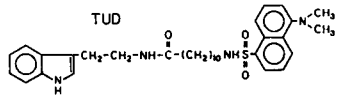

M-Pos249

THE INTERACTION OF MILK XANTHINE OXIDASE WITH BISULFITE. K. M. Fish, V. Massey, R. H. Sands and W. R. Dunham (Intro. by J. L. Oncley), Department of Biological Chemistry and Biophysics Research Division, The University of Michigan, Ann Arbor, MI 48109-2099

Bisulfite ion competitively inhibits xanthine oxidase activity. The ability of HSO_3^- to bind at the molybdenum center is controlled by pH due to the pK_a of 6.91 of SO_3^{2-}/HSO_3^-. The K_d of the enzyme bisulfite complex is 4.5×10^{-5} M at pH 7.0 and 25°C.

The relative magnitude of extinction changes in the optical absorption spectra, the number of inhibitor ions reversibly bound, and the number of electrons required for complete bleaching of the visible spectrum of the MXO:HSO_3^- complex were all dependent on the percentage of fully functional xanthine oxidase. Binding of HSO_3^- causes perturbations of the visible spectrum: the maximum extinction changes at 320 and 422 nm were calculated to be ~4300 and ~2150 $M^{-1}\,cm^{-1}$ respectively. The stoichiometry of reversible binding was determined to be one HSO_3^-/active Mo center.

Combined optical and epr analyses of anaerobic dithionite titrations revealed that the relative redox potentials of the $Mo^{+6/+5}$ and $Mo^{+5/+4}$ couples decreased by ~35 and 45 mV respectively on binding bisulfite.

The finding that bisulfite has a profound effect on the redox properties of xanthine oxidase necessitates a re-evaluation of dithionite titrations previously carried out with this enzyme at neutral and low pH's since bisulfite produced as an oxidation product of dithionite binds to the enzyme during the course of titration. (NIH grant GM32785 and NSF grant DMB-8803843).

M-Pos250

SOLUTION CONFORMATION AND STABILITY OF THE ZINC FINGER PEPTIDE ZFY-6 STUDIED BY RAMAN SPECTROSCOPY. Tiansheng Li, Michael A. Weiss and George J. Thomas, Jr. (Intro. by Renee Becka), Division of Cell Biology and Biophysics, School of Basic Life Sciences, University of Missouri-Kansas City, Kansas City, MO 64110.

The peptide, KPYQCQYCEYRSADSSNLKTHIKTKHSKEK, which comprises 30 residues of the sixth zinc-finger domain of the human male-associated ZFY protein (ZFY-6), has been investigated in solution by laser Raman spectroscopy to determine the dependence of conformation upon Zn binding. A Raman band near 330 cm^{-1}, assigned to Zn-ligand stretching vibrations, identifies the zinc-coordinated form of the folded peptide (zinc finger). Relative intensities of Raman amide I components, near 1653 and 1679 cm^{-1}, clearly differentiate the more highly α-helical secondary structure of the zinc-associated complex from the less α-helical structure of the zinc-free (oxidized) form. The secondary structure change which accompanies oxidation is consistent with a loss of helicity affecting 8 ± 2 peptide residues. In solution at pH 7, the zinc-free form of ZFY-6 exhibits a sharp Raman band at 510 cm^{-1}, indicating formation of a disulfide bridge with gauche/gauche/gauche (g/g/g) configuration of the Cα-Cß-S-S-Cß-Cα network. Additionally, oxidation alters other side chain configurations, including conversion of one tyrosine phenolic group from the role of exclusive hydrogen bond acceptor in the zinc finger to that of both acceptor and donor in the zinc-free form. In solution at low pH, Zn is also displaced from the finger structure with formation of disulfide bridges, as indicated by Raman disulfide markers. Conformational transitions of ZFY-6 in neutral (pH 7) and acidic (pH 3.5) solutions will be discussed in relation to 2D-NMR studies of the folded peptide (M. Kochoyan et al., manuscript submitted).

Supported by NIH Grant AI11855.

M-Pos251

VIBRATIONAL SPECTROSCOPY AS A PROBE OF SULFHYDRYL GROUP STRUCTURE AND INTERACTIONS IN PROTEINS. Huimin Li, James M. Benevides and George J. Thomas, Jr., Div. Cell Biol. and Biophys., School of Basic Life Sciences, University of Missouri, Kansas City, MO 64110

The cysteine sulfhydryl group plays an important role in structural biochemistry. It is capable of donating and accepting hydrogen bonds with solvent molecules as well as with other protein groups. Cysteine ligand coordination is fundamental to enzyme activity and nucleic acid recognition. We have undertaken a systematic Raman study of model mercaptans and cysteine thiols in order to provide an effective spectroscopic probe of the S-H group and its biologically relevant configurations and interactions in aqueous and crystalline proteins. The study of aliphatic and aromatic mercaptans in both polar and apolar solvents and of L-cysteine and glutathione in the crystal provides a basis for interpreting the S-H stretching region of the Raman spectrum in terms of hydrogen bond donation by S-H, hydrogen bond acceptance by S, and rotamer populations of the cysteinyl side chain. The frequency interval of the Raman S-H stretching vibration (σ_{SH}) is diagnostic of S-H donors which are hydrogen bonded strongly (2525-2560 cm^{-1}), moderately (2560-2575 cm^{-1}) or weakly (2575-2580 cm^{-1}). When the S-H group is not hydrogen-bonded, e.g. at high dilution in CCl_4, we find $\sigma_{SH} \approx 2585 \pm 5$ cm^{-1}. Hydrogen-bond acceptance by S, in the absence of S-H donation, elevates σ_{SH} slightly (≈4 cm^{-1}). Normal mode analysis provides complementary data to understand the effects of rotamer population on the S-H and C-S stretching frequencies. Since the S-H region of the Raman spectrum contains no interference from other molecular vibrations, the established correlations should be applicable to resolving different cysteine interactions and side-chain orientations in proteins.

Supported by N.I.H. Grant AI11855.

M-Pos252

A GENERAL RACK MECHANISM FOR ENZYME FUNCTION Rufus Lumry, Chemistry Department, University of Minnesota, Minneapolis, Mn 55455.

The discovery of the "knot-matrix" construction of enzymes has allowed a more detailed description of the "rack" mechanism of enzymic catalysis and regulation. Each catalytic function depends on the closure process of two functional domains each consisting of one knot and its associated matrix. In this process the enzyme groups participating chemically, which are held at the knot surface at least one per knot, are forced mechanically into the substrate in a configuration closely approximating the transition state. Each substrate has a distinct reaction coordinate determined by size, chemical nature of reacting group and sidechains, and stereochemistry. The central feature of the process is the contraction of the matrices in which their free volume is greatly reduced. Studies of serine proteases by Bone et al. (Biochemistry 28,7600(1989)) and by Mangel and coworkers(Ibid, 29, 5925(1990)) show that even in the acyl-enzyme state the average free volume is reduced by 30 to 50% depending on the shape and size of substrate alky sidechain. The actual reduction in the matrices is considerably larger. One consequence is that the matrices, which have considerable motility in the free enzyme, resemble glasses in the acyl-enzyme states. Further motion along the reaction coordinate toward the transition state into a metastable state from which the passage to the transition state is conventional probably involves further contraction generating still higher potential energy in the assembly of reacting atoms. Our best estimate is that the lifetime of the metastable state is within one order of magnitude of 1ns. The popular "transition-state-stabilization" mechanism for catalysis is not consistent with these observations unless conformational dynamics is included. The two mechanisms are then similar except in the way the potential energy is used to decrease the activation free energy. The expansion-contraction device is essential for redistribution of conformational free-energy. Thus, for example, the free energy of substrate binding is utilized to change the enthalpy/entropy balance so as to favor contraction.

Palendromy in the functional domains of enzymes having zymogen precursors appears to be common despite the evolutionary cost. It is not found in dimeric enzymes produced by gene duplication.

"Knot tricks" based on completion of a knot by a missing sidechain provided by the other protein of a dimeric enzyme will be described.

M-Pos253

KINETICS OF GLUCOSE-6-PHOSPHATE BINDING TO HUMAN GLUCOSE-6-PHOSPHATE DEHYDROGENASE WITH AND WITHOUT GLYCEROL. Omoefe O. Abugo. Molecular Dynamics Section, Laboratory of Cellular and Molecular Biology, NIH/NIA, Gerontology Research Center, Baltimore, Maryland.

Previous kinetic results have shown the binding of glucose-6-phosphate (G6P) to the B variant of the enzyme glucose-6-phosphate dehydrogenase (G6PD) to be michealian in nature. At higher concentrations of the G6P substrate than had been previously utilized, it has, however, been observed that the enzyme exhibits negative co-operativity, indicating the presence of an additional weak binding site.

In the presence of glycerol under non-denaturing conditions, the observed negative co-operativity is found to be abolished, resulting in the elimination of the additional weak binding site. Kinetic studies at different temperatures do suggest that in the presence of glycerol, perturbations of the protein hydration lead to conformational changes in the G6PD molecule, resulting in the deformation of the weak binding site.

M-Pos254

EARLY KINETICS OF ALDOSTERONE SECRETION FROM *ZONA GLOMERULOSA* CELLS OF RAT.

Terry M. Dwyer, Attila Szebeni and Manis J. Smith. Department of Physiology and Biophysics. University of Mississippi Medical Center, Jackson, MS 39216-4505.

Aldosterone secretion is recognized to be regulated by activation of the synthetic pathway, requiring 10's of minutes, and by trophic increases in cell number, precursor stores and enzyme levels, requiring days to weeks. The early changes in secretory rate were studied by perfusing freshly dissected adrenal capsules from rat in a thermostatically controlled chamber. The perfusate was M199 with a HCO_3/CO_2 buffer. This preparation is enriched in the *zona glomerulosa* cells that are specific for aldosterone secretion. Perfusate poor in oxygen (4%) yielded aldosterone secretion that fell with time; rapid switching to 95% O_2 resulted in a increase in aldosterone release peaking at 4 min and returning to baseline by 20 min. Preincubation with the precursor corticosterone yielded a similar increase that was sustained. Stimulating secretion by changing bath K from 4 to 6 mM resulted in a similar peak transient of aldosterone secretion at 30 s followed by a slower increase in secretory rate. This slower increase in aldosterone secretion can be prevented by limiting the exposure of the cell to 6 mM K.

This work was sponsored by grants from NIH and the American Heart Association, Mississippi Affiliate.

M-Pos255

CALORIMETRIC DETERMINATION OF THE EFFECT OF IONIC STRENGTH ON THE ENZYME KINETICS AND THERMAL STABILITY OF YEAST CYTOCHROME C OXIDASE. Paul E. Morin and Ernesto Freire, Biocalorimetry Center and Department of Biology. The Johns Hopkins University, Baltimore, MD 21218.

The kinetic parameters for the enzymatic reaction of yeast cytochrome c oxidase with its biological substrate cytochrome c have been measured using a titration microcalorimeter to monitor the heat produced or absorbed with respect to time. This technique allows determination of both the energetics and the kinetics of the reaction under a variety of conditions within a single experiment. Experiments performed in buffer systems of varying ionization enthalpies allow determination of the number of protons absorbed or released during the course of the reaction. For cytochrome c oxidase the intrinsic enthalpy of reaction was determined to be -16.5 kcal/mole with one (0.96) proton consumed for each ferrocytochrome c molecule oxidized. Variation of salt concentrations from 0-200 mM KCl in the presence of 10 mM phosphate, pH 7.40 results in a biphasic dependence of activity upon ionic strength with a peak activity observed near 40 mM KCl. The salt effect on the kinetics of the yeast enzyme is similar to that described for the enzyme purified from other biological sources. Despite the strong salt dependence of the reaction kinetics, the enthalpy for the reaction was found to be independent of the salt concentration in the reaction medium. Thermal stability studies of the enzyme indicate that in the absence of salt the calorimetric profile is characterized by two well defined peaks centered at 51°C and 60°C. At high salt concentrations the high temperature peak shifts downwards by 3°C. Additional experiments involving direct transfer of the enzyme from low to high salt conditions yield very small transfer enthalpy changes (-20 ± 5 kcal/mole cytochrome c oxidase) that remain constant within the experimental error throughout the salt concentrations tested. These results indicate that the salt effect on the oxidase molecule is likely of entropic origin. (Supported by NIH Grant GM37911 and RR-04328.)

M-Pos256

THE TRANSVERSE TUBULE Mg^{2+}-ATPase IS A HIGHLY GLYCOSYLATED, MULTIPLE SUBUNIT ENZYME. T.L. Kirley, Department of Pharmacology and Cell Biophysics, University of Cincinnati, Cincinnati, Ohio 45267-0575.

The major ATPase activity present in transverse tubules isolated from rabbit skeletal muscle is the Mg^{2+}-ATPase. This enzyme hydrolyzes nucleotides in the presence of millimolar Mg^{2+} or Ca^{2+}. It is not related to the E_1E_2, F_0F_1, and the vacuolar ATPases, as judged by a variety of enzymatic criteria. It also does not appear to be an ectoenzyme. The Mg^{2+}-ATPase was first isolated in active form in this laboratory (Kirley, J. Biol. Chem. 263, 12682-12689 (1988)). In that work, the main protein had a molecular weight of approximately 100 kDa. In the present study, the purification scheme was improved by the addition of a high performance size exclusion chromatography (HPSEC) step, and a highly active preparation has been obtained (specific activities of up to 70,000 μmoles ATP hydrolyzed/mg protein/hr). In addition to the approximately 100 kDa subunit seen previously, there is also a 160 kDa band and a diffuse band at approximately 70 kDa. The 160 kDa α subunit was poorly recovered from the native gel used previously, explaining why it was not described earlier. The 70 kDa protein runs as a diffuse, hard to detect band which is clearly seen only after deglycosylation. All three of these putative subunits comigrate with the Mg^{2+}-ATPase activity as a single band on native gels, but they are not linked by intermolecular disulfide bonds. Deglycosylation with PNGase-F showed that all three subunits are N-glycosylated at multiple sites, the 160 kDa (α subunit) protein having a core molecular weight of 131 kDa, the 97 kDa (ß subunit) protein having a core molecular weight of 84 kDa, and the 70 kDa (γ subunit) having a core molecular weight of 50 kDa. Similar results were obtained using trifluoromethanesulfonic acid to chemically deglycosylate the purified Mg^{2+}-ATPase. Densitometry of Coomassie blue stained gels indicate that the subunit stoichiometry of the Mg^{2+}-ATPase is $\alpha_1\beta_3\gamma_1$.

Supported by NIH RO1 AR38576

M-Pos257

STEREOCHEMISTRY OF THE CONCERTED ENOLIZATION CATALYZED BY Δ^5-3-KETOSTEROID ISOMERASE (KSI). A. Kuliopulos, G.P. Mullen, L. Xue, and A.S. Mildvan. Johns Hopkins School of Medicine, Baltimore, MD 21205.

Multiple kinetic isotope effects show the rate-limiting step of the KSI reaction to be the concerted enolization of the bound substrate (Biochemistry 29, 7491). The Y55F + Y88F double mutant of KSI, which decreases both k_{cat} and K_M by only 4-fold, retains as the only aromatic residues Tyr-14, which functions as the general acid, 3 histidines, and 10 phenylalanines. 1D and 2D NMR (TOCSY) spectra of the Y55F + Y88F mutant at 600 MHz, deuterating the phe rings, permit unequivocal assignment of the aromatic proton resonances of Tyr-14 at 6.66 ppm (3,5H) and 6.83 ppm (2,6H) and reveal its pK_A to exceed 10.9. Binding of the product analog 19-nortestosterone (19-NT) induces downfield shifts of 0.12 and 0.06 ppm of the 3,5H and 2,6H resonances of Tyr-14, possibly due to the deshielding effect of the 3-keto group of the steroid. 2D NOESY spectra of the enzyme-19-NT complex reveal an NOE indicating proximity between the 3,5 protons of Tyr-14 and the 2α-proton of the steroid (2.35 ppm) but no NOE's to the 4-proton (5.88 ppm) or to the 6α-proton of the steroid (2.48 ppm). Partial deuteration of 19-NT reveals a 7-fold smaller NOE to the 2β-proton. These data place the phenolic ring of Tyr-14 beside the 2-position of the steroid and far from the 4- and 6-positions, ruling out an orientation of the phenolic ring symmetrically above or below the A-ring of the steroid. The positioning of Tyr-14 beside the steroid permits hydrogen bonding of the phenolic -OH to a lone electron pair rather than to the π electron pair of the 3-keto group of the substrate. Since Asp-38 deprotonates the axial 4β-position from above the A-ring, the overall stereochemistry of the concerted enolization is orthogonal.

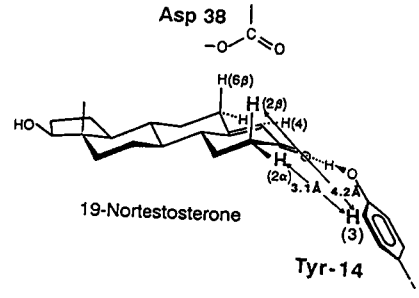

M-Pos258

NONENZYMATIC GLYCOSYLATION OF ALDOLASE. Aydin Örstan and Ari Gafni. Institute of Gerontology, The University of Michigan, 300 N. Ingalls, Ann Arbor, MI 48109-2007.

Rabbit muscle aldolase is nonenzymatically glycosylated by its substrate fructose-1,6-diphosphate (FDP) in 0.1 M phosphate buffer, pH 7.5, at 37°C. The process results in the inactivation of the enzyme accompanied with the development of an end product with an emission peak at 428 nm. Although the rate of inactivation of the enzyme is not sensitive to the concentration of FDP in the range 0.1-10 mM, the fluorescence obtained after incubation with 10 mM FDP (curve 1) is six fold larger than that obtained with 0.5 mM FDP (curve 2). This indicates that more than one FDP molecule may be involved in the formation of the fluorescent end product. The spectrum of glycosylated aldolase (excited at 370 nm) resembles the normalized spectrum obtained from a solution of lysine and ribose heated at 75°C (curve 3). Thus, nonenzymatic glycosylation may always produce the same product regardless of the starting materials and incubation conditions. Aldolase is also inactivated by fructose-1-phosphate and to a lesser extent by fructose-6-phosphate. Degradation of aldolase by cathepsin B has been monitored using polyacrylamide gel electrophoresis and fluorescamine. Compared to aldolase incubated without FDP, glycosylated enzyme is degraded to a greater extent by cathepsin B. This result suggests that nonenzymatic glycosylation may be one of the regulatory factors of the in vivo half life of aldolase.

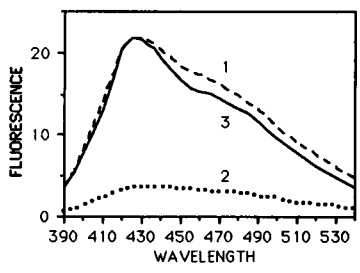

M-Pos259

ELECTROCONFORMATION COUPLING (ECC) IN THE ECTOENZYME NUCLEOTIDE DIPHOSPHOHYDROLASE. M. D. Rosenberg, T.Y. Tsong, R. Strobel, and D.S. Liu, Depts. of Biochemistry and Genetics and Cell Biology, University of Minnesota, St. Paul, MN 55108

Tsong *et al.* have shown that the coulombic interaction between an enzyme and an alternating electric field (AC) can cause an enzyme to oscillate between conformational states. Analyses suggest that the AC can cause the transmembrane potential to oscillate locally, thus, enhancing the activity of membrane proteins. The integral membrane transport ATPases have been used to demonstrate this phenomenon. We have studied the affects of AC on another integral membrane ATPase that is not part of a transport system. Ecto nucleotide diphosphohydrolase (EC 3.6.1.5) has been purified 40,000 fold using chromatographic separations, gel electrophoresis and monoclonal antibody affinity chromatography. The enzyme is in micellar form having been solubilized from membrane microvesicles by NP-40 and is a homogeneous protein (80kd) with high specific activity (approximately 200 U/mg) and high stability at room temperature. Samples were incubated at 37°C, pH7.4, and stimulated in an AC field (field strength 10 V/cm) at varying frequencies. Activity was measured prior to and following 10 minutes of stimulation. A sharp optimal frequency window was found at 1 kHz resulting in a 2.5 fold increase in activity. These results lend further support to the ECC model and the concept that membrane enzyme activity is sensitive to local and time-dependent fluctuations of the electrical field. Reference: Tsong, T.Y. (1990) Ann. Rev. Biophys. Biophys. Chem. 19, 83-106.

M-Pos260

INTERMEDIATE STATES OF B_{12} ENZYME CATALYSIS: HOMOLYTIC vs. HETEROLYTIC Co-C BOND CLEAVAGE. *M. Wirt, I. Sagi, & M. Chance, Department of Chemistry, Georgetown University, Washington, DC 20057.*

Knowledge of the mechanism of Co-C bond cleavage in B_{12} dependent enzymes is critical to understanding the mechanism of B_{12} enzyme catalysis. To investigate the relationship between geometry of the intermediate and Co-C bond cleavage, the structures of the lower valence Co(I) and Co(II) B_{12} intermediates in solution are analyzed by X-ray edge and EXAFS spectroscopy. Integration of pre-edge transitions, followed by comparison of these intensities to model compounds, provides a means for predicting geometric conformations. The edge spectrum of the Co(I) B_{12} species contains a moderate intensity 1s-4p + shake-down (SD) peak and no 1s-3d transition. Comparison of these features with model compounds shows that the structure of Co(I) B_{12} is distorted square planar. For enzymes, such as methionine synthetase (Harder et. al., *Biochem.*, **28**, 1989, p. 9080) to promote Co(I) formation and heterolytic Co-C bond cleavage, a weakening and/or cleavage of the Co-dimethylbenzimidazole (DMB) bond is required.

Homolytic cleavage of the Co-C bond results in the formation of the Co(II) B_{12} intermediate. X-ray edge data shows the geometry of Co(II) B_{12} to be five coordinate distorted square pyramidal. This result is consistent with the recent crystal structure of Krautler et. al.(*J. Amer. Chem. Soc.*, **111**, 1989, p. 8936). Using EXAFS spectroscopy, we have analyzed the structure of Co(II) B_{12} in solution. Average Co-N (equatorial) distances to the corrin ring are estimated at 1.88 $\pm$ 0.02 Å, and the Co-N_d distance to the (DMB) ligand of 1.99 $\pm$ 0.03 Å. Our results indicate that as Co-C bond homolysis occurs, the Co-N_d bond becomes much stronger, while the Co-N equatorial distances show minimal change. We will present EXAFS results of Co(I) B_{12} and demonstrate that modulation of the Co-DMB bond is a key mechanism in promoting homolytic vs. heterolytic cleavage.

This research is supported by CSRS U.S. Department of Agriculture under grant #90-37200-5357 of the Program in Human Nutrition.

M-Pos261

METHYLCOBALAMIN HETEROLYSIS: PLATINUM BINDING TO AMIDES MIMICS ENZYMATIC CLEAVAGE. *E. Chen, J. Barriocanal, K. Taraszka & M. R. Chance, Department of Chemistry, Georgetown University, Washington, DC 20057.*

Adenosylcobalamin and methylcobalamin (MeB_{12}) dependent enzyme systems undergo homolytic and heterolytic cleavage of the Co-C bond. However, it is unclear how enzymes interact with cobalamins to promote heterolysis *vs.* homolysis. Previous studies (Fanchiang et al., *JACS*, **101**, 1979, p. 1442) show that demethylation of MeB_{12} by Pt^{IV} to generate aquocobalamin (AqB_{12}) and a methyl carbanion is accelerated by Pt^{II}. Therefore, the heterolytic cleavage mechanism may be examined using platinum compounds.

Recent FTIR studies (Taraszka et. al., *Biochemistry*, submitted; Taraszka et al., *Biophys. J.*, **57**, p. 49a) have identified the Amide I (C=O) stretching mode of the corrin ring amide side chains for B_{12} compounds. The MeB_{12} amide I band decreases by as much as 30 cm^{-1} upon addition of increasing equivalents of Pt^{II}. We have identified a time window during which shifts of the amide I band are not accompanied by changes in the MeB_{12} optical spectrum, suggesting that Pt^{II} couples with the side chains to form a Pt^{II}-MeB_{12} complex. The complex exhibits a corrin ring mode at the frequency expected for MeB_{12}. However, at later times this mode shifts to reflect AqB_{12}, the presence of which is verified by the optical spectrum. Since there are no further changes in the position of the amide I band it appears that the complex is stable. The effect of the platinum-amide interaction on the axial ligand is seen by reactions of Pt^{II} with cyanocobalamin. In addition to the above amide band shifts there is a shift of the -CN stretching frequency to 2140 cm^{-1} from 2134 cm^{-1}, indicating that the Co-C bond is weakening. Other consequences of complex formation such as changes in the intensity of the corrin ring mode and shifts of a second corrin ring breathing mode may explain how heterolysis is accelerated. Studies of Pt^{II} and Pt^{IV} interactions with other cobalamins will also be reported.

This research is supported by CSRS U.S. Department of Agriculture under grant #90-37200-5357 of the Program in Human Nutrition.

M-Pos262

RADICAL REDUCTION IN MEMBRANES OF NORMAL AND SICKLE RED BLOOD CELLS ASSOCIATED WITH ANTIOXIDANTS, Yin Zhang and L. W.-M. Fung, Department of Chemistry, Loyola University of Chicago, Chicago, IL 60626

The efficiency of radical scavenging in human red blood cell membranes by intracellular antioxidants was studied by spin label electron paramagnetic resonance methods. A pseudo first order spin label reduction rate constant was determined and used as an index for the effectiveness of antioxidant system toward radicals in cell membranes. The average rate constant of normal red blood cells was 4.06 $\pm$ 1.80 x 10^{-3}/min (n=50). The activities of several major antioxidant enzymes and the concentrations of membrane-associated vitamin E in these blood cells were measured to determine the effects of individual antioxidant on the radical reduction in cell membranes. We found that the spin label reduction rates for normal cells do not correlate well with the activities of superoxide dismutase (SOD), catalase and glutathione peroxidase (GSH-Px) and the level of vitamin E. However, the addition of NADPH, which provides reducing equivalents in reactions that are critical in protecting against oxidant damage, increased the reduction rate of spin labels in membranes.

We also measured the reduction rate constants and enzyme activities in sickle red blood cells, and found that the average reduction rate and the variation in rate values from sickle patients were much higher (10.94 $\pm$ 7.54 x 10^{-3}/min, n=17) than those of normal. The activities of SOD in sickle cells are lower than those in normal cells, while the activities of GSH-Px are higher than those in normal. However, there are no significant difference in catalase activities and vitamin E concentrations between normal and sickle cells.

We propose that certain intracellular reducing component(s), not yet identified, is responsible for reducing the spin labels in membranes and is competing for substrates with SOD, catalase and GSH-Px in various redox reactions in red blood cells.

(Supported by NIH and Loyola University of Chicago)

M-Pos263

CLASSICAL RAMAN SPECTROSCOPIC STUDIES OF NADP COFACTORS BOUND TO DIHYDROFOLATE REDUCASE BY DIFFERENCE TECHNIQUES. Jie Zheng, Yong Q. Chen, Janet Grimsley, Joseph Kraut, and Robert Callender*. Physics Department(J.Z., Y.C., and R.C.), City College of New York, NY. NY 10031, and Department of Chemistry(J.G. and J.K.), University of California, San Diego, La Jolla, CA 92093.

Dihydrofolate reductase (DHFR) is an extensively studied enzyme that catalyzes the NADP-dependent reduction of dihydrofolate to tetrahydrofolate. We have used sensitive classical Raman difference spectroscopy to study the interaction between the NADP coenzymes and DHFR. The binding of the NADPH and $NADP^+$ coenzymes to DHFR causes significant changes in their Raman spectra relative to spectra obtained in the absence of enzyme. The molecular motions of the bound adenine moiety of those coenzymes produce Raman bands that are essentially identical to those found for adenine in hydrophobic solvents. This suggests that adenine binds to a very hydrophobic environment in DHFR. Pronounced changes in the Raman spectrum of the nicotinamide moiety of NADPH are observed upon binding; some of these changes are understood and will be discussed in term of specific hydrogen bonding patterns and strengths.

M-Pos264

STRUCTURAL STUDIES OF TRANSGLUTAMINASE-INHIBITOR COMPLEXES BY ^{13}C SOLID-STATE NMR.

Michèle Auger, Ann E. McDermott & Robert G. Griffin, *MIT, Cambridge MA, 02139*, Valerie Robinson, A.L. Castelhano, R. Billedeau, D.H. Pliura & Allen Krantz, *Syntex (Canada) Mississauga, Ontario, L5N 3X4.*

Transglutaminases are calcium-dependent enzymes that catalyze the exchange of primary amines for ammonia at the γ-carboxamide group of peptide-bound glutamine residues. The molecular weight of guinea pig liver transglutaminase (a monomer of M_r 76,620) is quite large by the standards of high-resolution NMR. We have used solid-state ^{13}C NMR to study the mechanism of inhibition of the enzyme transglutaminase by 3-halo-4,5-dihydroisoxazole inhibitors. These inhibitors were conceived on the assumption that they inhibit transglutaminase by attack of an enzyme active site cysteine thiol on the dihydroisoxazole ring. The tetrahedral intermediate formed could then break down with the loss of the halide group and the subsequent formation of a stable thioimine adduct. We have compared the ^{13}C CPMAS spectra of the chloro, bromo and thioethyl dihydroisoxazole inhibitors and the results indicate that the chemical shift of the C3 carbon is sensitive to the nature of the heteroatom. Subtraction of the natural abundance ^{13}C spectrum of the enzyme from that of the enzyme inhibited by C3 labelled chloro-dihydroisoxazole reveals a broad peak at 156 ppm. The chemical shift of this peak is very close to that obtained for the 3-thioethyl model compound and suggests the formation of a stable thioimine enzyme adduct. Similar results were obtained for the lyophilized enzyme and for frozen solutions of the enzyme in the absence and presence of Ca^{2+}.

M-Pos265

CRYSTAL STRUCTURE AND CONFORMATION OF 2,7-BIS-[PIPERIDINOPROPOXY]-9H-FLOUREN-9-ONE, AN ANALOG OF TILORONE.

Kanthi Dasari and T. Srikrishnan, Center for Crystallographic Research, Roswell Park Cancer Institute, Buffalo, New York 14263

Tilorone is an orally active pharmacologic agent that protects mice against infections with RNA and DNA viruses and is also the only known small molecule that is an interferon inducer. It is shown to influence the immune mechanism and has antitumor and anti-inflammatory properties. It has been postulated using energy calculations to act by an intercalating mechanism preferentially intercalating between A-T base pairs (Chen, Gresh & Pullman, Nucl. Acid Res. 16, 3061-3073 (1988)). Twenty-eight different analogs of tilorone have been synthesized by changing the substituents at the 2,7 positions of the central chromophore, fluoren-9-one and have been tested for their antiviral activity (Andrews et al., J. Med. Chem. 17, 882 (1974)). Structural studies of these analogs have been undertaken as a first step in a structure-function study of these compounds. Crystals of the title compound in the monohydrate form are triclinic, space group P1, with a = 7.068(2), b = 9.030(3), c = 23.635(3), α = 103.91(2), β = 108.49(2), γ = 93.84(4)° , V = 1371.9Å^3, Z = 2, D_o = 1.17 g/c.c, D_c = 1.168 g/c.c. The structure was solved with CAD-4 data (5702 reflections, 1873>3σ) using the SHELX-86 programs and refined to a current R value of 0.063. The propoxy is in a zig-zag conformation and coplanar with the central fluorenone chromophore. The two end piperidine rings are in the preferred chair conformation. The crystal structure is stabilized by C-H···O hydrogen bonds and stacking interactions involving the fluorenone rings. Attempts are being made to crystallize some of the other tilorone analogs as well as complexes of the title compound with dinucleotide model compounds to understand the details of the interaction of tilorone with nucleic acids. Work supported by New York State Dept. of Health, ACS-IN54W8 and in part by NIH GM24864. Thanks are due to Dr. Fiel for a gift of the sample.

M-Pos266

THE INFLUENCE OF PHYSICAL CHARACTERISTICS OF LIPOSOMES CONTAINING DOXORUBICIN ON THEIR PHARMACOLOGICAL BEHAVIOR.

D. Goren[1,2], A. Gabizon[1] and Y. Barenholz[2] (Introduced by R. Taylor)[3].
[1] Department of Oncology, Hadassah University Hospital, Jerusalem, Israel; [2] Department of Membrane Biochemistry, Hebrew University - Hadassah Medical School, Jerusalem, Israel; [3] Department of Biochemistry, University of Virginia, Charlottesville, Virginia.

We have investigated the behavior of two populations of doxorubicin (DXR)-containing phospholipid vesicles with regard to various physical and pharmacological parameters. DXR containing liposomes were prepared by ultrasonic irradiation, the lipid composition being phosphatidylglycerol (or phosphatidylserine), phosphatidylcholine and cholesterol. The vesicles were fractionated into oligolamellar vesicles (OLV) and small unilamellar vesicles (SUV) by preparative differential ultracentrifugation (150,000 gx1 h). Unentrapped DXR was removed by gel exclusion chromatography. OLV and SUV liposomes had almost identical lipid composition but differed in size (mean diameters, 247 ± 113 nm and 61 ± 16 nm, respectively) and number of lamellae (two for OLV, one for SUV). Drug entrapment per unit of lipid was three to five-fold higher in OLV than in SUV. In both liposome populations more than 95% of the entrapped drug was membrane-associated. Physical studies on these two vesicle populations revealed higher motional restriction and greater susceptibility to iodide-mediated fluorescence collisional quenching of DXR in the small vesicles. OLV showed superior stability in the presence of plasma as determined by the fraction of DXR retained by the vesicles. It was also found that the tissue distribution of DXR in SUV follows a pattern different from that of DXR in OLV and resembles that of soluble DXR. In accordance with these differences in patterns of tissue distribution, animal studies demonstrated that DXR in OLV is significantly less toxic than DXR in SUV and more effective in a tumor model with predominant involvement of the liver. These results indicate that vesicle size and/or number of lamellae play an important role in optimizing liposome-mediated delivery of DXR, and that oligolamellar liposomes are distinctively superior to small unilamellar liposomes when "fluid phase" formulations with bilayer-associated DXR are considered.

M-Pos267

A COMPARISON OF MOLECULAR ELECTROSTATIC POTENTIALS EVALUATED FROM AB INITIO AND SEMI-EMPIRICAL MOLECULAR ORBITAL WAVEFUNCTIONS.

JAMES D. PETKE, COMPUTATIONAL CHEMISTRY, UPJOHN LABORATORIES, KALAMAZOO, MI 49001

THE SELECTIVE BINDING OF A MOLECULE TO A RECEPTOR IS INFLUENCED BY A NUMBER OF FACTORS INCLUDING STERIC, HYDROPHOBIC, AND ELECTROSTATIC LIGAND-RECEPTOR INTERACTIONS. ELECTROSTATIC ASPECTS OF BOTH LIGAND-RECEPTOR COMPLEMENTARITY AND LIGAND SIMILARITY MAY BE INVESTIGATED USING THE MOLECULAR ELECTROSTATIC POTENTIAL (MEP) EVALUATED OVER VAN DER WAALS SURFACES OR AT SELECTED POINTS IN SPACE. IDEALLY, ACCURATE MEPs MAY BE OBTAINED FROM AB INITIO ELECTRONIC WAVEFUNCTIONS. HOWEVER, IN PRACTICE SUCH WAVEFUNCTIONS ARE COSTLY TO OBTAIN, AND MEPs CALCULATED FROM SEMI-EMPIRICAL WAVEFUNCTIONS OR POINT CHARGE MODELS ARE USED. THIS WORK PRESENTS A DETAILED COMPARISON OF THE MEP OBTAINED FROM MINIMUM AND EXTENDED BASIS SET AB INITIO MOLECULAR ORBITAL WAVEFUNCTIONS, AND SEMI-EMPIRICAL WAVEFUNCTIONS WITH MNDO, AM1, AND PM3 PARAMETERIZATIONS. CALCULATIONS ON SEVERAL LARGE MOLECULES SHOW GENERALLY THAT EACH OF THE SEMI-EMPIRICAL METHODS GIVES A REASONABLE QUALITATIVE REPRESENTATION OF THE AB INITIO MEP. QUANTITATIVE DIFFERENCES BETWEEN AB INITIO AND SEMI-EMPIRICAL POTENTIALS APPEAR TO VARY WITH THE CHOICE OF PARAMETER SET, THE MNDO PARAMETERIZATION PROVIDING THE MOST CONSISTENT RESULTS RELATIVE TO THOSE OF MINIMUM BASIS SET AB INITIO CALCULATIONS.

M-Pos268

INTENSITY AND ANISOTROPY DECAYS OF [LEU⁵]-ENKEPHALIN TYROSYL FLUORESCENCE BY 10 GHz FREQUENCY-DOMAIN FLUOROMETRY.

I. Gryczynski, G. Laczko, W. Wiczk and J.R. Lakowicz, University of Maryland School of Medicine, Department of Biological Chemistry and Center for Fluorescence Spectroscopy, Baltimore, Maryland 21201.

The technique of frequency-domain fluorometry has been extended to 10 GHz using the harmonic content of a picosecond laser source, a special 6μ microchannel plate photomultiplier tube with a grid before the anode and microwave electronics for cross correlation detection (Lakowicz et al., *Rev. Sci. Instrum.* 61:2331-37, 1990). This new instrument was used to resolve the complex picosecond intensity and anisotropy decays of the tyrosyl emission of [Leu⁵]-enkephalin. Enhanced resolution of the frequency-domain measured tyrosyl anisotropy decay was obtained by using different amounts of acrylamide quenching followed by global analysis. The data indicates a 44 ps correlation time for local tyrosine motions, and a 219 ps correlation time for overall rotational diffusion of the pentapeptide. Our data are consistent with initial loss of fluorescence anisotropy from r_o = 0.4 to a value of r_∞ = 0.326 (measured in propylene glycol at -60°C) occurring during the first picosecond after excitation. However, our data do not unequivically demonstrate the existence of this 1 ps component.

To test the resolution limit of our 10 GHz fluorometer, we measured intensity and anisotropy decays of NATyrA in the presence of 0.5 M acrylamide at 70°C. A short correlation time of 8 ps with 0.2 ps accuracy was measured.

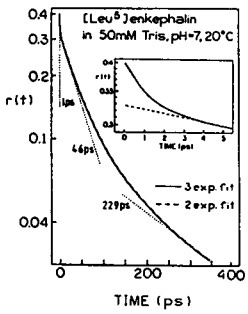

M-Pos269

OXYTOCIN AND [ARG⁸]-VASOPRESSIN TYROSINE-TO-DISULFIDE BRIDGE DISTANCE DISTRIBUTIONS RECOVERED WITH FREQUENCY-DOMAIN FLUORESCENCE ENERGY TRANSFER MEASUREMENTS.

H. Szmacinski, W. Wiczk, M.N. Fishman, P.S. Eis, J.R. Lakowicz, University of Maryland School of Medicine, Department of Biological Chemistry, Baltimore, MD 21201 and M.L. Johnson, University of Virginia, Department of Pharmacology, Charlottesville, VA 22908

Oxytocin and [Arg⁸]-vasopressin have two intrinsic chromophores in common, the phenol side chain of Tyr² and the Cys¹-Cys⁶ disulfide bridge. Their respective emission and absorption spectra indicate that the tyrosyl phenol fluorescence (donor) will be attenuated by fluorescence resonance energy transfer (FRET) to the nearby disulfide bridge (acceptor). The Asu¹'⁶-analogs, in which the disulfide bridge is substituted by CH_2-CH_2, were used as the reference donor-only compounds. Energy transfer was observed by measuring the donor frequency response in the absence and presence of acceptor with frequency-domain fluorometry. The R_o values were calculated using the absorbance spectrum of cystine, or the difference absorbance spectrum (hormone minus Asu-analog), and the emission spectrum and quantum yield of the Asu-analog. In each case the calculated R_o was about 8-9 Å.

Fitting of the frequency-domain phase and modulation data to a Gaussian distance probability function indicates that the average inter-chromophoric distance ($\bar{r}$) is similar in both compounds, $\bar{r}$ = 6.36 Å for oxytocin and $\bar{r}$ = 6.72 Å for vasopressin. However, the distance distribution of vasopressin is narrower (hw = 2.13 Å) than that of oxytocin (hw = 3.63 Å), which is consistent with restriction of the tyrosine phenol motion due to its stacking with the side chain of Phe³. Finally, the fitted distance distribution functions are compared with histograms describing the distance between the middles of the chromophores during the course of long, *in vacuo*, molecular dynamics runs using the computer program CHARMm and the QUANTA 3.0 parameters.

M-Pos270

MECHANISMS OF WATER NMR RELAXATION IN MACRO-MOLECULE SOLUTION

Chen Lin, T. F. Egan, H. E. Rorschach and C. F. Hazlewood
Baylor College of Medicine, W. M. Rice University, Houston, Texas

Among various models proposed for the mechanism of water NMR relaxation in the macro-molecule solution, two models given by Kimmich[<1>] and Rorschach[<2>] predicts the correct frequency dispersion behavior based relaxation processes associated with the motion which has wide spectrum of correlation times. In Kimmich's model, the continues diffusion of water molecule on the rugged macro-molecule surface generates correlation time $\tau_c = (D_{\|}q^2)^{-1}$ for a spatial Fourier component of the macro-molecule surface q, where $D_{\|}$ is translational diffusion constant. Rorschach's model suggested that the vibration of the macro-molecule chain with the associated water produce the long correlation time $\tau_c = (f\mu q^2)^{-1}$, where f is the chain tension and μ is chain mobility. Our experimental results on Ribonulease-A and on its unfolded state Oxidized Ribonulease-A shows a strong relation between the frequency dispersion of relaxation with the conformation of the macro-molecule. Our study on Poly-amino Acid also suggested that the dynamics of the macro-molecule has an important influence on the relaxation too. Rorschach's polymer dynamics model also predicts a frequency independent term in T_2 relaxation, we will discuss how can we take advantage of it to study the dynamics of the macro-molecule in solution.

1. G. Schauer, P. Kimmich and W. Nusser, Deuteron Field-cycling Relaxation Spectroscopy and Translational Water Diffusion in Protein Hydration Shells, Biophys. J. Vol 53 397:404 (1988)
2. H. E. Rorschach and C. F. Hazlewood, Protein Dynamics and NMR Relaxation Time T_1 of Water in Biological System, J. Mag. Res. 70:79 (1986)

M-Pos271

SOLUTION CONFORMATIONS OF PIRENZEPINE DERIVATIVES VIA MOLECULAR MECHANICS AND MOLECULAR DYNAMICS.

Leonore A. Findsen and Kari J. Seger, *College of Pharmacy, University of Toledo, Toledo, OH 43606*

The determination of accurate solution conformations of drug molecules is one of active study. In biological systems, the generated conformations of these molecules can be used to determine the structure of a receptor where there is no direct experimental data available for the macromolecule. This study compares the vacuum and solution conformations, and charge distributions of derivatives of known selective antagonists of muscarinic receptors. The two muscarinic receptor subtypes studied are the postsynaptic M1 receptor and the presynaptic M2 receptor. The two selective antagonists of these receptors are pirenzepine (M1) and AF-DX 116 (M2) shown below. To reduce some of the degrees of freedom in the compounds, additional ring systems are added to constrain the location of the carboxyl group with respect to the pyperazine ring. The different low energy conformations are determined via vacuum molecular mechanics calculations and solution molecular dynamics calculations as the saturation of the pyperazine ring is varied. The relative positions of the nitrogens in the ring system are compared as a function of saturation for each of the receptor subtypes. The charge distribution of the compounds are also compared as a function of saturation and nitrogen placement. In conjunction with the experimental activities as they become available, the theoretical conformations and charge distributions will help in the determination of which molecular properties determine activity and selectivity of these two receptor subtypes.

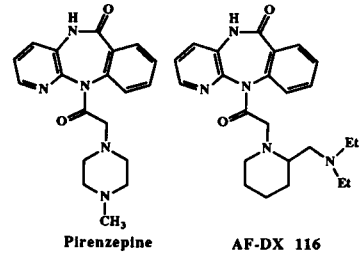

M-Pos272

THE ORIGIN OF THE MAGNETIC FIELD DEPENDENCE OF PROTON SPIN-LATTICE RELAXATION IN HETEROGENEOUS SAMPLES LIKE TISSUES.

Robert G. Bryant, C. C. Lester, D. Mendelson, C. L. Jackson. Department of Biophysics and Department of Chemistry, University of Rochester Medical Center, Rochester, New York 14642

The solvent proton spin-lattice relaxation rate in heterogeneous samples including tissue is complicated by the magnetic dipole-dipole coupling between mobile solvent spins and immobile spins of the matrix. A consequence of the relaxation coupling is that the observable relaxation rate constants are not elementary but are roots of coupled differential equations that include the responses of both the solid and liquid components and a magnetization transfer rate that connects the two populations. Though the field dependence of the solvent spin relaxation has been known for many years, the origin has not been understandable in terms of modifications of the solvent proton mobility. We have shown that he field dependence of the observed solvent proton relaxation rate in heterogeneous systems is dominated the magnetic coupling to the behavior of the solid components of the heterogeneous system. In particular for protein and tissue systems, the field dependence of the water proton relaxation is determined by the field dependence of the solid proton population which provides a direct measure of the internal fluctuation spectrum of the protein or matrix. These systems may be modelled with a magnetic field independent magnetization transfer rate constant implying rapid water-surface motions. Further, the relaxation rate of the solvent may be indirectly controlled by the addition of paramagnetic relaxation agents to the solid spin system even if the paramagnetic centers do not permit the rapid exchange of protons with first-coordination-sphere metal ion positions.

M-Pos273

VIBRATIONAL DYNAMICS OF THE *CIS*-PEPTIDE GROUP

Noemi G. Mirkin and Samuel Krimm
Biophysics Research Division, University of Michigan, Ann Arbor, MI 48109, USA

While the *trans*-peptide group predominates in the stable polypeptide chain of proteins, some non-proline *cis*-peptide groups are found.[1] Recent resonance Raman studies under conditions of high laser pulse energies[2,3] also indicate that *trans*-N-methylacetamide (NMA) can be photoisomerized to *cis*-NMA. It is therefore important to have a detailed understanding of the vibrational dynamics of the *cis*-peptide group. We have computed the *ab intio* geometry and force field at the Hartree-Fock level using a 4-31G* basis set of *cis*-NMA, for both the isolated molecule and with two H_2O molecules hydrogen-bonded to it, and have obtained its normal modes. The computed harmonic force constants of *cis*-NMA were scaled using the 10 scale factors obtained by optimizing the force field for *trans*-NMA to its matrix-isolated frequencies.[4] Good agreement with experiment required the modification of only one scale factor, that for CN stretch being changed from 0.74 to 0.84. These scale factors were then transferred unchanged to the hydrogen bonded *cis*-NMA system. The results for the isolated molecule show good agreement with experimental data and in particular the changes from *trans*-NMA[4]. For the hydrogen-bonded system the calculations confirm the assignments made in the resonance Raman studies[2,3] and also show that the normal modes as well as the frequencies are significantly affected by hydrogen bonding to the solvent. Thus, isolated molecules may not be adequate models for the normal modes of molecules that interact strongly with solvent. This research was supported by NSF grants DMB-8816756 and DMR-8806975

1. Steward, D.E.; Sarkar, A.; Wampler, J.E. J. Mol. Biol. 1990, 214, 253-260.
2. Wang, Y.; Purrello, R.; Sprio, T.G. J. Am. Chem. Soc. 1989, 111, 8274-8276.
3. Song, S.; Asher, S.A.; Krimm, S.; Shaw, K.D. J. Am. Chem. Soc., in press.
4. Mirkin, N.G.; Krimm, S. J. Mol. Struct., in press.

M-Pos274

SELF-CONSISTENT ENERGY PARAMETERS IN A SPECTROSCOPICALLY DETERMINED FORCE FIELD (SDFF) FOR MOLECULAR MECHANICS AND DYNAMICS.

K. Palmö, L-O. Pietilä, and S. Krimm, Biophysics Research Division, University of Michigan, Ann Arbor, MI 48109, USA

We have previously reported on a method by which scaled *ab initio* force fields and structures can be transformed to molecular mechanics force constants and reference geometry parameters, provided that reasonable parameters for the nonbonded interactions are known[1]. When testing this SDFF procedure on N-methylacetamide and some alanine dipeptides, a major difficulty was to find parameters of the van der Waals interactions that were reasonably consistent with the *ab initio* results. It became evident that adjustment of these parameters was needed as a complement to the original method. In this work the computational technique has been further developed, and a set of parameters for nonbonded interactions can now be adjusted towards consistency simultaneously with the calculation of the molecular mechanics valence force field and reference geometry. In order to take full advantage of the procedure, *ab initio* results for several conformations of a group of related molecules should be available. The method is being applied to a series of non-hydrogen-bonded alanine dipeptides with the purpose of constructing a complete molecular mechanics energy function capable of reproducing vibrational frequencies as well as structures. A fixed set of atomic charges is used, but the van der Waals parameters are optimized using the self-consistency criterion. Initial values for the barrier heights of the torsion potentials, and for cross terms involving torsions, are calculated from the quadratic force constants obtained in the transformation. For practical reasons, the number of force constants in the valence force field is reduced by neglecting the cross terms that do not significantly affect the vibrational frequencies. Part of the quadratic energy parameters are finally reoptimized to the original (scaled) *ab initio* data. Research supported by the Monsanto Co. and NSF grants DMB-8816756 and DMR-8806975.

1. K. Palmö, L.-O. Pietilä, and S. Krimm, J. Comp. Chem., in press.

M-Pos275

ENERGY MINIMIZED PREDICTED STRUCTURES FOR FIVE BOVINE CASEINS AND THE COILED/COIL DOMAIN OF TROPOMYOSIN G: CORRELATION WITH FTIR.

Thomas F. Kumosinski, Eleanor M. Brown and Harold M. Farrell, Jr., USDA, Eastern Regional Research Center, Philadelphia, PA 19118

To develop protein structure-function relationships in the absence of available crystallographic data, energy minimized three dimensional models were constructed for five bovine caseins, which are considered aperiodic and the fibrous coiled/coil region of tropomyosin G. Here non-globular proteins were used to minimize the effects of close-packing of multiple domains. The five caseins ($alpha_{S1}$-A, $alpha_{S1}$-B, beta-, kappa-, and $alpha_{S2}$-) contain varying amounts (5 to 17 mole percent) and distribution of proline throughout their single polypeptide chains. All initial structures were built, using the Sybyl-Mendel Molecular Modeling program, incorporating results of several sequence based prediction methods and deconvolution FTIR data. All structures were then energy minimized using a Kollman Force Field. To maximize the probability of obtaining a lowest energy state, the simulated annealing procedure was employed. All final structures showed agreement with FTIR results and with particular attention paid to the types of turns present. New FTIR assignments for several turns are in agreement with proteins of known x-ray crystal structures. The coiled/coil region of tropomysin G was constructed from two 40 residue pieces in an alpha-helix conformation. This initial structure was completely unstable with an energy of around 22,000,000 Kcal. Energy minimization and simulated annealing resulted in a non-classical screw-type helix with a stabilization energy of around -25 Kcal/residue. All structures were in global agreement with known physical chemical and biochemical information from the literature.

M-Pos276

SPIN LABEL EPR STUDIES OF MODIFIED AND OXIDIZED SPECTRIN FROM HUMAN ERYTHROCYTE MEMBRANES, Benito O. Kalaw and L. W.-M. Fung, Department of Chemistry, Loyola University of Chicago, Chicago, IL 60626

We have used spin label electron paramagnetic resonance methods to study the segmental motions of chemically perturbed spectrin-actin systems which include spectrin-actin crosslinked with glutaraldehyde or oxidized with diamide, phenyl hydrazine, or hydrogen peroxide. We found an increase in the spectral parameter W/S ratios with increasing perturbant concentration in all systems studied, indicating slight increases in the weakly immobilized motions in the perturbed systems.

SDS gel electrophoresis data indicated about 80 % of the spectrin heterodimers in the spectrin-actin complexes formed high molecular weight species in the perturbed systems.

We have also studied the isoelectric point (pI) of these systems and found a linear relationship between the W/S ratios and the pI of the modified samples.

Our results indicate charge modifications to provide slightly more mobilized, rather than immobilized, segmental motions in spectrin-actin systems when perturbed by crosslinking or oxidant molecules.

(Supported by NIH and Loyola University of Chicago.)

M-Pos277

THE BENDING OF CALMODULIN MAY BE MODULATED BY ITS TARGET PROTEIN. **Juan-Luis Pascual-Ahuir** and **Harel Weinstein**, Department of Physiology and Biophysics, Mt. Sinai School of Medicine, CUNY, New York, NY 10029.

Calmodulin (CAM) is an EF-hand calcium binding protein which activates many cellular processes through its interaction with a variety of other proteins in the cell. Each of the four EF-hand motifs in CAM contains a Ca^{2+}-binding loop flanked by an alpha-helix. In the x-ray structure, the fourth and fifth helix, and the 7 residues placed between them form a long tether helix that is extended and exposed to the solvent. However, some experiments in solution demonstrated that in presence of Ca^{2+} the radius of gyration of CAM is smaller than that of the x-ray structure. Futhermore the radius of gyration decreases more when CAM binds to its target proteins. Some models of interaction of CAM with several of its target proteins show that in order to achieve the correct interaction orientation, the tether helix is likely to be bent, suggesting that the bending of this long alpha-helix plays an important role in the activity of CAM. In a number of molecular dynamics simulations on CAM, starting from the x-ray structure under various conditions, the tether helix becomes distorted producing a bent structure. However, the nature of the bending differs as a function of the initial conditions of the run, and the time at which bending occurs varies from 80 to 500 ps into the simulation, depending on the trajectory. We have analyzed a variety of kinetic factors involved in the process of bending in the various trajectories. We hypothesize on the role that the target proteins play in the molecular rearrangement based on the nature of the structure and the bends obtained in the simulations. The process appears to be dependent on the dynamics and the structure of a network of hydrogen bonds, including those in the helical backbone, water-backbone hydrogen bonds, water-sidechain hydrogen bonds, and sidechain-backbone hydrogen bonds. The relation we find between the bending and the exposure of hydrophobic patches, that are otherwise sterically inaccessible, further supports the role of this modified structure in the function of CAM.

SUPPORT: NIH Grant GM-41373. COMPUTATIONS: Pittsburgh Supercomputer Center, Cornell National Supercomputer Facility, the Advanced Scientific Computing Laboratory of NCI at the Frederick Cancer Reserach Facility, and the University Computer Center of CUNY.

M-Pos278

INDUCTION OF PROTEIN AGGREGATION IN NEPHROMIMETIC SOLUTIONS

Elizabeth A. Myatt and Fred J. Stevens
Argonne National Laboratory
Argonne, IL 60439-4833

Bence Jones proteins are immunoglobulin light chains which form covalent and/or noncovalent dimers. Their copious production by monoclonal plasma cells during multiple myeloma can result in their excretion by the kidneys in mg/ml concentrations. The milieu of the renal tubule differs substantially from the isotonic neutral conditions of plasma. In the renal tubule, urea and sodium chloride concentrations can readily reach an osmolarity of 0.6 each, and the pH can vary from 7 to 4. We have shown by small-zone size-exclusion chromatography that these solution conditions profoundly affect the self-association of Bence Jones proteins by promoting dimerization and, in some cases, higher order aggregation. At physiologically relevant protein concentrations, some of these proteins exhibit a continuum of aggregates having molecular weights which range from 45,000 (i.e., dimer) to in excess of 300,000. A few form polymers of well-defined molecular weights, while others do not aggregate under any of the solution conditions tested. When aggregation beyond the dimer stage occurs, it is concentration-dependent and reversible. In most cases, little or no polymerization tendency is observed in standard phosphate buffered saline solutions. To a significant degree, chromatographic conditions that mimic the physiological conditions of the nephron favor the formation of high molecular weight oligomers. The occurrence of oligomer formation correlates well with the ability of the protein to form pathologically significant tubular deposits in the nephron of the myeloma patient.
This work is supported by the U.S. Department of Energy, Office of Health and Environmental Research, under Contract No. W-31109-ENG-38.

M-Pos279

HELICAL STRUCTURE OF PAP PILI

Minfang Gong, Esther Bullitt and Lee Makowski
Department of Physics, Boston University
Boston, MA 02215

We report here the results of X-ray fiber diffraction experiments and electron microscopy of the Pap pili.

Pap pili are filamentous surface appendages of E. coli about 75Å in diameter and 1 μm in length. Expression of these adhesion pili causes E. coli to infect the human urinary tract. Pap pili are composed of a major structural protein and several minor proteins. The major protein, PapA, is a 15,700 dalton protein composed of 163 amino acids synthesized with a 22-amino acid signal peptide. The bulk of the Pap pili is made up of a helical arrangement of PapA. The helical symmetry of the structure was determined by indexing the X-ray diffraction pattern from magnetically oriented Pap pili fibers. Analysis of equatorial X-ray data determined the radial density distribution of protein in the pili. This result was confirmed using scanning transmission electron microscopy. Electron micrographs of negatively stained pili will be used to calculate a three dimensional reconstruction of their structure. This will be used in coordination with X-ray data to obtain a structural image to the highest possible resolution. The possible implications of these results are discussed.

M-Pos280

HYDROGEN ION BINDING BY TMV, HELICAL PROTEIN AND STACKED DISK PROTEIN.

Ragaa A. Shalaby[1] and D.L.D. Caspar[2], [1]Point Park College, Pittsburgh, PA 15222; [2]Rosenstiel Basic Medical Sciences Research Center, Brandeis University, Waltham, MA 02254.

Hydrogen ion titration experiments were performed on TMV, TMV helical protein and stacked disk protein in KCl solution at 20°C, at different ionic strengths. Hydrogen ion binding was followed as a function of pH between pH 3.7 and pH 9, pH 4.0 was arbitrary, taken to represent zero hydrogen ion binding. Comparing the difference in the binding pattern between μ=0.10 and μ=0.01, we observe that, for all three species, a maximum difference occurs around pH 6 and is about 1.5, 1 and 1.5 H+/m more at μ=0.1 than at μ=0.01 for TMV, helical protein and stacked disk protein, respectively. When we take the difference of H+ ion binding between TMV and helical protein at the same ionic strength, we observe a maximum of 2 more H+ ions bound per protein monomer in the helix than in TMV at μ=0.20 and a difference of one H+/m at μ=0.10. A maximum excess of 1.5 H+/m is bound to the stacked disk as compared to TMV at μ=0.20. This difference drops down to one H+/m when μ=0.10. Comparing the binding by helical protein to that by stacked disk protein, we observe that below pH 7, stacked disks bind more than helical protein. Above pH 7, the pattern is reversed and helical protein binds more than stacked disk protein.

These data indicate that alteration in electrostatic interactions due to changes in the ionic environment may lead to large shifts in the pK of the H+ ion binding groups in the virus or protein particle. Competitive binding of K+ and H+ to the same sites on the protein may also contribute to the effects seen. Also, the presence of the RNA in TMV, and the disorder in the structure of the inner loop in the disk would have observable effects on the binding pattern.

M-Pos281

THE PERMEABILITY OF BACTERIOPHAGE CAPSIDS.

Gary A. Griess, Saeed A. Khan, and Philip Serwer, Department of Biochemistry, The University of Texas Health Science Center at San Antonio, TX 78284-7760.

Knowledge of the permeability of bacteriophage capsids is needed for analysis of mechanisms of capsid assembly, capsid transformations and DNA packaging [references are in Griess, G.A., Khan, S.A., and Serwer, P. (1990) Biopolymers, in press]. Although permeability variants of the capsid of bacteriophage T7 have been isolated by use of buoyant density centrifugation [Serwer, P. (1980) J. Mol. Biol. 138, 65-91), quantitative analysis of the permeability of bacteriophage capsids has not yet been made. In the present study, the permeability of wild-type bacteriophage T4 (T4wt) and a T4 osmotic-shock resistant mutant (T40s41) have been compared by use of a DNA-specific probe, ethidium, and a protein-specific probe, bis-ANS, the latter found here to bind (binding was measured by fluorescence enhancement) only to sites interior to the outer surface of the DNA-enclosing outer shell of the T4 capsid. T4wt was found impermeable to both bis-ANS and ethidium at 25°C. However, raising temperature to 50-55°C made T4wt permeable to both probes, without inactivation of T4wt. In contrast, T40s41 was permeable to both probes at 25°C. The binding of both probes was first order (rate constant = k*). The value of k* for T40s41 was a function of the type and concentration of anion present in the 10-100 μM range, in the presence of 500 mM chloride ion. The following ions decreased k* (in order of decreasing effectiveness): ATP, phosphate, sulfur, acetate. Fluoride, iodide and glutamate were ineffective. Release of DNA from T4 increased equilibrium binding of bis-ANS and raised k* to a value too high to measure. Bacteriophage T7 also bound bis-ANS at a rate that was measurable before expulsion of DNA, but too high to measure after expulsion. Analysis by SDS polyacrylamide gel electrophoresis revealed that incubation of T7 with bis-ANS caused selective loss of internal proteins.
Supported by NIH (GM24365) and the Robert A. Welch Foundation (AQ-764).

M-Pos282

NUCLEATION OF VIRUS CRYSTALS STUDIED BY ELECTRON MICROSCOPY* S. D. Durbin† and G. Feher††, †Dept. of Physics and Astronomy, Carleton College, Northfield, MN 55057 and ††Physics Dept., Univ. of California, San Diego, La Jolla, CA 92093.

The formation of crystalline nuclei is the first step in protein crystallization. The nucleation process has been studied by quasielastic light scattering, but this method is indirect and requires a model-dependent analysis of the spectral distribution of the scattered light.[1] We have studied nucleation using the method of freeze-etch electron microscopy[2] to observe directly the distribution of dimers, trimers, ...n-mers in solutions of tomato bushy stunt virus[3] (see Figure). From the distribution of aggregates of various sizes, we calculated association constants for the particular solution. We examined conditions that led to crystallization, to amorphous precipitation, and to no changes in the solution. As the supersaturation of the solution was raised toward the value typically used for crystallization, there was a rapid increase in the number of larger aggregates. Under conditions favorable for crystallization, the association constant tended to increase with the size of the aggregate, though no particular aggregate appeared to be unusually stable. We also observed the shapes of the aggregates, i.e. whether they tended to be compact and well ordered (heading towards crystals) or extended and poorly ordered (heading towards amorphous precipitate). One interesting observation was that even under the usual crystallization conditions, many large aggregates were poorly ordered, reflecting the statistical difficulty in forming a crystalline nucleus.

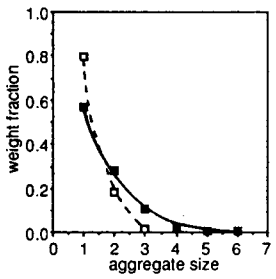

Size distributions of aggregates under conditions leading to crystallization (full line) and no changes (dashed line).

[1]See, e.g.: G. Feher and Z. Kam (1985) in Methods in Enzymology, Vol. 114, Eds. C.H.W. Hirs et al, pp.77-112.
[2]S.D. Durbin and G. Feher (1990) J. Mol. Biol. 212, 763.
[3]We thank S.C. Harrison for supplying the virus.

*Work supported by NIH.

M-Pos283

TRANSFECTION OF E. COLI BY Pf1 VIRAL RF-DNA PRODUCES Epf1, A VIRUS WITH A STRUCTURE LIKE Pf1 THAT INFECTS P. AERUGINOSA. L. G. Kostrikis[1,2], S. A. Reisberg[1], and L. A. Day[1]. [1]The Public Health Research Institute, 455 First Avenue, New York, N.Y. 10016, and [2]Chemistry Department, New York University, New York, N.Y. 10003

Pf1 is a filamentous single-stranded circular DNA virus with a unique structure that infects *Pseudomonas aeruginosa, strain K.* It is the only filamentous virus with a stoichiometry of one nucleotide per protein subunit, and its DNA structure is the most extended known, with proposed DNA models calling for phosphates at the center. Although Pf1 cannot directly infect *E. coli* MM294 or *E. coli* JM109, these strains have been transfected with the double-stranded form of Pf1 DNA (RF DNA) so that they export low levels of virus. The transfected *E. coli* create plaques on lawns of *P. aeruginosa* by exporting the virus, and both transfected and untransfected *E. coli* survive within the plaques, but outside the plaques the untransfected *E. coli* are killed. The double-stranded form of the 7.4 kb viral DNA isolated from the transfected *E. coli* is methylated, whereas that from the normal host is not. The amount of viral coat protein in the transfected cells is approximately 1/10 the amount in the normally infected host.

Some of the exported virus, named Epf1, has the buoyant density (1.285 g cm^{-3}), the length (20,000 Å), and the mass-per-length of Pf1. Further, by monitoring changes in virion length for both Epf1 and Pf1 induced by a temperature change, we have observed behavior that is predicted from a known transition in Pf1 virion symmetry. The structure features shared by Pf1 and Epf1 indicate that *E. coli* assembles Epf1 with the DNA structure and the coat protein symmetry of Pf1. Thus, the specific information required for assembling the unusual Pf1/Epf1 structure is carried in the viral genome, with the many host functions required for assembly and export being available in *E. coli* as well as *P. aeruginosa.* The ability of *E. coli* to provide such functions for this virus was unexpected because of differences both in the export systems of the two bacteria and in structural symmetries of their viruses.

The electron microscopy to be presented was done in collaboration with M. Simon and J. S. Wall of the Brookhaven National Laboratory, Upton, New York 11973

M-Pos284

Quasielastic and Total Intensity Light Scattering Studies of the Hydrodynamic Properties of Cartilage Proteoglycan

David Zangrando, Alex M. Jamieson, John Blackwell
Department of Macromolecular Science
Case Western Reserve University
Cleveland, Ohio

ABSTRACT

Dynamic and static laser light scattering methods were employed in conjunction with viscosity measurements to determine the Mandelkern-Flory-Scheraga (MFS) parameter [1] , B , for bovine nasal septum (BNS) proteoglycan subunit (PGS) in 4M GdHCL and in 0.15M NaCl. By way of comparison, the MFS parameter was also determined for the proteoglycan aggregate (PGA) by similar methods in 0.15M NaCl solution.

The ratio of the hydrodynamic radii obtained from the intrinsic viscosity (Rhn) and the translational diffusion coefficient (Rhf) , p2= Rhn/Rhf, was determined , as well as the radius ratio p1=Rgz/Rhf, where Rg is the z-average radius of gyration obtained from static light scattering, and Rhf is the reciprocal z-average Stokes radius, <1/Rhf>z.

For branched-chain molecules, p1 and p2 are known to depend numerically on branch frequency, branch type, and molecular polydispersity. Even after correction for polydispersity, our experimental results for both PGA and PGS give B and p2 values significantly below the hard-sphere limit of conventional hydrodynamic theory.

A review of proteoglycan literature was performed in order to determine if such hydrodynamic behavior had been previousely observed and if any explanation had been proposed. In addition, a review of the experimental hydrodynamic properties of synthetic star-branched polymers was carried out for further comparison with our results.

Lastly, recent theories developed to explain the effects of branching on hydrodynamic behavior are discussed as well as Monte Carlo simulations. Each approch appears to better approximate the spatial and relaxational characteristics of the synthetically produced or computer-generated branched structures than the older and often used Kirkwood-Riseman (KR) theory. These more recent theories have found values for B and P1 and P2 below the lower limits set by the KR model. This may indicated that our results are not inconsistant with recent hydrodynamic modeling.

M-Pos286

A CATASTROPHE THEORY MODEL OF CORNEAL STROMAL SWELLING. L. Stephen Kwok. *Lions Eye Research Laboratories, Dept. Ophthalmology, LSU Medical Center School of Medicine, New Orleans, LA.*

The corneal stroma shows a biphasic timecourse of swelling in 0.174 M NaCl. A discontinuity is frequently found when hydration reaches the region of 10-14 kg H_2O/kg dry wgt in predried and fresh corneal specimens. This biphasicity can be interpreted in terms of an elementary cusp catastrophe proposed by Thom, with log t and log Q as control parameters, and $\sqrt{H}$ as the state variable. (Where t = time, Q = stromal charge, and H = hydration.) Corneal swelling is modelled as an example of a space equivalent unfolding of a Riemann-Hugoniot type cusp with a moving transition plane. A thermodynamic potential with two attractor regions, each with a local minimum, governs corneal stromal swelling. Transitions to the second phase followed a "saturation convention", whereby the second minimum is preferred upon availability. It is proposed that the transition plane coincides with the uncoupling of interfibrillary linkages or "springs" in the corneal stroma, associated with a critical stromal charge $\approx 1 \times 10^{-7}$ mole e^- for a hydration ≈ 10 kg H_2O/kg dry wgt. It appears that long-range interactions within the interfibrillary matrix, due to the presence and behaviour of the stromal proteoglycans, are capable of structural effects.

(Supported in part by USPHS Grants EY03311 to S.D. Klyce, and EY02377 from the National Eye Institute.)

M-Pos285

"POLYELECTROLYTE PROPERTIES OF PROTEOGLYCANS"

Wayne F. Reed, Xiao Li, Snehasish Ghosh, Christopher E. Reed, Martha Burt, and Robert M. Peitzsch, Physics Department, Tulane University, New Orleans, Louisiana 70118

Static and dynamic light scattering results are presented for glycosaminoglycans (GAGs) of different size and structure; short chains (Heparin and Chondroitin Sulfate), long chains (hyaluronate) and branched structures (proteoglycan monomers). The static data are interpreted in terms of apparent persistence lengths, and their scaling laws, corrections due to excluded volume, and second virial coefficient theories. Comparisons are also made with Monte Carlo simulation results. The existence and behavior of scattering peaks in the visible light range for proteoglycans at low ionic strength is discussed from the points of view of local ordering and the correlation hole. Diffusion coefficients are related to the linearized coupled hydrodynamic mode theory and compared to non-free draining and free draining hydrodyanmic models in the zero polymer concentration limit. The notion of the 'extraordinary' hydrodynamic phase is discussed. Finally, the results concerning complexes of GAGs with polycations (e.g. Heparin-histamine and hyaluronate-Polylysine) and the stability and characteristics of such structures are presented. Supported by National Science Foundation Grant No. DMB-8803760

M-Pos287

CONFORMATION AND DYNAMICS OF LEWIS BLOOD GROUP OLIGOSACCHARIDES BY NOESY SIMULATION AND TRAJECTORY CALCULATION.

Perseveranda Cagas, Chaitali Mukhopadhyay and C. Allen Bush.
Dept. of Chemistry and Biochemistry, University of Maryland, Baltimore County, Baltimore MD 21228 U.S.A.

Complete ^{1}H NMR assignments for the Lewis oligosaccharides Lacto-N-fucopentaose 1 (LNF-1), Lacto-N-fucopentaose 2 (LNF-2), Lacto-N-difucopentaose 1 (LND-1) and a blood group A type 1 pentasaccharide have been made using standard 2-dimensional correlation techniques. To study the 3-dimensional structures of these oligosaccharides, nuclear Overhauser data (2D-NOESY) for carbon-bound and acetamido protons were obtained in $D_2O(H_2O)$ and in DMSO-$D_2O(H_2O)$. Using a full spin analysis, 2D-NOESY peaks were simulated as a function of the internal coordinates of model oligosaccharides and compared with observed NOE's. Results of the NOESY simulations indicate a narrow range of conformations in which NOE's agree with experiment. Molecular dynamics simulations of di-, tri- and tetrasaccharide fragments were performed. The trajectory calculations of various glycosidic dihedral angles show that while the disaccharide unit can have significant torsional transitions about the glycosidic linkage, such transitions are less frequent in tri- and tetrasaccharides and are usually within the range of 10 degrees. The range of glycosidic angles obtained from these dynamics simulations agree well with those obtained from NOESY experiments.

Research supported by NIH Grant GM-31449.

M-Pos288

CORRELATION OF MOLECULAR MODELLING WITH 1 AND 2D NMR OF A ß-(1,3);(1,6) MACROCYCLIC GLUCAN ASSOCIATED WITH *BRADYRHIZOBIUM JAPONICUM* USDA 110.

P.L. Irwin, P.E. Pfeffer, T.F. Kumosinski and D.B. Rolin
Eastern Regional Research Center, ARS, Philadelphia, PA 19118

Considerable evidence suggests that some oligosaccharides are crucial to the successful colonization of legume roots by nitrogen fixing bacteria. We have isolated a 14 membered ring ß-glucan containing a repeating unit of 3 consecutively linked ß-(1,3) and 4 consecutively linked ß-(1,6) glucose units. In addition each sequence of ß-(1,3) linked glucose units contained a single, non-reducing, unsubstituted glucose linked at the C-6 position as well as a phosphocholine group attached primarily to one of the two unsubstituted C-6 positions of the ß-(1,3) linked residues. An energy minimized 3D structure was built using a Kollman Force field within the Tripos Sybyl Mendel molecular modeling program. The final *in vacuo* structure contains a hydrophobic as well as a hydrophilic exterior surface and a hydrophilic 18 Å cavity. A hydrated structure was built with 104 H_2O molecules added to the internal cavity. The resulting energy minimized complex yielded a stabilizing energy of 140Kcal due to the presence of water. Proton NMR studies of this molecule in $DMSO_{d6}$ demonstrated that certain OHs have a different chemical shift (5.00 ppm) than H_2O (3.3 ppm). 2D NOESY (chemical exchange) measurements demonstrated that exchange between these sites was relatively slow (16 sec^{-1}). Molecular models indicate that stacking of alternate hydrophilic and hydrophobic faces of the cycles in addition to intermolecular ion pairing between phosphocholine groups can result in the formation of cylindrical assemblies capable of binding water. Such structures may be responsible for controlling water activity within nodule encapsulated nitrogen fixing bacteroids as well as in the free living bacteria.

M-Pos289

A MOLECULE OF N-ACETYL GLUCOSAMINE IS N-LINKED TO THE α-SUBUNIT OF THE Na-PUMP. Carlos H. Pedemonte and Jack H. Kaplan. Dept. of Physiology, University of Pennsylvania, Philadelphia, PA 19104.

We have recently demonstrated that the Na-pump α-subunit has N-linked carbohydrates attached in the cytosolic side of the cell membrane (Pedemonte C. H., Sachs G. and Kaplan J. H., Proc. Natl. Acad. Sci., USA, in press). The conclusion that the oligosaccharides are bound to asparagine residues of the α-subunit polypeptide was based in the observation that the protein-carbohydrate linkage is hydrolyzed by peptide-N-glycosidase F (an enzyme specific for N-linked sugars) and not by alkaline hydrolysis (more sensitive for O-linked oligosaccharides). The orientation of the α-subunit glycans with respect to the membrane was studied by using right-side-out vesicles prepared from kidney outer medulla. The acceptor sites on the α-subunit were available for galactosylation by bovine milk galactosyltransferase only after permeabilization of the vesicles with saponin. The higher galactosylation is due to the opening of the vesicles and not to a direct effect of saponin on the Na-pump protein. This was demonstrated by using SDS or other physical methods (French press and sonication) to permeabilize the vesicles instead of saponin. These experiments confirm our previous conclusion that the sugar moieties bound to the α-subunit of the Na-pump are cytosolic oriented. The oligosaccharides released from the α-subunit of the Na-pump by treatment with peptide N-glycosidase F (PNGase) were separated by gel filtration in a P-2 column. The elution volume correlates with that of a standard prepared by attaching [^{14}C]-Gal to N-acetyl glucosamine by using UDP-[^{14}C]-Gal and galactosyltransferase. In a different experiment, the radioactive oligosaccharides cleaved by PNGase and separated from the protein in a Sephadex G-50 column were acetylated and separated by thin layer chromatography (TLC). The Rf of the [^{3}H]-Gal labeled sample coincided with those of the [^{14}C]-Gal-GlcNAc standard and also with a nonradioactive standard Gal-GlcNAc (from Sigma). Therefore, these experiments suggest that the PNGase-sensitive carbohydrate component of the Na-pump α-subunit is a single GlcNAc molecule.

M-Pos290

PREDICTED 3D STRUCTURES AND DYNAMICS OF CYCLIC ß-(1,2) GLUCANS.

P.E. Pfeffer[1], T.F. Kumosinski[1], P.L. Irwin[1], D. B. Rolin[1], K. J. Miller[2], R. Zauhar[3], and A. Benesi[4].
[1] Eastern Regional Research Center, Philadelphia, PA 19118 and [2]Dept. of Food Science and [3]Biotechnology Institute, and [4]Dept. of Chemistry, Pennsylvania State University, University Park, PA 16802.

The ß-(1,2) cyclic glucans are produced by a number of species of fast growing *Rhizobium* and *Agrobacterium* as mixtures with ring sizes ranging from 17-33 members (major forms 18-24) [1]. Although their role has not been firmly established, some evidence suggests that they may effect osmotic regulation in these bacteria [2]. Recent studies have shown these glucans to be excellent candidates as hosts for large guest molecules such as drugs and vitamins [3]. ^{13}C NMR solution studies of uncomplexed (1,2) cyclic glucans have demonstrated that the molecules have rapidly averaged dynamic structures with no discernable conformational preferences. However, in the presence of guest molecules the cyclic structures may assume more rigid domains. Three dimensional molecular models, [ring sizes 18-24], of the cyclic ß-(1,2) glucans were constructed using the Tripos Sybyl-Mendel modeling system assuming a trisaccharide as a repeating unit with a set of 3 different Φ and Ψ dihedral angle pairs. These structures were energy minimized using a Kollman Force Field with electrostatics. All atom partial charges were calculated using the Gasteiger method. The above methodology was tested for (1,4) cyclic glucans (both α and ß) which yielded energy minimized structures in agreement with those derived from X-ray crystallography. All structures revealed a hydrophobic interior and a hydrophilic exterior. Molecular dynamics calculations as well as ^{13}C NMR measurements of (1,2) cyclic glucans were obtained for apo and drug encapsulated forms to determine if binding imposed induced conformational rigidity. These dynamic structures were then contrasted with comparable guest bound and free a and ß (1,4) cyclodextrins.

[1] Benincasa, M., G.P. Cartoni, F. Coccioli, R. Rizzo, and L.P.T.M. Zevenhuizen 1987 J. of Chromatography 393, 263-271.
[2] Miller, K.J., J.E.P. Kennedy, and V.N. Rheinhold 1986 Science 231, 8-51.
[3] Koizumi, K., Y. Okada, S. Horiyama, T. Utamura, T. Higashiura and M. Keda 1984 J. of Inclusion Phenomena 2, 891-899.

M-Pos291

STABILITY, STRUCTURE AND CATALYTIC ACTIVITY OF THE METAL CHELATES OF POLYMERIC AMINOSUGARS. K.S. Rajan, S. Mainer and F.C.G. Hoskin, IIT Research Institute, Chicago, IL., and John Walker and John Halliday, U.S. Army Natick RD&E Center, Natick, MA (Intro. by C. Narasimhan).

The formation and thermodynamic stability of Cu(II)-chelates of glucosamine and its dimeric, trimeric and tetrameric oligomers in the presence of N,N,N',N'-tetramethylethylenediamine (TMEN) were investigated in aqueous media at μ = 1.0 (KNO_3) and 25 C. The stability constants which were determined for the 1:1 and 1:2 chelates of Cu(II) with glucosamine, chitobiose, chitotriose and chitotetrose were respectively: β_2 = 9.88,9.61, 10.50, 6.84 and 8.24 and β_2 = 17.96, 17.53, 17.15, 10.83 and 11.91. Results of electronic absorption, CD and ESR spectral studies combined with an equilibrium analysis indicated bidentate coordination of Cu(II) involving the amino- and hydroxyl groups of the oligomers. Further, the charge transfer and the d-d transition bands of the ternary complexes involving the oligomers and TMEN exhibited both wavelength shifts and inversion of configuration when compared to the binary complexes. The catalytic activity of the chelates for the decomposition of toxic organophosphorus compounds has been investigated and the results are discussed in terms of a possible mechanism.

M-Pos292

CALCULATION OF THE SURFACE ENERGY FOR HEXAGONAL AND LAMELLAR STRUCTURES FOR A LIPID MEMBRANE.

Dr.IRINA VAYL

The goal of this work is to evaluate the change in surface energy due to structural transition in lipid membrane between lamellar and hexagonal phases. The potential surface energy is determined using graphs representa tion in the pairwise approximation. Each graph corresponds to some interaction between two molecules and for homogeneous one-component plane surface depends on intermolecular distance. The potential function for pair molecules is discribed by LJ and Coulomb potentials. The formulas for calculation of the number of identical graphs have been derived for both structures. The density of surface energy have been calculated for the hexagonal and lamellar structures of DPPC membrane.

M-Pos293

MEAN FIELD STOCHASTIC BOUNDARY MOLECULAR DYNAMICS SIMULATION OF PHOSPHOLIPIDS IN A MEMBRANE

Hans De Loof[1], Richard W. Pastor[3], Jere P. Segrest[1,2], and Stephen C. Harvey[1]; Departments of [1]Biochemistry and [2]Medicine, University of Alabama at Birmingham, Birmingham, AL 35294; and [3]Biophysics Laboratory, Center for Biologics Evaluation and Research, Food and Drug Administration, 8800 Rockville Pike, Bethesda, MD 20892.

We have extended the single chain mean field simulations of Pastor *et al.* (*J. Phys. Chem. 89*, 1112 [1988]) to a complete two chain molecule, dipalmitoylphosphotidyl choline (DPPC). The potential energy function for the molecular dynamics (MD) simulation is similar to the standard AMBER force field, with the following modifications: the term for torsional rotations about covalent bonds is a Ryckaert-Bellemans potential (a power series in cos ϕ); to represent the packing effects of neighboring molecules, we have added both a Marcelja mean field (with the energy inversely proportional to the distance between the terminal carbon of the chain and a plane representing the lipid/water interface) and a Maier-Saupe potential (with a negative dispersion energy proportional to the sum of the order parameters along the chain). The force constants in these last two terms were adjusted until a very long MD simulation (102 ns) converges to give values for the order parameters and spin-lattice relaxation times that are close to those from experiment.

We then examined a hexagonally close-packed array of seven DPPC molecules, using a hybrid simulation method, with normal molecular dynamics at the center and Langevin dynamics (a stochastic boundary) with reduced mean field and dispersion potentials at the edges of the system. Optimum parameters give nearly identical behavior to all molecules, whether at the center or in the boundary layer, with convergence again approaching experimental results.

A wide range of interesting motions is observed. Our results indicate the need for long simulations with carefully chosen parameters, if one hopes to obtaine meaningful information on model membrane systems using molecular dynamics or similar approaches.

M-Pos294

Patterson Analysis and Gaussian Modeling in the Interpretation of Difference Electron Density Profiles

Howard S. Young, Victor Skita, and Leo G. Herbette. Biomolecular Structure Analysis Center, Univ. of Conn. Health Center, Farmington, CT 06032

The time-averaged location of Class III antiarrhythmic and 1,4-dihydropyridine calcium channel (DHP) drugs within bovine heart phosphatidylcholine lipid bilayers was determined by small angle x-ray diffraction. Patterson analysis of resultant intensity functions allowed identification of autocorrelations indicating the drug location within the bilayer. Gaussian modeling of experimental electron density profiles confirmed the correct interpretation of the difference electron density profiles. The combined analyses allowed calculation of the appropriate difference electron density profile in the absence of an absolute scale. The Class III drugs bretylium and clofilium were found to occupy locations 19Å and 13Å, respectively, from the hydrocarbon core center of the membrane bilayer, while the DHP nimodipine was located at 16Å from the bilayer center. These methods are being applied to investigations of local anesthetic interactions with the acetylcholine receptor membrane in order to establish a structural basis for Hille's (1977) theory of anesthesia that involves both the lipid bilayer and protein components of a biological membrane. (Supported by the Department of Higher Education High Technology Program and Miles Pharmaceuticals, West Haven, CT)

M-Pos295

MOLECULAR MODELS FOR CHOLESTEROL-INDUCED FLUID-PHASE IMMISCIBILITY IN MEMBRANES.

M. B. Sankaram and T. E. Thompson, Department of Biochemistry, University of Virginia Health Sciences Center, Charlottesville, VA 22908.

Cholesterol is known to induce the formation of immiscible fluid phases in lipid bilayers. With increasing concentration of cholesterol in phosphatidylcholine-cholesterol mixtures at temperatures above the main transition of the pure phospholipid, a transition from an acyl-chain disordered fluid phase (ℓ_d phase) to a relatively more ordered fluid phase (ℓ_o phase) takes place via an intervening ℓ_d-ℓ_o mixed phase region. To determine the location of cholesterol in the lipid bilayer, we measured the effect of 50 mol% cholesterol on the isotropic chemical shifts of the carbonyl carbons of the phospholipid molecule using magic-angle spinning NMR methods. The results of this study suggest that cholesterol is anchored in the lipid bilayer by a hydrogen bond between its 3-ß hydroxyl and the sn-2 carbonyl of the phospholipid. We also studied the effect of a spin-labelled phospholipid on the spin-lattice relaxation rates of the phospholipid and cholesteryl carbons in the ℓ_d and the ℓ_o phases using magic-angle spinning NMR methods. These results taken together with our previous considerations of hydrophobic mismatch indicate that the cholesterol-induced fluid phase immiscibility is a result of an isothermal structural transition at the molecular level. This transition involves a conversion from the ℓ_d phase where cholesterol spans the entire bilayer to a structure for the ℓ_o phase where each monolayer contains the steroid molecules.

Supported by NIH grant, GM-14628.

M-Pos296

THE USE OF BROMINATED LIPIDS AS STRUCTURAL ISOMORPHS IN MEMBRANE X-RAY DIFFRACTION. Michael C. Wiener and Stephen H. White. *Department of Physiology and Biophysics, University of California, Irvine, CA 92717.*

Typical bilayer x-ray diffraction experiments yield Fourier density profiles that are on relative scales. The determination of an absolute scale profile increases the information obtainable from bilayer diffraction. In our development of quasi-molecular modeling methods and the joint refinement of neutron and x-ray diffraction data (Wiener and White, *Biophysical Journal*, in press), the determination of absolute scale structure factors is essential. Inspired by the earlier work of Franks (*Nature*, 276, p.530-532, 1978) on the use of halogenated cholesterol for absolute scaling, we investigated the use of halogenated lipids in a similar role. We synthesized the bromolipid 1-oleoyl, *2-9,10*-dibromostearic PC (OBPC) and investigated its use as a structural isomorph in dioleoyl PC (DOPC) bilayers. X-ray diffraction experiments on a series of DOPC-OBPC mixtures reveal that OBPC is a superb isomorph for DOPC. The profiles of 0-100 mol% OBPC-DOPC mixtures are virtually identical except for a well-defined bromine distribution which is very similar to the double bond distribution of DOPC. Moreover, the phases of DOPC structure factors obtained from these experiments agree with those obtained from conventional swelling experiments. We conclude that halogenated membrane components hold considerable promise in bilayer x-ray diffraction and will be suitable for many of the applications of specific deuteration in neutron diffraction. These include: (1) obtaining the absolute scale of x-ray diffraction experiments, (2) phasing structure factors, and (3) determining accurately the distributions of specific regions of the bilayer. (Supported by NIH grant GM37291 and NSF grant DMB880743).

M-Pos297

MEYER-OVERTON--FROM OIL TO ENTROPY: THE ENERGETIC BASIS OF ANESTHETIC ACTION IN MEMBRANES.

Nathan Janes,* Jack W. Hsu, Emanuel Rubin, and Theodore F. Taraschi, Thomas Jefferson University, Department of Pathology and Cell Biology, 1020 Locust St., Philadelphia, PA 19107

"Narcosis commences when any chemically indifferent substance has attained a certain concentration in the lipoids of the cell" as determined by oil solubility. (H.H. Meyer, 1901).

This statement implies that anesthesia is a colligative property of solutes in membranes. Colligative thermodynamics implicates two factors of primary importance for anesthetic potency. We propose that the anesthetic locus involves (1) a low enthalpy event which coincides with (2) large changes in configurational entropy or solute partitioning. Our model predicts that the absolute concentration of solute in the membrane is not the decisive factor, as Meyer predicted. Rather of crucial importance are changes in partitioning (or solute concentration) in the locus microenvironment, which entropically drive the interchange between the putative conscious and unconscious conformers.

Experimental support for these criteria is obtained from equilibria in model membranes. The influence of the solute n-hexanol on the low enthalpy ($\Delta H = 0.83$ kcal) gel ($L_{\beta'}$) to ripple ($P_{\beta'}$) equilibrium (pretransition), and the high enthalpy ($\Delta H = 5.03$ kcal) $P_{\beta'}$ to liquid-crystalline L_α main transition of dimyristoyl lecithin (DML) was examined. Hexanol partition coefficients, obtained using a dual radiolabel centrifugal method, indicated substantial changes in solute partitioning for both equilibria. A dramatic stabilization (depression of the pretransition temperature) of the ripple phase was observed at general anesthetic concentrations (3-5 mole% intramembrane). Agreement with theory was excellent. For instance, an increase in partitioning of 22.2 molal units occurred for $L_{\beta'} \rightarrow P_{\beta'}$, corresponding to intramembrane hexanol concentrations of 3.7% in $P_{\beta'}$, and a $7.1 \pm 1.0^{\circ}C$ stabilization was observed (theory $6.6^{\circ}C$). In contrast, the relatively high enthalpy $P_{\beta'} \rightarrow L_\alpha$ equilibrium was, as predicted, much less sensitive to the alcohol, since increased solute partitioning in L_α did not dominate the relative enthalpy increase (at 8.3%, $0.9 \pm 0.6^{\circ}C$ observed, $1.6^{\circ}C$ theory). Similar results are obtained for the low enthalpy equilibrium between the L_α and hexagonal (H_{II}) phases of dioleoyl phosphatidylethanolamine in the presence of hexanol. Supported by PHS AA07215, AA07463, AA07186, AA00088.

M-Pos298

VIDEO ENHANCED MICROSCOPIC STUDIES OF THE MELTING AND FORMATION OF TUBULES FROM A DIACETYLENIC PHOSPHOLIPID

B.R. Ratna, A.S. Rudolph, B. Kahn and R. Shashidhar
Center for Bio/Molecular Science & Engineering
Code 6090, Naval Research Laboratory
Washington D.C. 20375-5000

A diacetylenic phospholipid, 1-2-bis alkadiynoyl-sn-glycero-3-phosphocholine, when dispersed in water or alcohol/water, forms hollow cylinders (called "tubules") on cooling below the chain melting temperature. Electron microscopy shows that these tubules are formed by helically wrapped bilayers. We have carried out optical microscopic studies of the melting and formation of tubules. On heating, the bilayers constituting the wall of the tubule melt and unwrap. Polarization microscopy shows that the melted phase is the liquid crystalline L_α phase. On further heating (in the ethanol\water medium), there is a continuous swelling of the bilayers, until finally an optically clear solution with no visible birefringence is observed. On cooling this isotropic-like liquid, fluid filaments which exhibit pronounced fluctuations are observed. These filaments are highly metastable and coalesce. On further cooling, tubules are seen to emerge from this condensed state. The nature of the fluid filaments and their role in tubule formation will be discussed.

M-Pos299

DIACETYLENIC ETHER AND ESTER LIPIDS: BILAYER STRUCTURE, SYNTHESIS AND PROPERTIES

David G. Rhodes[1], Zhenchun Xu[2] and Robert Bittman[2]
1. Biomolecular Structure Analysis Center, Dept. Radiology U. of Connecticut Health Center, Farmington, CT 06032
2. Department of Chemistry and Biochemistry, Queens College of CUNY, Flushing, NY 11367

Four diacetylenic phosphatidylcholines (PC's) have been synthesized and the structures of bilayers of these lipids determined at low resolution by low angle x-ray diffraction. The PC's have 18 carbon chains but differ with respect to the ether/ester linkage at sn-1 and sn-2 and the relative position of the diynoyl moiety:
diester-PC 1 - bisacetylenic unit as C4-C7 of each chain
diester-PC 2 - bisacetylenic unit as C4-C7 of sn-1 and C5-C8 of sn-2
diester-PC 3 - bisacetylenic unit as C10-C13 of each chain
diether-PC 4 - bisacetylenic unit as C4-C7 of sn-1 and C5-C8 of sn-2

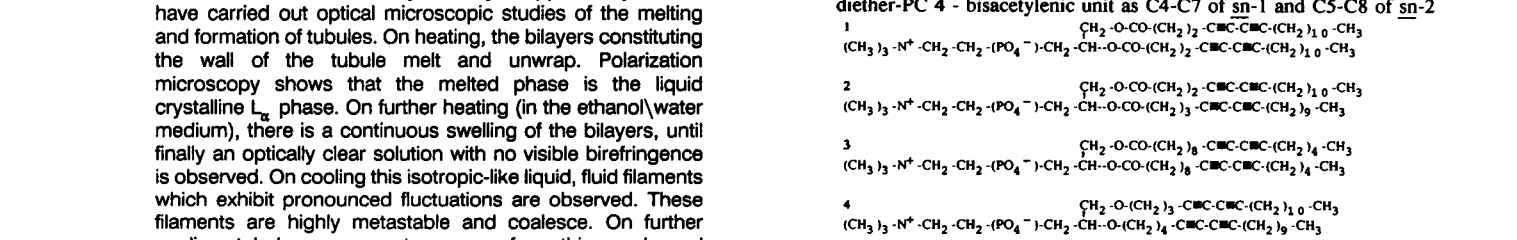

We find that only 1 exhibits the 'typical' bilayer profile, while 2, 3 and 4 show evidence of interdigitation and/or significant disorder. Only 1 polymerized effectively; this derivative polymerized in seconds to a deep blue. The color turned red irreversibly at 40°C. Polymerized liposomes of 1 underwent osmotic swelling with urea, glycerol, and acetamide more rapidly than did liposomes of palmitoyl-oleoyl-PC , but the initial rates of swelling of polymerized liposomes of 1 were 3-10 times lower than those of unpolymerized liposomes of 1.

Supported by NSF #CTS-8904938 (DGR) and NIH #HL-16660 (RB).

M-Pos300

MEMBRANE PHASE STATE DURING CELL GROWTH BY LAURDAN GENERALIZED POLARIZATION.

T. Parasassi, O. Sapora*, M. di Stefano, G. Lanzilli and G. Ravagnan. Instituto di Medicina Sperimentale, CNR, and *Institito Superiore di Sanita, Roma, Italy.

The sensitivity of Laurdan emission and excitation spectra to phospholipid phase state has been used to detect modifications of growing cell membranes. In phospholipid vesicles Laurdan shows a 40 nm red shift passing through the gel to the liquid-crystalline phase. In mixed phase vesicles quantification of the two coexisting phases can be achieved by the Laurdan Generalized Polarization (GP)(1). The GP offers the advantage of rapid measurements with no need of calibration. Moreover, all properties of the "classical" polarization still pertain to the GP. A technique to label cell membranes with the minimum perturbation of the membrane itself while maintaining the cell viability has been developed. Laurdan GP values were measured in proerythropoietic K562 cells in the G0 phase and after 12 hours of non-synchronous growth. The GP values were considerably higher in the cells G0 phase with respect to the growing cells, indicating a higher molar fraction of gel phase phospholipids in G0 cells. Quantification of membrane coexisting phases has been achieved taking into account the contribution of cholesterol. (1) Parasassi, T., De Stasio, G., d'Ubaldo, A. and Gratton, E., Biophys.J. 57 (1990) 1179.

M-Pos301

QUENCHING INTERACTION BETWEEN LUMINESCENT AND SPIN-LABELED ANTIBODIES: A PROBE OF CELL SURFACE PROTEIN ORGANIZATION

Janos Matko, Kazuo Ohki & Michael Edidin
Dept. Biol., The Johns Hopkins Univ., Baltimore, MD, 21218

The fluorescence quenching by nitroxide radicals of fluorescein and Tb^{3+} conjugated antibodies was studied in solution and on cell surfaces. The spin labels proved to be effective quenchers, but the quenching reaction showed characteristic temperature and viscosity dependence arguing against the diffusion controlled collisional mechanism proposed earlier and assumed in many cases in the quenching analysis. Time-resolved luminescence measurements, solvent-dependence of the quenching as well as the spectral overlap and its elimination by ascorbate, in correlation with abolishing the quenching, all suggest the Forster type energy transfer as the dominant mechanism in the quenching. Two cell lines, a transformed human fibroblast, VA2, and a human lymphoma, JY, were labeled with fluorescein or Tb^{3+}-labeled KE2 monoclonal antibodies developed against MHC Class I antigens. Spin-labeled antibodies quenched both luminescences effectively, indicating that the cell surface distribution of the antigens is not random/dispersed but rather a dynamic equilibrium of monomeric and dimeric forms or even larger aggregates. FCET measurements with fluorescent donors and acceptors led to the same conclusion. No quenching was observed when FL-transferrin (on VA2 cells) or FL-SIg (on JY cells) were applied as fluorophores to the spin labeled KE2 quenchers. Application of the Tb^{3+}/spin label pairs rather than classical fluorescent donor-acceptor pairs has the advantage of the independence of the orientation factor. (Supported by grant from NIH.)

M-Pos302

SOLID-STATE NMR STUDIES OF MEMBRANE BOUND FILAMENTOUS BACTERIOPHAGE COAT AND PROCOAT PROTEINS

Y. Kim*[1], J. Richards[2], J. Tomich[3], and S.J. Opella[1]

[1]Department of Chemistry, University of Pennsylvania, Philadelphia, PA 19104

[2]Division of Chemistry and Chemical Engineering, California Institute of Technology, Pasadena, CA 91125

[3]Division of Medical Genetics, Children's Hospital of Los Angeles, 4650 Sunset Blvd., Los Angeles, CA 90027

Solid-state NMR structural studies can be performed on membrane proteins oriented in lipid bilayers between glass plates. The structural information is in the form of orientations of bonds and chemical groups with respect to the plane of the bilayer. Parallel studies of protein dynamics can be performed on unoriented samples by analyzing the motional averaging of powder pattern lineshapes. Both experimental approaches have been applied to the coat and procoat proteins from a class I bacteriophage (fd) and a class II bacteriophage (Pf1). All of these species are typical membrane proteins with both hydrophobic membrane spanning helices and amphipathic bridging helices parallel to the plane of the bilayer. They have mobile N- and C- terminal residues as well as mobile loops connecting the helices.

M-Pos303

ORIENTATIONAL ORDER IN THE INTACT MEMBRANES AND DERIVED LIPOSOMES OF ACHOLEPLASMA LAIDLAWII STRAIN B: A DEUTERIUM NMR STUDY. M. A. Monck*, M. Bloom§, M. Lafleur*, R.N.A.H.Lewis#, R.N.McElhaney# and P.R.Cullis*. *Dept. Of Biochemistry, §Dept. of Physics, U.B.C., Vancouver, Canada V6T 1W5, #Dept. fof Biochemistry, University of Alberta, Edmonton, Alberta, Edmonton Canada, T6G 2H7.

We have investigated the dependence of the lipid chain orientational order in a biological membrane upon its lipid composition. Deuterium nuclear magnetic resonance spectroscopy has been used to measure the order in the plasma membrane of the bacterium Acholeplasma laidlawii strain B (ALB) as well as in liposomes composed of extracted ALB membrane lipids. ALB is a useful biological organism for study because the lipid fatty acid composition of the plasma membrane can be readily manipulated. Using this property, perdeuteriated palmitic acid (16:0d31) was incorporated into the membrane as a probe for determining order parameters. A second fatty acyl chain which was varied was also incorporated. The following membrane fatty acyl chain compositions were examined: 16:0d31/14:0, 16:0d31/18:1Δ9, 16:0d31/18:1cΔ9, 16:0d31/18:2cΔ9, Δ12.

Quadrupolar splittings and the orientational order profiles were measured from the depaked spectra of the above systems. With a variation in the second fatty acyl chain from 14:0 to 18:2cΔ9.Δ12 the maximum quadrupolar splittings decreased by approximately 10%. No consistent trends in the lipid headgroup compositions were observed. However, the range of maximum quadrupolar splittings obtained for the intact membrane systems was narrower than that obtained for the liposomal systems by more than a factor of two. It appears that the extent of change in orientational order is damped in the intact membrane as compared to the rehydrated lipid bilayer.

Also examined was cholesterol incorporation into ALB lipid membranes. With respect to membrane order, the ^{2}H-NMR spectra of the ALB membranes in which cholesterol incorporation was studied did not differ from the corresponding spectra where the samples lacked cholesterol. Spectra taken at increasing temperature intervals above 37°C did not show a significant decrease in membrane order while a subsequent spectrum taken at 37°C showed a significant increase in membrane order. ALB samples which were lyophilized and then rehydrated to form liposomal membrane systems gave ^{2}H-NMR spectra that indicated a highly ordered lipid bilayer compared to a bilayer lacking cholesterol. Finally, ALB samples containing 2,2,4,4,6d5-cholesterol as the ^{2}H-NMR probe gave spectra showing isotropic behaviour. The indication here is that cholesterol is present in the ALB samples but is not located within the lipid bilayer at an orientation normal to the bilayer plane. A discussion of the results as they pertain to the various aspects of modulation will be presented.

M-Pos304

Imaging red and white blood cells in buffer with the Atomic Force Microscope

Hans-Jürgen Butt and Paul K. Hansma*
Max-Planck-Institut für Biophysik, Kennedyallee 70, 6000 Frankfurt 70, Germany; *Dept. of Physics, University of California, Santa Barbara, CA 93106

The atomic force microscope (AFM) is part of a new breed of microscopes, the scanning probe microscopes. Single atoms could be resolved with the AFM on hard materials. As the AFM combines a possible high resolution with the opportunity to image in water, it is a promising tool for investigating the surface structure of cells.

When we tried to image untreated mammalian cells in buffer, the cells turned out to be too soft to be imaged repeatedly. To increase their rigidity the cells were fixed with 1% glutaraldehyde for 1 min. Then red and white blood cells could been imaged for hours in buffer solution. Surface features down to 5 nm were resolved with the AFM.

M-Pos305

FOCAL CONTACT FORMATION IS RESPONSIBLE FOR CELL-SUBSTRATE STRENGTHENING RESPONSE: ANALYSIS OF THE CENTRIFUGAL ASSAY FOR CELL ADHESIVENESS. Daniel A. Hammer, School of Chemical Engineering, Cornell University, Ithaca NY 14853.

The centrifugal force to remove a cell from a surface is a useful measure of cell attachment strength. However, the results of this assay depend on the length of time that a cell is allowed to bind and spread on the surface before cell detachment; the longer the cell is incubated on the surface, the more difficult it is to remove. Fluorescent labelling of the cytoskeleton, interference reflection microscopy, and studies with metabolic inhibitors all suggest that this strengthening response depends on the reorganization of the cytoskeleton and the formation of focal contacts - patches of very tight adhesiveness - between the cell and surface.

We present a simple mathematical model in which we compare the strength of adhesiveness of the cell during four different states of the spreading and strengthening response: initial contact, spreading with uniform distribution of receptor-ligand bonds, spreading with focal contact formation, and solidification by focal contact communication across the cell length. In our modeling, we show how parameters such as receptor number, cell size, ligand density, receptor-ligand affinity, the density of cytoskeletal gelation centers, the number of receptor binding molecules in these centers, and their affinity for the cytoplasmic tail of the receptor, all affect the strength of cell-substrate attachment in each state. We show that the strengthening response observed in many reports using this assay is almost entirely attributable to the presence of cytoplasmic gelation centers which thermodynamically drive the clustering of receptors into small patches of very high density. The analysis suggests two simple ways in which a cell can alter its adhesiveness: through expressing different levels of cytoskeletal molecules, or changing the affinity of interaction between the cytoskeleton and transmembraneous adhesion receptors. For example, a two order of magnitude change in affinity between adhesion receptor and the cytoskeletal molecule talin can induce a two order of magnitude increase in the strength of attachment as measured by centrifugation, even when focal contacts comprise as little as 0.1% of the gross cell-substrate contact region. The model is compared to results on fibroblast adhesion to fibronectin measured by Lotz et al., J Cell Biol 109;1795-1805 (1989).

M-Pos306

MEASURING VESICLE FUSION RATES USING FLUORESCENCE ASSAYS: SOME CONSIDERATIONS REVISITED.

A. Walter*, J.L. Banschbach, D. P. Siegel.*Department of Physiology and Biophysics, Wright State University, Dayton, OH 45435 and Procter and Gamble Co., P.O. Box 398707, Cincinnati, OH 4523 9-8707.

In using fluorescence assays of membrane fusion, it is implicitly assumed that the presence of the fluorescent probes do not perturb the vesicles and that the rates determined in hand-mixing experiments truly represent the initial fusion kinetics. We examined these assumptions for divalent cation-induced fusion of PS vesicles prepared by high-pressure extrusion through 0.1 μm filters. Because of long-standing speculations about the relevance of chain-melting transitions to the fusion process, we measured the influence of the components of two frequently-used assays on the T_c of POPS. Tb, DPA, and ANTS had no significant effect, but DPX at assay concentrations (90 mM) depressed T_c from 11° C to a temperature ≤ 0° C. A similar effect occurred in bovine brain PS. Whether the DPX also affects the fusion process is not known, but the result clearly suggests that DPX alters the initial state of the membrane, making this compound suspect for fusion rate determinations. In hand-mixing studies of fusion or leakage rates, a concentrated stock of vesicles or divalent cation is added to a reaction mixture, and the fluorescence vs. time curves often appear sigmoidal. The mixing time in these studies is ca. 1 sec. However, identical studies done with a stopped flow mixer (1:1 volume mixing with a 10 msec dead time) result in monotonic curves. By calculation of the fluorescence level corresponding to dimerization of all vesicles, it can be shown that most vesicles have formed dimers or multimers within <5 sec at concentrations in which fusion appears to be rate-limiting (50 μM bovine brain PS with 5 mM Ca^{2+}; 60 μM PS with 3.75 mM Ca^{2+}). It is proposed that stopped-flow mixing experiments provide more reliable determinations of initial kinetics.

M-Pos307

POLYMORPHISM OF UNPOLYMERIZED AND POLYMERIZED LIPID-WATER MEMBRANE SYSTEMS.

F.Osterberg, J. Cerne, E. Shyamsunder and S.M. Gruner, *Physics Department, Princeton University*; and H. Lamparski and D. F. O'Brien, *Department of Chemistry, University of Arizona*

X-ray diffraction and NMR have been used to study the polymorphism of aqueous dispersions of a polymerizable PC (SorbPC), mixed with DOPE in a molar ratio 1:3. In the unpolymerized state, the system exhibits complex phase behaviour. Freshly hydrated suspensions exhibit X-ray diffraction that is characteristic of non-lamellar phases in combination with a disordered component. Upon heating, the system eventually forms a phase with hexagonal symmetry. The non-lamellar phases are presumed to be inverted phases because they swell to a limited degree in excess water. The system exhibits very sluggish phase transition behaviour involving very long-lived intermediate states that are strongly dependent on the thermal history of the sample. This thermal history dependence was investigated by cycling the system between -30 C and 65 C. At -30 C the system is in the gel phase. Upon thermal cycling the system reproducibly forms an inverted hexagonal (H_{II}) phase, at the expense of the cubic and disordered phases observed in the freshly prepared samples. Interestingly, upon photopolymerization, the system continues to exhibit the occurrence of non-lamellar phase transitions. Additional studies to investigate whether the occurrence of non-lamellar phases in photopolymerized lipid is due to a selective demixing of unpolymerized lipid, or whether the polymerized membranes are actually undergoing non-lamellar phase transitions will be reported.

This work was supported by grants from the NIH, DOE, and ONR.

M-Pos308

THE INTERACTION OF CORD FACTOR (α,α-D-TREHALOSE-6,6'-DIMYCOLATE) WITH PHOSPHOLIPID ASSEMBLIES.

B.J. SPARGO, L.M. CROWE, B.L. BEAMAN, J.H. CROWE. Departments of Zoology and Medical Microbiology and Immunology, University of California, Davis.

Cord factor (CF) or α,α-D-trehalose-6,6'-dimycolate is a cell wall glycolipid of human pathogenic bacteria such as Mycobacterium tuberculosis, Nocardia asteroides, and Corynebacteria diphtheria that has been linked to toxicity and persistence of the pathogen. Recently, we have demonstrated (Spargo, *et al.* (1990) Proc. Nat. Acad. Sci., in press) that cord factor inhibits calcium-induced fusion of unilamellar vesicles. We postulated that cord factor inhibits fusion either by steric hinderance by the trehalose head group or by increasing hydration of the membrane surface each of which would reduce the likelihood that two opposing membranes would come in contact sufficient for fusion. Increased hydration would reduce the potential for calcium-induced dehydration of the membrane surface, a step thought necessary for completion of the fusion event.

We have attempted to distinguish between these possible mechanisms in the current study. The effects of cord factor on membrane properties such as fluidity, lipid packing, and membrane hydration were investigated. Fluorescence anisotropy data suggest that cord factor reduces the liquid crystalline to gel transition temperature of acidic phospholipid in the presence of calcium. CF in DMPC:POPA Langmuir-Blodgett films increases the surface area from 0.64 nm^2/molecule to 0.92 nm^2/molecule. The amount of membrane surface-associated water as measured by DSC demonstrated that CF increases the mole water/ mole lipid ratio from 8.1 in the absence of CF to 30.9 in its presence. These findings suggest that CF interacts directly with bilayers and that its presence in the bilayer increases the hydration barrier to fusion.

Supported in part by grants 2RO1-AI20900 from the National Institutes of Health (BLB), DCB-89-18822 from the National Science Foundation (JHC) and NA85AA-D-SG140 from the California Sea Grant College Program (JHC).

M-Pos309

EFFECT OF AMPHIPATHIC COMPOUNDS ON POLY(ETHYLENE GLYCOL)-INDUCED FUSION OF MEMBRANE VESICLES COMPOSED OF 1,2-DIPALMITOYL-3-*SN*-PHOSPHATIDYLCHOLINE

Gail F. McIntyre, Derek J. Parks, Donald Massenburg, and Barry R. Lentz. (Intro. by Walter Shaw). *Dept. of Biochemistry & Biophysics, University of North Carolina at Chapel Hill, NC 27599.*

Poly(ethylene)glycol (PEG) does not induce fusion of dipalmitoylphosphatidylcholine (DPPC) large, extruded, unilamellar vesicles (LUVET); however, it does cause aggregation and lipid transfer between these vesicles (Burgess *et al.*, Biochemistry 1990, submitted). The abilities of several amphipathic compounds to induce fusion between vesicles caused to aggregate by PEG has been tested. These compounds have been hypothesized to play a role in various cellular processes requiring membrane fusion. Vesicles which contained 0.5 mol% L-α-lysophosphatidylcholine, 5 mol% platelet activating factor, or 0.5 mol% palmitic acid fused in the presence of 30%, 25%, and 20% (w/w) PEG, respectively. Vesicles containing 1,2-dipalmitoylglycerol, 1,2-dioleoyl-*sn*-glycerol, 1-oleoyl-2-acetyl-*sn*-glycerol, or monooleoyl-*rac*-glycerol, at reasonable surface concentrations (up to 5 mol%), did not fuse in the presence or absence of PEG. From these results, it appears that there are general structural features associated with amphipathic bilayer perturbants that induce fusion of DPPC LUVET in the presence of the aggregating polymer, PEG. Successful fusogenic amphipaths contained a long chain hydrocarbon moiety to insert into the hydrophobic region of the lipid bilayer as well as a polar headgroup that, either because of its charge or bulky structure, had a larger effective cross sectional area than that of the hydrocarbon region. There was no correlation between the abilities of these amphipaths to induce phase separation or non-lamellar phases and their abilities to support fusion of pure DPPC LUVET in the presence of high concentrations of PEG. These results are discussed in terms of the type of disrupted lipid packing that could be expected to favor fusion. *Supported by USPHS Grant GM-32707.*

M-Pos310

DETERMINATION OF THE RAPID KINETICS OF LIPID EXCHANGE INDUCED BY POLY(ETHYLENE GLYCOL) USING THE SLM® FOURIER TRANSFORM PHASE AND MODULATION SPECTROFLUOROMETER

Stephen W Burgess+, Jogin R Wu+, Kerry Swift#, and Barry R Lentz+ +Dept. of Biochemistry & Biophysics, Univ. of North Carolina Chapel Hill, NC 27599 #SLM-Aminco 810 W. Anthony Drive Urbana, IL 61801

Rate constants were determined for the transfer of the fluorescent lipid probe DPHpPC between large, unilamellar extrusion vesicles composed either of dipalmitoyl phosphatidylcholine (DPPC[1]) or of DPPC mixed with a small amount (0.5mol%) of lyso phosphatidylcholine (Lyso PC[1]). Transfer of the lipid probe in the presence of varying concentrations of poly(ethylene glycol) (PEG[1]) was monitored using the SLM 48000-MHF Multi-Harmonic Fourier Transform phase and modulation spectrofluorometer to collect multifrequency phase and modulation fluorescence data sets on a millisecond time scale. Using a simple two-state model for initial lipid transfer, we performed fluorescence lifetime analyses on the multifrequency data sets to obtain the fractional contribution of donor and acceptor probe populations to the average fluorescence lifetime. The fractional fluorescence intensity of each population was used to calculate the mole fraction of probe in each population as a function of time following rapid mixing of vesicles with PEG. The rate of transfer of lipid at PEG concentrations <35% (w/w) was much more rapid than transfer in the absence of PEG and increased linearly with increasing PEG concentration. At ~35% (w/w) PEG, the rate constant for lipid transfer increased dramatically for both DPPC and DPPC/lysoPC vesicles. Fusion of the lysoPC-containing vesicles first occurred at 30% (w/w) PEG. These results are interpreted in terms of a distinct interbilayer structure associated with the intimate bilayer contact induced by high concentrations of PEG. This interbilayer structure promotes rapid lipid transfer and may be involved in membrane fusion. *Supported by USPHS Grant GM-32707.*

M-Pos311

MECHANISM OF POLY(ETHYLENE GLYCOL)-INDUCED LIPID TRANSFER BETWEEN PHOSPHATIDYLCHOLINE LARGE UNILAMELLAR VESICLES

Jogin R. Wu & Barry R. Lentz. Intro. by Jan Hermans. *Dept. of Biochemistry & Biophysics, Univ. of North Carolina, Chapel Hill, NC 27599.*

Experiments with a specially designed dialysis chamber were performed to assess three possible mechanisms of poly(ethylene glycol) (PEG)-induced rapid lipid transfer between large unilamellar vesicles (LUVET) composed of dioleoylphosphatidylcholine (DOPC): 1] transfer between aggregated vesicles, 2] transfer through an aqueous medium of lowered dielectric constant, and 3] transfer *via* a PEG carrier. The results showed that vesicle close contact as a result of PEG dehydration was largely responsible for the rapid lipid transfer observed in the presence of PEG. The rate and extent of lipid transfer were also examined at 10wt% PEG and analyzed in terms of a two-state model especially developed to account for the initial rate of lipid transfer as followed by the fluorescence lifetime of DPHpPC as a fluorescent lipid probe. Analysis revealed that two rate processes were involved in DPHpPC transfer between bilayers both in the absence and presence of PEG. Since the maximum extent of transfer was 50%, trans-bilayer diffusion of DPHpPC seemed not to contribute to either process. The fast process in the presence of PEG was identified as due to rapid inter-bilayer monomer diffusion between closely apposed vesicles, and, in the absence of PEG, as due to monomer diffusion through the aqueous phase. The slow process in both cases seemed to reflect specific properties of the DPHpPC probe, perhaps reflecting the tendency of this probe to segregate into microdomains in the plane of the membrane. The Arrhenius activation energy for the fast process at temperatures from 10 to 48 °C was 15.3 ± 0.3 kcal/mol and 10.6 ± 0.5 kcal/mol in the absence and presence of PEG, respectively. The slow process was invariant with temperature. From these studies, we conclude that PEG enhances the rate of inter-vesicle lipid transfer by forcing dehydration and aggregation of vesicle bilayers, thereby altering the properties of the aqueous phase between membranes. *Supported by USPHS Grant GM32707.*

M-Pos312

^{31}P NMR SPECTROSCOPY OF THE THERMOTROPIC PHASE BEHAVIOR OF BINARY MIXTURES OF PHOTOPOLYMERIZABLE PC'S AND DOPE.

Judith A. Barry, Henry Lamparski, and David F. O'Brien (Intro. by V. J. Hruby). *Department of Chemistry, University of Arizona, Tucson, AZ 85721*

The effect of photopolymerization of lipids on the thermotropic phase behavior has been studied with ^{31}P NMR spectroscopy. Both a SorbPC, with polymerizable dienes near the ends of the chains, and a DenPC, which polymerizes adjacent to the acyl linkage near the headgroup, were mixed with DOPE in molar ratios of 3:1 DOPE:SorbPC and 3.6:1 DOPE:DenPC. The SorbPC and DenPC were photopolymerized to varying degrees by exposure to ultraviolet light. Each mixture was slowly heated from 25° to 100°C, and a ^{31}P NMR spectrum acquired every 2° to 5° in the region of a phase transition. In all mixtures, both polymerized and unpolymerized, heating from the L_α phase caused the formation of a phase with isotropic symmetry. The isotropic NMR signal is analogous to spectra observed in other lipid systems, which have been identified as cubic structures by complimentary X-ray diffraction studies. Supported in part by NIH Postdoctoral Fellowship EY06111 (J.A.B.).

M-Pos313

PHOTOINDUCED DESTABILIZATION OF LIPOSOMES.

H. Lamparski, U. Liman, D. A. Frankel & D. F. O'Brien. *Department of Chemistry, University of Arizona, Tucson, AZ 85721.*

The stabilities of two-component liposomes composed of the photopolymerizable SorbPC and either DOPE or DOPC were examined via fluorescence leakage assays. Ultraviolet light exposure of the liposomes yields poly(SorbPC) which phase separates from the remaining monomeric lipids. Photoinduced destabilization was observed only in liposomes composed of DOPE/SorbPC, and only in samples that consist at least in part of oligolamellar liposomes. Photopolymerization of 100 nm diameter unilamellar DOPE/SorbPC (3/1) liposomes does not induce leakage. These observations on liposomes coupled with collaborative ^{31}P NMR and X-ray diffraction studies on extended bilayers of these same lipids, indicate that the bilayer destabilization involves the formation of nonlamellar lipid structures. The current data suggest that liposome leakage may be mediated by the formation of an isotropically symmetric structure, e.g. an interlamellar attachment (ILA), between the lamellae of the oligolamellar liposomes. Supported in part by the NSF.

M-Pos314

ENERGY STORAGE AND MEMBRANE ELECTROFUSION IN RABBIT ERYTHROCYTE GHOSTS.

Yankuan Wu, Joseph G. Montes, and Raymond A. Sjodin, Department of Biophysics, School of Medicine, University of Maryland at Baltimore, Baltimore, MD 21201

Electrofusion yields in rabbit erythocyte ghosts were determined in experiments performed at low (10^7 cells/ml) population density. Three different treatments were compared: 1) current-first (CF) protocol; 2) pulse-first (PF) protocol, using either a single pulse or a train of three pulses of about the same energy as the single pulse; 3) a combined treatment consisting of PF of alternating ("APF-CF") or same polarity ("PF-CF") followed by one "final" pulse. At low final pulse strength (200V/mm), yields were about the same for the CF, PF, and PF-CF protocols; at higher final pulse strength (400V/mm), yields improved considerably and CF gave the same yields as PF-CF. Thus, fusion yields for PF and CF were not additive in the PF-CF protocol, suggesting saturability of the long-lived fusogenic state and possible identity of that state with that occurring in CF. Fusion yields induced by either APF-CF or PF-CF, and with different time spacing (0-60s) between prepulses, were also compared with each other and with the yields in the controls. There was no significant difference in fusion yield when the ghosts were treated with a train of different prepulse(s) of the same total energy; furthermore, alternating the polarity of the prepulses and changing the time spacing had no effect on yield, suggesting that "memory" of a preceding prepulse could not be "erased" by reversing the polarity of a subsequent prepulse, and that the prepulses contributed the same to the fusion yield whether they were reversed or not. Thus, the storage of energy in the membrane can be saturated under certain circumstances. This means that the long-lived fusogenic state and the "normal" cell electrofusion state may have the same mechanism.

M-Pos315

THE ADDITIVITY OF PULSE ENERGY AND THE ROLE OF THE ELECTRIC FIELD STRENGTH IN THE ELECTROFUSION OF RABBIT ERYTHROCYTE GHOSTS

Raymond A. Sjodin, Yankuan Wu, and Joseph G. Montes Department of Biophysics, School of Medicine, University of Maryland at Baltimore, Baltimore, MD 21201

Electrically induced membrane fusion can be produced in two ways. One is the normal electro-fusion protocol (CF protocol). The other means is the PF protocol, a reverse process of the CF protocol. To study the relationship between the long-lived fusogenic state and the "normal" electrofusion state and the possible mechanisms of membrane fusion, fusion yield for rabbit erythrocyte ghosts was determined using a "PF-CF" protocol, whereupon ghosts are first treated with a train of prepulses of the same electrical characteristics and then immediately subjected to a typical CF protocol. The polarity of the prepulses in a train can be either the same ("PF-CF") or alternating ("APF-CF"). In our studies, experiments were conducted in a suspension of low cell population density (10^7 cells/ml) in a 20 mM sodium phosphate buffer (pH 8.5). Fusion yields were generally not increased with an increase in the number of prepulses beyond two; instead, a small decrease in the yields was typically observed. Nonetheless, fusion yields were still increased by using a couple of prepulses which have the same or alternative polarities before applying the final pulse. Varying the decay half time ($T_{1/2}$) (i.e., the power) of the prepulses had little or no effect on the fusion yields in most of the experiments, indicating that changing the electric field strength is the major way to increase the fusion yield. The results clearly show that the effect on membrane fusion events of the electric energy delivered by the pulses is not additive, but rather suggest saturability of the long-lived fusogenic state and possible identity of that state with the state occurring with the usual electrofusion protocol, at least under certain conditions. Since the effect of electric pulses on the cell membrane could conceivably be reversible, we performed experiments whose purpose it was to "erase" the "memory" of previously applied prepulses by applying subsequent prepulse of the same energy but opposite polarity. There was no significant difference in fusion yield whether the polarity of prepulses was alternated or not. These results appear to favor an electropore hypothesis rather than a point-defect hypothesis, and suggest that the mechanism for both the long-lived fusogenic state and the usual electrofusion state may be the same.

M-Pos316

INDUCTION OF AGGREGATION AND HEMIFUSION OF ACIDIC LIPOSOMES BY A CALCIUM OR BARIUM-DEPENDENT PROTEIN FROM BOVINE TISSUES.

Milton de la Fuente, George Lee, Harvey B. Pollard. Laboratory of Cell Biology and Genetics, NIDDK, Bethesda, MD 20892.

Searching for a Ba^{2+}-dependent protein mediator in exocytosis, we have recently purified to homogeneity a 36 KD protein (G36), that aggregates chromaffin granules in the presence of Ca^{2+} or Ba^{2+}, but not Mg^{2+}. This activity is inhibited by phenothiazine drugs such as trifluoperazine and promethazine, as in the analogous calcium dependent process mediated by synexin. Preliminary experiments indicated that G36 binds to lipids, and we therefore pursued a study of the ability of this protein to aggregate and fuse liposomes. Liposomes were prepared using the extrusion technique, and aggregation was followed by changes in turbidity. Membrane mixing was studied using the RET assay. Fusion was determined by the ANTS/DPX and the fluorescein dextran methods. We found that G36 rapidly aggregates acidic liposomes made of PS, PS:PE, PA:PE and PI:PE in the presence of Ca^{2+} or Ba^{2+} but not Mg^{2+}, at pH below 6.5. G36 also induces hemifusion, as defined by membrane mixing. However, in distinction to synexin, G36 does not promote complete fusion, as determined by volume mixing experiments. Fusion, however, occurs rapidly if small amounts of arachidonic acid are added to the system, as is necessary for fusion of intact chromaffin granules by synexin. We conclude that G36 a candidate for the predicted mediator of the Ba^{2+}-dependent fusion step during exocytosis and do not exclude the further possibility of its involvement in Ca^{2+}-dependent events.

M-Pos317

SINGLE CELL ASSAY OF EXOCYTOSIS FROM RAT PANCREATIC ISLET B CELLS USING PERFORATED PATCH RECORDING.

Kevin D. Gillis and Stanley Misler, The Jewish Hospital and Department of Electrical Engineering, Washington University, St. Louis, MO 63110.

A reasonable hypothesis for stimulus-secretion coupling in the insulin secreting B cell is that glucose metabolism --> cell depolarization --> Ca^{2+} entry via voltage dependent channels --> $Ca^{2+}{}_i$-dependent exocytosis of insulin storage granule contents. The combination of phase detection with whole cell recording permits monitoring of depolarization-induced Ca^{2+} currents (I_{Ca}) and the resulting changes in membrane capacitance ΔC_m which are associated with vesicle exocytosis during the secretion. Here we have combined phase detection with the perforated patch variant of whole cell recording (PPR), which allows prolonged maintenance of cell metabolism and $Ca^{2+}{}_i$ buffering, to explore the links between Ca^{2+} current, or electrical activity, and insulin granule exocytosis in isolated islet B cells. Previous studies indicated that PPR maintains depolarization-induced changes in C_m (Biophys J. 57:491a).

Following one or more pulses of membrane depolarization which activate Ca^{2+} currents, single islet cells (C_m = 3.3-5.8 pF), patched with pipettes containing a $CsCl/CsSO_4$ solution and bathed in 5 mM Ca^{2+} + 1 mM IBMX Ringer's, display $Ca^{2+}{}_o$-dependent increases in C_m. ΔC_m shows a very similar bell-shaped dependence on clamping voltage as does peak inward Ca^{2+} current (I_{Ca}); both are maximal between +10 and +20 mV. Single 100 msec pulses to +20 mV, which evoke ~20 pA Ca^{2+} currents, produce 10-100 fF ΔC_m's. Both ΔC_m and I_{Ca} are blocked by addition of 50 μM Cd^{2+}. When a series of 100 msec pulses to +10 mV is applied, the first pulse produces a maximum ΔC_m. Subsequent pulses produce rapid depression of ΔC_m that can be relieved following several minutes of quiescence. Preliminary experiments suggest that secretogogue (e.g. glucose or tolbutamide) stimulated increases in C_m can be measured by periodically switching from the current clamp recording mode, where the cell is allowed to generate its own electrical activity, to the voltage clamp recording mode, which permits C_m measurements.

Support: NIH DK37380.

M-VCR2

PROTEINS ON SEA URCHIN CORTICAL GRANULES MEDIATE CALCIUM TRIGGERED VESICLE FUSION

Steven S. Vogel & Joshua Zimmerberg (LBM, NIDDK, National Institutes of Health, Bethesda, MD 20892)

Using both video-enhanced light-microscopy, and a light scattering assay, we find that aggregates of purified sea urchin cortical granules fuse with each other when perfused with ≥ 10 μM calcium (50% fusion at 32 μM). Both micromolar calcium and granule/granule contact are required concurrently for fusion (though the order of presentation is not important); isolated granules do not lyse (~1%) when exposed to 100 μM calcium. Further evidence that membrane fusion has occurred comes from observing hydrated contents leaking out of a corner of the granule-syncytium, clumps of contents are seen moving under the syncytium membrane distances much larger than several granule diameters. Considering that we often find syncytium whose contents are not undergoing Brownian motion, we presume that content hydration is not required for granule/granule fusion. Indeed, this reaction does not even require added cytoplasmic proteins (such as NSF or synexin) or cytoplasmic organic factors (such as ATP, GTP, arachidonic acid, or acyl Co-A), thus the mechanism for calcium triggered vesicle fusion must reside on the vesicles themselves. In addition, our finding that granule/granule fusion (using up to 500 μM calcium) is inhibited by proteolysis (with trypsin, 1 mg/ml for 1 h at RT), and by treatment with the protein modifying reagent NEM (1 mM for 30 min at RT), argues that, as in viral fusion, the sea urchin cortical reaction is mediated by vesicular membrane proteins that do not require water soluble organic co-factors.

M-Pos318

FUSION OF HIV-1 WITH LIPOSOMES AND ERYTHROCYTE GHOSTS.

Charles E. Larsen, Dennis R. Alford, Shlomo Nir*, Myra Jennings**, Kyung-Dall Lee, and Nejat Düzgüneş. Cancer Research Institute, University of California, San Francisco, CA 94143-0128; *Seagram Centre for Soil and Water Sciences, The Hebrew University, Rehovot 76100, ISRAEL; and **Comparative Oncology Laboratory, University of California, Davis, CA, 95616.

We investigated the kinetics of membrane fusion between HIV-1 and phospholipid vesicles and erythrocyte ghost membranes and studied the effects of pH, divalent cation, target membrane composition, and viral trypsinization on this process. Sucrose gradient purified HIV-1 was labeled with octadecyl rhodamine B chloride (R_{18}), and fusion was monitored continuously as the dilution of probe into target membranes. Ultrastructural analysis of the virus and reaction products by scanning electron microscopy was also utilized to confirm the results of the R_{18} assay. HIV-1 fusion is strongly dependent upon the lipid composition of target membranes. For anionic liposomes, fusion with pure cardiolipin (CL) liposomes > CL/dioleoylphosphatidylcholine (DOPC) (3:7) > phosphatidylinositol (PI) ≥ phosphatidic acid (PA) > phosphatidylserine (PS) vesicles at neutral pH. HIV-1 fusion with pure DOPC liposomes is dramatically slower than with anionic liposomes, and dilution of PS with either PC or PE also greatly reduces the rate of fusion with HIV-1. Reduction of pH from 7.5 enhances the rate of HIV-1 fusion with CL, CL/DOPC (3:7), PS, PI and PA vesicles but does not affect fusion with pure DOPC liposomes. Physiologically relevant concentrations of calcium stimulate HIV-1 fusion with several liposome compositions and with erythrocyte ghost membranes. Trypsinization of HIV-1 results in loss of fusion activity towards CL liposomes under certain conditions. Recombinant soluble CD4 (rCD4) and bovine serum albumin (BSA) inhibit HIV fusion to the same extent over a broad concentration range. The fusion products of HIV-1 and CL are composed of one virus and one or more liposomes, but the HIV-liposome products show a dramatic retardation in their fusion with plain liposomes. HIV-1 fusion with CL vesicles is temperature dependent. In conclusion, HIV-1 can fuse with model membranes lacking the known viral receptor, CD4, or any other protein, and rCD4 inhibition of HIV-1 fusion is not specific. HIV-1 fusion with model membranes shares similarities (but also distinct differences) with other lipid enveloped viruses such as Sendai and influenza. This work was supported by USPHS Grant AI25534 (ND), U.S.-Israel Binational Science Foundation grant 86-00010 (ND/SN) and fellowships (CEL) from the American Cancer Society (PF-3394) and NIH (AI08117).

M-Pos319

FUSION OF BOVINE LEUKEMIA VIRUS (BLV) WITH CELLS AND LARGE UNILAMELLAR LIPOSOMES.

F. Defrise-Quertain, V. Vonèche*, L. Giurgea**, D. Portetelle* and J-M. Ruysschaert.
Laboratoire de Chimie Physique des Macromolécules aux Interfaces, Université Libre de Bruxelles, CP206/2 1050 Bruxelles, Belgium; *Faculty of Agronomy, 5800 Gembloux, Belgium and **Institut Pasteur du Brabant, rue Engeland, 1180 Bruxelles, Belgium.

Bovine Leukemia Virus (BLV) is a transactivating retrovirus which induces after a period of latency lymphoid tumors in ruminants (Burny et al, 1987). Structurally and functionally, BLV is related to human T lymphotropic viruses HTLV-I and HTLV-II. BLV contains two envelope associated glycoproteins: the external protein gp51 interacts with the receptors on the target cell membrane and the transmembrane protein gp30 induces fusion . Up to now, very little is known about the molecular mechanisms leading to BLV entry into the host cell. Fusion between BLV and natural or model membranes was studied using the assay for lipid mixing based on the relief of self-quenching of octadecyl rhodamine B chloride (R18). Purified BLV was labeled with the fluorophore according to published procedures. After labeling and purification, BLV-R18 was still able to induce syncytia on CC81 cells, usually used for BLV as fusion indicator cells. During interaction of BLV-R18 with large unilamellar vesicles (LUV), fusion was always faster and more important with LUV made of pure cardiolipin. All other lipid compositions tested (eggPC, PC/PE/SM/chol, PS....) were less prone to fuse. BLV-R18 particles bound to CC81 cells at 4°C fuse slowly with those cells at 37°C and pH 7.3 (maximum dequenching of 20% in one hour). The effect of lowering the pH and the temperature on the fusion kinetics is discussed. Well-known anti-gp51 monoclonal antibodies (MAbs) were also used to understand the fusion mechanism at the molecular level. The effect of MAbs directed against important biological epitopes as F, G and H on the R18 dilution into the cell membrane is currently under investigation.

REFERENCE.

A. Burny, Y. Cleuter, R. Kettmann, M. Mammerickx, G. Marbaix, D. Portetelle A. Van Den Broeke, L. Willems and R. Thomas, (1987) Cancer Surveys 6, 139-159

M-Pos320

FUSION GLYCOPROTEIN STRUCTURAL AND FUNCTIONAL DETERMINANTS OF SINDBIS VIRUS NEUROVIRULENCE.

Steven L. Novick and Diane E. Griffin, Departments of Medicine and Neurology, Johns Hopkins University School of Medicine, Meyer 6-181, 600 N. Wolfe St., Baltimore, MD 21205.

Sindbis virus is the type virus of the alphaviruses, positive-strand RNA viruses which are responsible for causing encephalitis in humans and other mammals. The mature virion consists of the viral genome in association with the capsid protein (C), enveloped within a lipid bilayer containing two surface glycoproteins, E1 and E2. The E1 protein contains the fusion activity necessary for viral entry within the endosome of the host cell, and the E2 protein mediates virus attachment to cell surface receptors. Recombinant viruses with single amino acid substitutions have previously been shown to have altered ability to induce cell-cell fusion, and also have altered neurovirulence in mice.

In order to determine the molecular events during virus-cell entry and their relationship to causing disease in an animal, quantitative measurements of virus-cell fusion were made as a function of amino acid substitutions in the E1 glycoprotein, using octadecyl Rhodamine B (R_{18}) labeled virus. Relief of self-quenching was monitored kinetically during fusion with unlabeled cells. Varying pH requirements for viral fusion with neuronal (N18) cells and baby hamster kidney cells (BHK) were observed, revealing a multistep conformational transition during virus-cell fusion. Temperature-dependent studies also showed differential activation energies for this conformational change. These data reveal information regarding the environment of the substituted amino acids within the protein. Pathogenesis studies in two-week-old mice further revealed differential mortality and time of death which can be correlated with the observed differences in fusion activation energies. This work supports the hypothesis that the thermodynamics of virus-cell membrane fusion play an important and limiting role in viral neurovirulence.

M-Pos321

THE EFFECT OF DTT TREATMENT ON BINDING AND FUSION OF RESPIRATORY SYNCYTIAL VIRUS TO MAMMALIAN CELLS.
L.A. Downing, J.M. Bernstein, and A. Walter (introduced by R. Putnam). Wright State University School of Medicine. Dayton, OH 45435.

The Respiratory syncytial virus (RSV) fusion protein (F) must be cleaved into two subunits to be functional. This cleavage exposes a hydrophobic amino acid sequence at the terminus of the F_1 subunit, but the subunits remain associated via a disulfide bond. In addition, there is a cluster of cysteine residues near the membrane spanning region of the fusion protein sequence that is highly conserved among paramyxoviruses. To begin to understand secondary structural requirements of F and the specific role of each of the subunits in the membrane fusion event, RSV was treated with DTT with the expectation that the F_2 portion and/or other structural disulfide bonds would be cleaved. Virus was incubated with or without 3 mM DTT, then labeled with the fluorescent probe octadecylrhodamine (R18) at self-quenching concentrations (85-95% maximal fluorescence). Upon fusion with mammalian cells (HELA or HEp2), the R18 probe disperses into the cell membrane and the subsequent increase in fluorescence is directly proportional to the extent of fusion. Virus was bound to cells on ice, excess virus removed and an aliquot cell-viral complexes was transferred to a cuvette containing buffer at 37 C to initiate fusion. Fusion was measured as percent increase in fluorescence; nonspecific R18 transfer was determined from heat-treated (80 C) R18-RSV. DTT pretreatment did not effect RSV binding to cells. However, the rate of fusion decreased to 47 (+23) % of control rates. Whether this effect is due to loss of the F_2 fragment or other structural changes remains to be determined.

M-Pos322

BILAYER STABILIZERS INHIBIT SENDAI VIRUS FUSION AT NEUTRAL pH BUT NOT ACID-INDUCED FUSION OF INFLUENZA VIRUS
James J. Cheetham[1], Leon C.M. Van Gorkom[1], Thomas D. Flanagan[2] and Richard M. Epand[1], [1]Dept. of Biochemistry, McMaster University, Hamilton, Ont. Canada and [2]Dept. of Microbiology, SUNY Buffalo, Buffalo, NY, USA.

Enveloped animal viruses infect cells, either by fusion with the plasma membrane at neutral pH (ie. Sendai and HIV), or fusion within the endosome at acidic pH (ie. influenza). Both of these processes are thought to be mediated by viral membrane glycoproteins. We have found that several amphipathic sterol derivatives which stabilize the bilayer phase of phosphatidylethanolamine (PE) membranes are potent inhibitors of Sendai virus induced haemolysis of erythrocytes and Sendai virus fusion to erythrocytes and PE containing liposomes, as measured by octadecylrhodamine dequenching. The site of action of these bilayer stabilizers is within the target membrane, and the charge of the amphiphile does not affect its activity. These same bilayer stabilizers however, seem to have little effect on the acid-induced fusion of influenza virus. This difference is not due to a loss of bilayer stabilization at lower pH. The fusion results are analyzed using a kinetic scheme incorporating rate constants for irreversible binding/rearrangement and fusion. We interpret these results as consistent with a model in which neutral pH fusion of Sendai virus is more dependent on the stability of the target membrane than is acid-induced fusion of influenza.

Supported by MRC grant MT-7654 (RME), NIAID grant AI26800 (TDF) and a NSERC pre-doctoral fellowship (JJC).

M-Pos323

Inhibition of Viral Membrane Fusion by Amphipathic Compounds. Philip L. Yeagle and Thomas Flanagan, (Intro. by G. Willsky) Departments of Biochemistry and Microbiology, University at Buffalo School of Medicine (SUNY), Buffalo, NY 14214.

We have examined the inhibition of membrane fusion involving large unilamellar vesicle (LUV) fusion with LUV and Sendai virus fusion with LUV. A contents mixing fluorescence assay (ANTS/DPX) was used for the former and lipid mixing assay (R_{18}) was used for the latter. These fusions have been previously characterized (J. Biol. Chem. 265, 12178 (1990)). The ability of castanospermine, fusidic acid, deoxycholate, and lysophosphatidylcholine to inhibit vesicle-vesicle fusion and virus-vesicle fusion was measured. The patterns of inhibition were different for these compounds. Castanospermine and lysophosphatidylcholine inhibited vesicle-vesicle fusion, but deoxycholate and fusidic acid did not. All but castanospermine inhibited virus-vesicle fusion. ^{31}P NMR was used to characterize the influence of these inhibitors on the lipid morphology. These compounds appear to inhibit membrane fusion by different mechanisms. This work was supported by a grant from the NIH (AI 26800).

M-Pos324

EFFECTS OF THE "FUSION PEPTIDE" FROM MEASLES VIRUS ON THE STRUCTURE OF N-METHYL DIOLEOYLPHOSPHATIDYLETHANOLAMINE MEMBRANES AND THEIR FUSION WITH SENDAI VIRUS†. Philip L. Yeagle*, Richard M. Epand§, Christopher D. Richardson¶ and Thomas D. Flanagan⊥, Departments of *Biochemistry and ⊥Microbiology, University at Buffalo School of Medicine and Biomedical Sciences, Buffalo, NY 14214; §Department of Biochemistry, McMaster University, Hamilton, Ontario; ¶Biotechnology Research Institute (NRC Canada), Montreal, P.Q.

^{31}P nuclear magnetic resonance (NMR) spectroscopy was used to study lipid organization in hydrated preparations of N-methyl dioleoylphosphatidylethanolamine and a "fusion peptide" with the sequence: FAGVVLAGAALGVAAAAQI, which corresponds to the amino terminus of the F1 subunit of the membrane fusion protein of measles virus. These amino acids are believed to mediate syncytia formation, host-cell penetration and hemolysis by infectious virus. The presence of the peptide at 0.5 mole percent significantly facilitated the formation of isotropic ^{31}P resonances. The effects at 1 mole percent were substantially enhanced over the effects observed at 0.5 mole percent, leading to a decrease in the onset temperature of the formation of the isotropic ^{31}P NMR resonances of about 30 °C. The formation of such isotropic ^{31}P NMR resonances was associated with an increased rate of fusion of large unilamellar vesicles (LUV) of N-methyl dioleoylphosphatidylethanolamine. However, only modestly enhanced fusion of octadecyl rhodamine-labelled Sendai virus with N-methyl dioleoylphosphatidylethanolamine LUV was observed when the "fusion peptide" was incorporated into the LUV. This work was supported by a grant from the National Institutes of Health (AI26800) and the Medical Research Council of Canada (MT7654).

M-Pos325

Peptides Representing the NH_2 Terminus (HA2) of Influenza Virus - Interaction with Membrane Models.

M. Rafalski,* A.Rockwell,* J.D.Lear,* A.Ortiz, J.Wilschut, W.F.DeGrado.*
*The Du Pont Co. PO Box 80328, Wilimington DE 19880 Univ. of Groningen, Bloemsingel 10, 9712KZ, Groningen, Holland.

At low pH the N-terminus of the Influenza hemagglutinin HA2 becomes exposed and available to bind and perturb nearby lipid membranes, faciliating fusion. Site specific mutations within this region of molecule severly affect its fusogenic activity (J.Cell Biol.**102**,11,1986). We have investigated the interaction of synthetic peptides, corresponding to the fusion segment (X31strain) with phospholipid (POPC) large unilamellar vesicles (LUV) and POPC monolayers. We have synthesized wild type and variant 20-residue peptides in which either Gly1 or Gly4 were replaced with Glu (E1, E4). All these peptides bind POPC LUVs with low μM range K_d's. Wild type and E4, but not E1 cause contents leakage of POPC LUV and penetrate POPC monolayer in a pH-dependent manner. Membrane interaction of these peptides correlates with their ability to form α-helical secondary structures in the bilayer. The E1 mutant binds to the membrane in a β-conformation. Our results suggest that conformation and depth of membrane penetration by these peptides are important for their functional activity.

M-Pos326

KINETICS OF pH-DEPENDENT FUSION INDUCED BY INFLUENZA HEMAGGLUTININ AND MUTANTS IN THE FUSION PEPTIDE. Christian Schoch and Robert Blumenthal NIH, Bethesda, Md.

We examined the fusogenic activity in cells of influenza hemagglutinin (HA), and of the following HA proteins altered in the amino-terminus of HA2 (fusion peptide) by site-directed mutagenesis (Gething et al, *J. Cell Biol.* **102**, 11-23,1986): M1 and M4, substitutions of GLU for GLY at positions 1 and 4 respectively, and M11, substitution of GLY for GLU at the 11 position. Following expression in Simian cells using SV40-HA recombinant virus vectors, we measured the kinetics of fusion with erythrocytes using a spectrofluorometric fluorescence dequenching assay (Morris et al, *J. Biol. Chem.* **264**, 3972-3978, 1989). In accordance with previous cell biological results M1 did not induce fusion, M11 showed the same pattern as the wild type (WT), and M4 showed a shift of about 0.4 in pH threshold. The overall kinetics of M4 and WT were similar in lag times for the onset of fusion, rise times and extent. A closer examination of the kinetic processes, however, revealed that the lag time could be dissected into at least two components: a commitment time of 5-10s, and a maturation time of 20-30s. Although the maturation times for WT and M4 were similar, the commitment time was more rapid with M4. These results are consistent with the notion that only the relatively rapid components in the overall fusion reaction depend on the structure of the fusion peptide, whereas the slower processes are governed by other factors.

M-Pos327

ROLE OF STERIC AND ELECTROSTATIC BARRIERS IN FUSION OF VESICULAR STOMATITIS VIRUS WITH CELLS
Anu Puri, Settimio Grimaldi and Robert Blumenthal, NIH, Bethesda, Md. (Intr. by D.S. Dimitrov).
Fusion of vesicular stomatitis virus (VSV) with cells and liposomes before and after treatment with neuraminidase was studied using the R18 dequenching assay. Desialylation of VSV significantly enhanced the extent of fusion with Vero cells but affected neither the pH-dependence nor the kinetics (e.g. delay times and initial rates). We measured about the same % binding of VSV and asialo-VSV to Vero cells. The enhanced fusion of asialo-VSV was observed both at the plasma membrane as well as via the endocytic pathway. Asialo-VSV showed enhanced fusion activity with negatively charged (phosphatidylcholine (PC)-phosphatidylserine (PS), 1:1 mole ratio) as well as uncharged (PC) liposomes indicating that intermembrane electrostatic effects did not play a significant role in viral fusion. According to our model, pH-dependent viral fusion occurs when the envelope proteins undergo pH-activated conformational changes while the virus is appropriately bound to the target membrane (Clague et al, *Biochemistry* **29**,1303, 1990). pH-dependent conformational transitions that occur while the virus is not in the proper apposition with respect to the target membrane, will result in a failure to fuse, or "desensitization". If the rates of activation reactions leading to fusion are slow relative to those of the desensitization pathway, suboptimal extents will be reached, whereas rapid activation rates will yield optimal extents. Preincubation of virus-cell complexes at subthreshold pH (6.5) caused desensitization of untreated virus whereas fusion of asialo VSV was not affected. These data are consistent with the notion that removal of steric constraints (e.g. sialic acid) results in more appropriately bound virus and hence an enhanced fusion efficiency.

M-Pos328

STRUCTURAL MODEL OF THE CONFORMATIONAL CHANGES OF INFLUENZA HEMAGGLUTININ THAT LEAD TO FUSION OF VIRAL AND CELL MEMBRANES
H. Robert Guy, Stewart Durrell, and Robert Blumenthal, Lab of Math. Biol., DCBD, NCI, NIH, Bethesda, MD 20892
Hemagglutinin (HA) is the protein on the surface of influenza virus that binds to sialic acid on cell membranes and induces fusion of viral and cell membranes. The HA consists of two disulfide linked glycopolypeptide chains, HA1 and HA2, which are arranged as a trimeric rod consisting of an α-helical stem extending some 10 nm from the virus membrane, surmounted by a globular top portion rich in β structure (Wilson et al, *Nature*, **289**,366-373). The C-terminal of HA2 contains the viral membrane spanning region, and the N-terminal contains the relatively hydrophobic fusion peptide. The sialic acid binding site is on a portion of HA1 that is at the top of the stalk. In our model, initial binding to the target membrane occurs when HA is in the neutral pH conformation. When the pH is lowered, the coiled-coil α helices in the HA2 stem interface dissociate (Doms and Helenius, *J. Virol.* **60**,833-839), and each monomer rotates by approximately 90° so that the long helices of the HA2 chain are parallel to the membrane surfaces. This conformational change pulls the two membranes closer together allowing the exposed fusion peptides to interact with the target membrane. In the model we currently favor, a hexagonal lattice is formed in which adjacent trimers interact. The long α helices of the HA2 chain of adjacent trimers form an antiparallel coiled-coil at a region that has two-fold symmetry; the transmembrane α helices in the viral membrane form a triple stranded coil-coil at the region of three-fold symmetry, and the fusion peptides may form a triple stranded structure that inserts into the target membrane at the region of three-fold symmetry.

M-Pos329

THE DELAY TIME FOR INFLUENZA HAEMAGGLUTININ-INDUCED MEMBRANE FUSION DEPENDS ON THE HAEMAGGLUTININ SURFACE DENSITY.

Michael J. Clague, Christian Schoch and Robert Blumenthal, NIH, Bethesda, Md. (Intr. by R.J. Rubin).

We have studied the kinetics of low pH induced fusion between erythrocyte membranes and membranes containing influenza haemagglutinin using assays based on the fluorescence dequenching of the lipophilic dye octadecylrhodamine B chloride. Stopped-flow mixing and fast data acquisition has been employed to monitor the early stages of influenza virus fusion. We have compared this with the kinetics observed for fusion of an NIH 3T3 cell line, transformed with bovine papilloma virus, which constitutively expresses influenza haemagglutinin (GP4f cells). Virus and GP4f cells both display a pH-dependent time lag before the onset of fluorescence dequenching, but of an order of magnitude difference, ~ 2 seconds versus ~ 20 seconds. We have adopted two strategies to investigate whether the difference in lag time reflects the surface density of acid-activated haemagglutinin, able to undergo productive conformational change. (i) Haemagglutinin expressed on the cell surface requires proteolytic cleavage with trypsin from an inactive HA0 form. We have limited the extent of proteolysis. (ii) By infection of CV-1 cells with a recombinant SV40 virus bearing the influenza haemagglutinin gene. The surface expression of haemagglutinin is a function of time post infection. For low pH induced fusion of both types of cell with erythrocytes, the lag time decreases with increasing haemagglutinin densities. We also show in the instance of virus fusion, that the magnitude of the delay time is a function of the target membrane character.

M-Pos330

THE MINIMAL NUMBER OF PROTEINS AT A MEMBRANE FUSION SITE AND THE DELAY TIME FOR FUSION.

Joe Bentz. Dept. Bioscience & Biotechnology, Drexel University, Philadelphia, PA, 19104.

The problem is to determine the minimal number of membrane fusion proteins which must aggregate together to create a fusion site. If this minimal fusion unit is ω, then the initial rate of fusion will be proportional to the number of aggregates of size ω (i.e. ω-lets) or larger. As the total surface density of the fusion protein increases, the number of ω-lets and higher order aggregates increases. Comparing the change in the number of fused liposomes to the change in the fusion protein surface density can fix the value of ω. We found that influenza hemagglutinin (HA) expressing fibroblasts fuse with a small constant fraction of bound glycophorin bearing liposomes (0.5 μm diameter), following a brief low pH incubation [1] and that **two or more** HA's were required at the fusion site. A general analysis [2] of the underlying kinetics proved that surface aggregation of the HA can occur on any time scale, with respect to the fusion kinetics, and the experimental protocol developed in [1] will produce the same estimates for the minimal fusion unit. Recently, it has been noted with similar systems that fusion shows a delay time, which is strongly temperature dependent [3,4]. It was proposed that this delay depends upon the aggregation of the fusion proteins. While this proposal is reasonable, we have found that the simplest description of the surface aggregation kinetics, which yields delay times consistent with those observed, also predicts that the delay time depends upon the inverse first power of the fusion protein surface density, regardless of the size of the minimal fusion unit. Thus, the delay time cannot be simply correlated with the minimal fusion unit.

(Supported by NIH grant GM31506).

[1] Ellens, H., Bentz, J., Mason, D., Zhang, F. and White, J. (1990) Biochemistry, in press.
[2] Bentz. J. (1991) in Advances in Membrane Fluidity, Drug & Anesthetic Effects. Vol. 5, Eds. R.C. Aloia, C.C. Curtain & L.M. Gordon. Alan R. Liss, Inc., New York, in press.
[3] Sarkar, D.P., Morris, S.J., Eidelman, O., Zimmerberg, J. and Blumenthal, R. (1989) J. Cell Biol. 109, 113-122.
[4] Spruce, A.E., Iwata, A., White, J.M. and Almers, W. (1989) Nature (London) 342, 555-558.

M-Pos331

FUSION OF INFLUENZA VIRUS WITH GLYCOPHORIN BEARING LIPOSOMES: ROLE OF THE TARGET MEMBRANE.

Dennis Alford[1],Harma Ellens[2] and Joe Bentz[1]. [1]Department of Bioscience and Biotechnology, Drexel University, Philadelphia, PA, 19104 and [2]Department of Drug Delivery, SmithKline Beecham, P.O. Box 1539, King of Prussia, PA, 19406-0939.

Previously, we have shown that two or more influenza hemagglutinin (HA) trimers are required at the fusion site using HA-expressing fibroblasts and glycophorin bearing liposomes (diameter ~0.5 mm) [1]. We have proposed fusion intermediates, within this aggregate of HA trimers at low pH,which are based upon a minimal alteration to the known neutral pH structure of HA and which should have reasonable activation energies [2]. In particular, we sought to account for the disposition of the bilayer lipids within fusion intermediates. The glycophorin bearing liposomes bind to the HA-expressing cells specifically through HA-glycophorin interactions and it was found that the low pH induced fusion between the cells and bound liposomes was mediated by HAs not bound to glycophorin. Thus, with respect to the target membrane, the fusion site involves just the lipid bilayer. While it is known that intact influenza virus can fuse with virtually any target bilayer, analysis of the fusion kinetics as a function of the target bilayer composition should permit elucidation of the fusion intermediates. Our first question is on the role of lipid phase behavior and lipid packing constraints.

Supported in part by research grant GM-31506 (JB) from the National Institutes of Health.

[1] Ellens, H., Bentz, J., Mason, D., Zhang, F. and White, J. (1990) Biochemistry, in press.
[2] Bentz, J., Ellens, H. & Alford, D. (1990). submitted.

M-Pos332

MATRIX FREE Na^+ OF ISOLATED PIG HEART MITOCHONDRIA.
D.W.Jung, K.Baysal & G.P.Brierley. Dept of Physiological Chemistry, The Ohio State University, Columbus, OH 43210.

The concentration of free Na^+ in the matrix of isolated pig heart mitochondria (PHM) has been monitored using the fluorescent probe SBFI developed by Tsien & coworkers (JBiolChem. 264:19449 & 19458, 1989). SBFI/AM loading into isolated mitochondria was more difficult than for BCECF/AM, mag-fura/AM or fura-2/AM and was greatly facilitated by the use of pluronic F-127. SBFI loads sufficiently to give signals approx 3-fold greater than non-loaded PHM. As reported for fibroblasts & lymphocytes the sequestered probe displays modified excitation spectra and increased quantum efficiency as compared to buffered salt soln. Calibration curves were generated in situ using ionophores (CCCP, nigericin and gramicidin) to equilibrate Na^+. Ratios (350/390Ex; Em=510) formed from net (loaded minus non-loaded) fluorescence intensities were plotted vs. Na^+ and curve fit to a rectangular hyperbola with a Kd of approx 48mM Na^+. The matrix free Na^+ of isolated PHM is too low to determine accurately (<0.2mM). PHM blocked with rotenone and oligomycin suspended in 0.1M KCl at pH 7.3 maintain a Na^+_{out}/Na^+_{in} gradient of approx 2 when titrated with NaCl up to 100mM. In the presence of succinate the gradient increases to greater than 8. The predicted pH gradients needed to account for these distributions due to Na^+/H^+ exchange alone are 0.3 and 0.9 (matrix alkaline), close to measured values. The addition of P_i to respiring mitochondria in the presence of 20mM Na^+ results in matrix acidification, a decrease in ΔpH and increased matrix Na^+. No significant change in matrix Na^+ was observed when Ca^{2+} was added to ruthenium red-blocked mitochondria. These results indicate the Na^+ gradient maintained across the inner mitochondrial membrane is dependent on the ΔpH and the endogenous Na^+/H^+ exchanger. The observations are consistent with those of Crompton & Heid (EurJBiochem 91:599, 1978) and indicate that the velocity of the Na^+/H^+ antiport relative to Na^+/Ca^{2+} antiport allows the Na^+/H^+ exchange to approach equilibrium. Supported in part by USPHS grant HL09364.

M-Pos333

FLUORESCENCE DIGITAL IMAGING OF INTRACELLULAR pH IN CULTURED NEONATAL RAT HEART CELLS.
VIRENDRA K. SHARMA AND SHEY-SHING SHEU, Department of Pharmacology, University of Rochester School of Medicine and Dentistry, Rochester, NY 14642.

The properties of the Na^+/H^+ exchange system have been studied in 1–2 day and 14–16 day old cultured cells from hearts of newborn rats. Intracellular pH (pH_i) was determined in BCECF-AM loaded cells using fluorescence digital imaging microscopy. The fluorescent ratio image, an indicator of pH_i, showed significant spatial heterogeneity. Areas of high fluorescence intensity occupied 35–40% of the total image. This heterogeneity was most probably caused by the mitochondria which are known to have a higher pH than cytoplasm.

The effect of phorbol ester, phorbol 12,13–dibutyrate (PDBu), on pH_i was also investigated. PDBu (100 nM) increased the pH_i of 1–2 day old myocytes from 7.10 to 7.92 (n = 5) and 14–16 day old cells from 7.15 to 7.55 (n = 5). This effect of PDBu on pH_i was completely blocked by pretreatment of heart cells with 20 μM dimethylamiloride (DMA), a Na^+/H^+ exchange inhibitor. PDBu also failed to increase the pH_i in myocytes pretreated with 0.1 μM staurosporine, a protein kinase C inhibitor.

pH_i recovery from NH_4Cl –induced acidification showed a similar time course in both age groups. Also the decrease in pH_i by 20 μM DMA during steady state had similar magnitude in both the groups of myocytes. These results suggest that Na^+/H^+ exchange system is present in cultured neonatal rat ventricular myocytes. Moreover activation of protein kinase C by PDBu leads to an increase in pH_i via Na^+/H^+ exchange. The greater PDBu–induced change in pH_i in younger myocytes is not due to higher Na^+/H^+ exchange activity in these cells. It is probably due to higher protein kinase C activity and/or a higher sensitivity to PDBu.

M-Pos334

CHARACTERIZATION OF THE CARBOXYL-TERMINAL REGION OF THE RABBIT CARDIAC Na^+/H^+ EXCHANGER.
L. Fliegel, M. Walsh*, C. Wong, J. Dyck, A. Barr. (Intr. by L.B. Smillie) Dept. of Pediatrics and Biochemistry, U. of AB, Edmonton, AB; *Dept. of Medical Biochemistry, U. of Calgary, Calgary, AB, Canada.

The Na^+/H^+ exchanger is a pH regulating protein which extrudes one H^+ in exchange for one Na^+ when intracellular pH decreases. We have isolated a rabbit cardiac Na^+/H^+ exchanger cDNA clone. To characterize the Na^+/H^+ exchanger protein, we expressed the carboxyl-terminal region of this cDNA clone as a fusion protein with β-galactosidase. cDNA of the Na^+/H^+ exchanger, coding for the carboxyl-terminal 178 amino acids, was cloned into the expression vector pEX1 which expresses proteins as a fusion product with β-galactosidase. Control and experimental pEX1-Na^+/H^+ exchanger cDNA were induced to produce the protein. Cells were lysed with a French press and the protein was solubilized from inclusion bodies with 1% sodium-N-lauroyl sarcosine. The fusion protein was purified using a p-aminophenyl-β-D-thiogalactopyranoside-agarose column. The purified experimental product and crude experimental extracts both reacted with an antibody produced against a synthetic peptide of the carboxyl-terminal 14 amino acids, thereby confirming the identity of the expressed protein. Limited digestion of the purified experimental protein with *Staphylococcus aureus* V8 protease followed by western blotting could localize the expressed portion of the protein to a 35 kD fragment. We studied the suitability of the expressed protein to act as a substrate for protein kinase mediated phosphorylation *in vitro*. Purified calmodulin dependent protein kinase II readily phosphorylated the Na^+/H^+ exchanger while this region of the protein was not a substrate for purified protein kinase C or for the catalytic subunit of cyclic AMP dependent protein kinase. This suggests that this region of the protein may be an important regulatory region *in vivo*.

To analyze the intron-exon structure of the rabbit gene encoding for this region of the protein we used polymerase chain reaction. Primers based on the cDNA sequence of the rabbit Na^+/H^+ exchanger were used and these showed that the C-terminal 200 amino acids are contained within one exon. In conclusion our studies show that this region of the protein encodes for a phosphorylatable protein which is contained within a single exon. Supported by MRC and AHFMR.

M-Pos335

PARTIAL PURIFICATION AND RECONSTITUTION OF THE Na^+-SELECTIVE Na^+/H^+ ANTIPORTER FROM BEEF HEART MITOCHONDRIA.
Z. S. Madar and K. D. Garlid. Department of Pharmacology, Medical College of Ohio, Toledo, Ohio 43699.

No identifying ligand exists for the Na^+/H^+ antiporter; therefore its purification for eventual structure-function studies must be followed by reconstitutive activity. The Na^+/H^+ antiporter, first demonstrated by Mitchell and Moyle (Eur. J. Biochem. 9, 149-155, 1969), is one of three mitochondrial antiporters that transport Na^+. The Na^+/H^+, K^+/H^+ and Na^+/Ca^{2+} antiporters each transport Na^+ electroneutrally, but their requirements differ sufficiently to distinguish among them. Mitochondrial proteins were extracted from beef heart SMPs, using Triton X-100, and fractionated on DEAE cellulose. Fractions were reconstituted into proteoliposomes containing the Na^+-selective fluorescent probe SBFI, and Na^+ uptake or efflux was measured with a spectrofluorometer. For initial screenings, we inhibited the K^+/H^+ antiporter irreversibly by treating Mg^{2+} depleted mitochondria with N, N'-dicyclohexylcarbodiimide (K. Garlid et al, J. Biol. Chem. 261, 1529-1535, 1986). The activity of the Na^+/Ca^+ antiporter was abolished by including 1 mM EGTA in the assay medium. We obtained a partially purified fraction free of the other carriers, as confirmed by the absence of Ca^{2+} stimulated Na^+ efflux and the absence of K^+/H^+ antiport. This fraction containing the Na^+/H^+ antiporter contains few proteins, and activity is purified 1000-fold. Li^+, a competitive inhibitor of the Na^+/H^+ antiporter (K. Garlid, in Cellular Ca^{2+} Regulation, Plenum Pub. Corp, 375-364, 1988), inhibited Na^+/H^+ antiport with K_i values of 1-1.5 mM (cis) and 40 mM (trans). Mn^{2+} inhibited Na^+/H^+ antiport with K_i = 0.5 mM. These results agree with those in intact mitochondria and confirm reconstitution of the beef heart mitochondrial Na^+/H^+ antiporter. This research was supported in part by NIH Grants HL 36573 and HL 43814.

M-Pos336

FUNCTIONAL RECONSTITUTION OF RAT UNCOUPLING PROTEIN EXPRESSED HETEROLOGOUSLY IN YEAST.

D.L. Murdza-Inglis, H.V. Patel, K.B. Freeman, Dept. of Biochemistry, McMaster Univ., Hamilton, Ontario L8N 3Z5 and P. Jezek, D.E. Orosz, K.D. Garlid, Dept. of Pharmacology, Medical College of Ohio, Toledo, Ohio 43699. (Introduced by E.E. Daniel)

Uncoupling protein (UCP) is found exclusively within the inner membrane of brown adipose tissue mitochondria where it functions to uncouple oxidative phosphorylation. By transporting protons back across the mitochondrial inner membrane into the matrix, UCP causes a decrease in the proton electrochemical gradient, thereby dissipating the energy stored in the gradient as heat. UCP also transports Cl^- and alkylsulfonates electrophoretically, but the physiological role of anion transport is not yet known. Both H^+ and anion transport are inhibited by purine nucleotides but only H^+ transport is activated by fatty acid. However, the mechanisms of ion transport have yet to be elucidated. In order to investigate structure/function relationships of UCP using site-directed mutagenesis, an expression system in yeast was developed by transforming yeast with an E. coli/S. cerevisiae shuttle vector containing the UCP cDNA under control of the Gal 1 promoter. A high level of expression of UCP was required because of the low molecular activity of H^+ and Cl^- transport by UCP. This was achieved by altering the translation start region in the rat UCP cDNA to one resembling a highly expressed yeast gene. We now report expression of 70-100 μg UCP/mg yeast mitochondrial protein, a level similar to that achieved in brown adipose tissue mitochondria of cold adapted rats. Furthermore, UCP purified from yeast mitochondria and reconstituted into proteoliposomes catalysed rapid, GDP sensitive Cl^- uptake and H^+ ejection, properties indistinguishable from those of the native protein. These studies can now be extended to define the molecular mechanisms of anion and H^+ transport and their regulation by fatty acid and purine nucleotides using site-directed mutagenesis.

M-Pos337

EFFECT OF INSULIN SUPPLEMENTATION ON DIABETES-INDUCED ALTERATIONS IN MITOCHONDRIAL ANION TRANSPORTER FUNCTION.

R.S. Kaplan, J.A. Mayor, R. Blackwell, R.H. Maughon, and G.L. Wilson. Dept. of Pharmacology, College of Medicine, University of South Alabama, Mobile, AL 36688.

We have previously shown that streptozotocin (STZ)-induced diabetes causes a decrease in the level of functional citrate transporter and increases in the levels of functional pyruvate and dicarboxylate transporters that can be extracted from rat liver mitoplasts. These changes were predicted based on diabetes-induced alterations in the activities of enzymes that comprise metabolic pathways to which these transporters either supply substrate or remove product and suggest a possible coordinated regulation. We have now examined the effect of insulin-supplementation of diabetic rats on the functional levels of these three transporters. Insulin treatment normalized the STZ-induced alterations in the functional levels of both the citrate and dicarboxylate transporters. Interestingly, with the pyruvate transporter insulin treatment caused a statistically significant change in the opposite direction to that observed in the diabetic animals (39% increase diabetic; 19% decrease insulin treated diabetic). We conclude that observed alterations in mitochondrial anion transporter function in experimental diabetes are a direct consequence of insulin deprivation since daily injection of insulin reversed such changes. To our knowledge this is the first report to demonstrate insulin regulation of the functional levels of mitochondrial transport proteins. (Supported by a Juvenile Diabetes Foundation International Research Grant and NIH Grant 5R29-GM38785 to R.S.K.).

M-Pos338

ON THE MECHANISM OF BUPIVACAINE-INDUCED UNCOUPLING OF MITOCHONDRIA.

X. Sun and K.D. Garlid. Department of Pharmacology, Medical College of Ohio, Toledo, Ohio 43699.

Bupivacaine, a tertiary amine local anesthetic, strongly stimulates mitochondrial respiration by an unknown mechanism. This action is not due to non-specific membrane damage or ion pair transport. Bupivacaine does collapse $\Delta\Psi$ and catalyzes transport of KOAc in the presence of valinomycin, contradicting the findings of Terada et al (J. Biol. Chem. 265, 7837-7842, 1990). We conclude that bupivacaine specifically mediates H^+ uniport in mitochondria, in agreement with Dabadie et al (FEBS Lett. 226, 77-82, 1987). These workers proposed that bupivacaine acts as a monomeric, cycling protonophore, a mechanism that conflicts with the hypothesis of Garlid and Nakashima (J. Biol. Chem. 258, 7974-7980, 1983): weak bases cannot catalyze significant proton transport because they are unable to delocalize their charge. With kinetic studies, we evaluated whether bupivacaine acts as a monomeric protonophore, a multimeric protonophore or a proton leak-inducer. H^+ transport was studied in the presence of valinomycin by following K^+ efflux with an ion electrode and KOAc uptake using light scattering. Kinetics exclude action as a monomeric protonophore. Bupivacaine could shield its charge by forming multimers; however, a comparison of data obtained by varying concentration with those obtained by varying pH conflict with this interpretation. All data show that transport rate depends exclusively on the third power of neutral bupivacaine base. We propose that bupivacaine accumulates within the membrane, where it provides solvation sites for intramembrane protons (H^+_3O), perhaps by positioning at protein:lipid interfaces. This increase in dielectric constant lowers the energy barrier to protons. The model is supported by the kinetic data and by the finding that bupivacaine-induced H^+ leak is more ohmic than endogenous leak, consistent with appearance of multiple sites (energy wells) along the H^+ pathway (Garlid et al, Biochim. Biophys. Acta. 976, 109-120, 1989). We conclude that bupivacaine is a proton-leak-inducer. Supported by NIH grant GM 31086.

M-Pos339

PURIFICATION AND RECONSTITUTION OF THE RAT LIVER MITOCHONDRIAL K^+ UNIPORTER.

M.G. Hegazy, F. Mahdi, X. Li, G. Gui, G. Mironova, A. Beavis, and K.D. Garlid. Department of Pharmacology, Medical College of Ohio, Toledo, Ohio 43699.

Mitochondrial K^+ content is maintained constant through regulation of two separate processes: the K^+/H^+ antiporter and the K^+ uniporter. In vivo, the K^+ uniporter mediates electrophoretic K^+ influx whereas the K^+/H^+ antiporter mediates electroneutral K^+ efflux (K. Garlid, in Integration of Mitochondrial Function, Plenum Publ. Corp., 257-276, 1988). Since K^+ is the major osmolyte of mitochondria, regulation of this futile K^+ cycle is required for mitochondrial volume homeostasis. The 82 kDa K^+/H^+ antiporter has been purified, reconstituted, immunologically characterized, cloned and partially sequenced. Work on the K^+ uniporter is at an earlier stage, but consensus is growing that this is a 53 kDa protein. Mironova, et al (Biophysics 26, 458-465, 1981) identified a 54-60 kDa protein that gave reconstitutive activity when incorporated into black lipid bilayers. Diwan and co-workers (BBRC 153, 224-230, 1988) identified and partially purified a 53 kDa mitochondrial protein that catalyzes K^+ uniport when it is incorporated into lipid vesicles. Identification was inconclusive because the protein fraction contained several 53 kDa and other proteins. We report purification to homogeneity of a 53 kDa protein from rat liver mitochondria that catalyzes K^+ uniport following reconstitution into liposomes. K^+ uniport was identified by its requirement for protonophore (CCCP). Significantly, the protein was discovered because it co-purified with the 82 kDa K^+/H^+ antiporter (Li, et al, J. Biol. Chem. 265, 15316-15322, 1990), which may indicate that these two K^+ porters are associated within the inner membrane. Analysis by SDS-PAGE and IEF shows a single protein band with M_r 53,000 and pI $\approx$ 6.5. Polyclonal antibodies raised to the 53 kDa protein do not react with the 82 kDa K^+/H^+ antiporter. Labeling of the 53 kDa K^+ uniporter by [^{14}C]dicyclohexylcarbodiimide requires matrix Mg^{2+}, whereas labeling of the 82 kDa K^+/H^+ antiporter is prevented by matrix Mg^{2+}. Supported in part by NIH grants HL 36573 and HL 43814.

M-Pos340

PURIFICATION OF THE SODIUM/CALCIUM EXCHANGER FROM BOVINE CARDIAC SARCOLEMMA.

John T. Durkin, Diane C. Ahrens, Jeffrey D. Hulmes, Yu-Ching E. Pan, and John P. Reeves, Roche Institute of Molecular Biology, Dept. of Protein Biochemistry, Roche Research Center, Nutley, NJ 07110

We have purified the exchanger from bovine cardiac sarcolemmal membranes by the following protocol: i) alkaline extraction (Philipson et.al.,1987, BBA 899:59) ii) solubilization in cholate; iii) anion-exchange on Affi-Gel 102; iv) density gradient centrifugation into polyoxyethylene-9-lauryl ether/glycerol; v) anion exchange on FPLC Mono-Q; and vi) desalting and repeating Mono-Q. Starting with 200 mg of sarcolemmal protein, we purify 40 μg protein. The specific activity of the purified exchanger is greater than 1 μmol calcium per mg protein per second, a purification factor of 40. SDS-PAGE and silver stain reveals two bands of apparent molecular weights 160 kDa and 120 kDa. No other proteins are present in sufficient quantities to account for the observed activity. On Western blots, both bands stain with antibodies to the canine cardiac exchanger (provided by K. Philipson, UCLA) and to the bovine retinal rod exchanger (provided by N. Cook, Max-Planck Institut, Frankfurt). The 160 and 120 kDa proteins have identical NH_2-terminal sequences: ETEM(E/A)G(E/P)GI(E/V)TG (parentheses denote ambiguous positions). The 160 kDa band may be an artifact of sample preparation for SDS-PAGE: its intensity increases, and the intensity of the 120 kDa band decreases, when the samples are boiled.

M-Pos341

SODIUM-CALCIUM EXCHANGE IN RENAL EPITHELIAL CELLS: INHIBITION BY MAGNESIUM AND DEPENDENCE ON CELL SODIUM AND METABOLIC ENERGY.

Rong-Ming Lyu, Lucinda Smith, and Jeffrey B. Smith. Dept. Pharmacology, Schools of Medicine and Dentistry, Univ. Alabama at Birmingham, Birmingham, Alabama 35294.

Na-Ca exchange was assayed by measuring the initial rate of 45Ca uptake or increases in cytosolic free Ca in LLC-MK2 cells. Replacing external Na with potassium failed to increase 45Ca uptake unless the cells were treated with ouabain. Ouabain increased intracellular Na from 15 to 67 mM. Replacing external Na with tetramethylammonium or potassium evoked about a six-fold increase in cytosolic free Ca in cells that were incubated with ouabain, but had little, if any, significant effect on free Ca in cells that were not treated with ouabain. Therefore, it is necessary both to increase cell Na and decrease external Na to produce detectable 45Ca influx via the exchanger. The high K1/2 for Na relative to cell Na apparently prevents Ca influx via the exchanger even at 140 mM external potassium. The dependence of Na gradient-dependent 45Ca uptake on cell Na gave a K1/2 of 27 mM and a Hill coefficient of 2.8 ± 0.3. Mg competitively inhibited 45Ca uptake via the exchanger (Ki = 80 ± 10 μM). Mg also inhibited Ca-stimulated 22Na efflux from Na-loaded cells. Because Mg failed to stimulate 22Na efflux, the exchanger does not cause detectable 22Na-Mg exchange. High external potassium (140 mM) decreased the potency of Mg 6.7-fold, increased the Vmax by 75%, and had no effect on the Km for Ca. The Vmax was 38.7 ± 7.0 and 22.4 ± 3.6 nmol/min mg and the Km for Ca was 220 ± 10 and 260 ± 50 μM in the presence of 140 mM KCl or N-methyl-D-glucamine chloride, respectively. Decreasing cellular ATP by treating the cells with deoxyglucose and a mitochondrial poison (oligomycin, antimycin A, rotenone, or dinitrophenol) strongly inhibited Na-Ca exchange. Glucose prevented the poisons from decreasing cellular ATP and Na-Ca exchange indicating that the poisons do not directly inhibit exchange. Repletion of ATP by removing the poisons and adding glucose restored exchange activity. The characteristics of Na-Ca exchange in the renal epithelial cells (including Vmax, Km for Ca, Ki for Mg and effects of potassium on Mg inhibition, as well as the dependence on metabolic energy) are very similar to those of the Na-Ca exchanger in rat aortic myocytes.

M-Pos342

COMPETITIVE AND NONCOMPETITIVE INTERACTIONS OF $[Na^+]_i$ and $[Ca^{2+}]_i$ IN THE Na^+/Ca^{2+} EXCHANGE SYSTEM IN GIANT CARDIAC MEMBRANE PATCHES: CHARACTERISTICS OF A MINIMUM MODEL.

D.W. Hilgemann / Dept. of Physiology, UTSW Med.Ctr., Dallas, TX, 75235.

The $[Ca]_i$- and time-dependence of inward I_{NaCa} and are expected to importantly control $[Ca]_i$ and E_m in cardiac muscle. In the presence of $[Na]_i$ (10-40 mM), the $[Ca]_i$-dependence of inward I_{NaCa} (i.e. Ca^{++} efflux) becomes steep (apparent slope, 1.4 to 2). In addition, $[Na]_i$ acts on the $[Ca]_i$ dependence of I_{NaCa} by both shifting the apparent K_d and reducing the maximum current. Upon removal of $[Na]_i$, $-I_{NaCa}$ recovers in an immediate and a slow phase (0.2-0.8 s^{-1}). The slow phase is removed by chymotrypsin, which also abolishes steepness of the $-I_{NaCa}$-$[Ca]_i$ relation in the presence of $[Na]_i$ and shifts inhibition of $-I_{NaCa}$ by $[Na]_i$ to higher $[Na]_i$. Chymotrypsin does not remove noncompetitive inhibition of $-I_{NaCa}$ by $[Na]_i$, and $[Na]_i$ is a strong (steep) inhibitor of both regulated and deregulated $-I_{NaCa}$ (K_d, 7 to 25 mM with 1 to 6μM $[Ca^{2+}]_i$; 'slope', 1.8). By contrast to $-I_{NaCa}$, cytoplasmic Ca^{2+}-Na^+ interactions with respect to $+I_{NaCa}$ exhibit a simple competitive behavior in chymotrypsin-deregulated patches; high sodium overcomes inhibition by up to 0.25 mM $[Ca^{++}]_i$.

All data on the chymotrypsin-deregulated system have been simultaneously fit by a least squares method to a simple consecutive exchange model with the following features: 1) Voltage-dependent sodium translocation. 2) Consecutive sodium binding. 3) Transition to an inactive state from fully unoccupied exchanger. 4) Exclusive binding of 2Na or 1Ca at 1st 2 Na binding sites with Na binding at 3rd site unchanged by Ca occupation.

Data on the regulated system is simulated by assuming additionally two inactivation processes; a sodium-independent process with Ca-dependent recovery and a Na-dependent inactivation process from the fully loaded cytoplasmic-oriented state.

M-Pos343

STEADY-STATE ION DEPENDENCIES OF CHYMOTRYPSIN-DEREGULATED CARDIAC Na^+/Ca^{2+} EXCHANGE CURRENT CONFORM TO CONSECUTIVE MECHANISM WITH VOLTAGE-DEPENDENCE IN THE SODIUM TRANSLOCATION PATHWAY.

D.W. Hilgemann & G.A. Nagel / Department of Physiology, UTSW, Dallas, TX, 75235; and Laboratory of Cardiac Physiology, The Rockefeller University, NY, NY, 10021.

Sodium-calcium exchange current (I_{NaCa}) was monitored in giant excised inside-out cardiac membrane patches (15-19 μm diameter;1-5 gigaohm seals) with perfusion of the pipette by the Soejima/Noma method (Pflügers Arch 400:424,1984). Secondary exchange modulation by cytoplasmic Ca^{2+} and Na^+ was removed with chymotrypsin (Hilgemann, Nature 344:242,1990) and complete ion dependencies of inward (-) and outward (+) I_{NaCa} were determined under zero-trans conditions. Nonspecific Ca-activated cation current was absent. $[Ca^{2+}]_i$-activated $-I_{NaCa}$ was completely removed by substitution of $[Na]_o$ for $[Li]_o$, and $[Na]_i$-activated $+I_{NaCa}$ was completely removed by substitution of $[Ca^{2+}]_o$ for $[Mg^{2+}]_o$. The $[Ca^{2+}]_i$-dependence of $-I_{NaCa}$ shifts from a half-maximum of 4 μM (or more) to 1 μM (or less) with reduction of $[Na^+]_o$ from 150 to 30 mM; it shifts to higher $[Ca^{2+}]_i$ with stimulation by hyperpolarization. The $[Na^+]_i$-dependence of $+I_{NaCa}$ shifts from a half-maximim of 15 mM (or more) to 8 mM (or less) with reduction of $[Ca^{2+}]_o$ from 5 mM to 0.15 mM; it shifts weakly to higher $[Na^+]_i$ or does not change with inhibition by hyperpolarization. The results are consistent with a consecutive exchange model and are inconsistent with charge movement in the calcium translocation pathway. Relatively small effects of E_m on the $[Na]_i$ dependence of $+I_{NaCa}$ are consistent with an E_m-dependent step subsequent to occlusion of Na_i from the cytoplasmic side (e.g. release of Na^+ ions at the external side, analgous to the sodium pump).

M-Pos344

MOLECULAR CLONING AND FUNCTIONAL EXPRESSION OF THE CARDIAC SARCOLEMMAL Na^+-Ca^{2+} EXCHANGER.

Debora A. Nicoll, Stefano Longoni, Kenneth D. Philipson.

Cardiovascular Research Laboratory, UCLA School of Medicine, Los Angeles CA 90024

A cDNA clone for the cardiac sarcolemmal Na^+-Ca^{2+} exchanger was identified by the ability of cRNA, copied from the clone, to induce the expression of exchanger activity in oocytes from *Xenopus laevis* (Science, in press). The exchanger clone encodes for a protein of 970 amino acids. A polypeptide corresponding to a segment of the exchanger protein was synthesized and used to generate a polyclonal antibody. The anti-peptide antibody recognizes proteins at 160, 120, and 70 kDa, thereby confirming that these proteins are associated with exchanger activity. We have identified a cleaved leader peptide, sites of glycosylation, and potential sites for calmodulin-binding, high-affinity Ca^{2+} regulation, and ion translocation. A model encompassing these features will be presented.

M-Pos345

IDENTIFICATION OF A PEPTIDE INHIBITOR OF THE CARDIAC SARCOLEMMAL Na^+-Ca^{2+} EXCHANGER

Zhaoping Li, Debora A. Nicoll, Anthony Collins, Donald W. Hilgemann, Adelaida G. Filoteo, John T. Penniston, John M. Tomich, and Kenneth D. Philipson (Intro. by J.S. Frank)
UCLA School of Medicine, University of Texas Southwestern Medical Center, Mayo Clinic, and Children's Hospital of Los Angeles.

The deduced amino acid sequence of the cardiac sarcolemmal Na^+-Ca^{2+} exchanger has a region which could represent a calmodulin binding site. As calmodulin binding regions of proteins often have an auto-inhibitory role, a synthetic peptide with this sequence was tested for functional effects on Na^+-Ca^{2+} exchange activity. The peptide inhibits the Na_i^+-dependent Ca^{2+} uptake ($K_I \sim 1.5\ \mu M$) and the Na_o^+-dependent Ca^{2+} efflux of sarcolemmal vesicles in a noncompetitive manner with respect to both Na^+ and Ca^{2+}. The peptide is also a potent inhibitor ($K_I \sim 0.1\ \mu M$) of the Na^+-Ca^{2+} exchange current of excised sarcolemmal patches. The binding site for the peptide on the exchanger is on the cytoplasmic surface of the membrane. The exchanger inhibitory peptide binds calmodulin with a moderately high affinity. From the characteristics of the inhibition of the exchange of sarcolemmal vesicles, we deduce that only inside-out sarcolemmal vesicles participate in the usual Na^+-Ca^{2+} exchange assay. This contrasts with the common assumption that both inside-out and rightside-out vesicles exhibit exchange activity.

M-Pos346

PURIFICATION AND IDENTIFICATION OF THE CARDIAC SARCOLEMMAL Na/Ca EXCHANGER.

A. Ambesi, E.E. Bagwell and G.E. Lindenmayer, Departments of Pharmacology and Medicine, Medical University of South Carolina, Charleston, S.C. 29425.

The cardiac sarcolemmal Na/Ca exchanger promotes the coupled movement of sodium and calcium across the cell membrane in a reversible, electrogenic manner linking changes in intracellular sodium and, partly, membrane potential to changes in intracellular free calcium and myocardial tension development. Purification of the Na/Ca exchanger from canine myocardium was accomplished using the following sequence: (1) isolation of sarcolemma (SL); (2) alkaline extraction of membranes; (3) solubilization with CHAPS; (4) DEAE chromatography; (5) concentration of active fraction; (6) HPLC gel filtration chromatography; (7) addition of cholate and phospholipids; (8) wheat germ agglutinin chromatography followed by (9) reconstitution into proteoliposomes. Specific activity was increased from 5.2 (SL) to 3766 nmol/mg/sec with recovery of 13.5% activity and 0.02% protein. SDS-PAGE (4-12% gradient) of the purified Na/Ca exchanger, under reducing conditions, revealed prominent proteins of 140, 120 and 75 kDa. Polyclonal antibodies developed against the reconstituted, purified Na/Ca exchanger recognized the three prominent proteins and two minor proteins of 100 and 85 kDa, and immunoprecipitated 98% of the Na/Ca exchanger from detergent-solubilized sarcolemma. Antibodies, antigen purified from each of the three prominent proteins, immunoprecipitated 80-95% of the Na/Ca exchanger and were found to cross-react with each of the other two prominent proteins as well as the minor 85 kDa protein but not with the minor 100 kDa protein. These data support the hypothesis that one or more of the three prominent proteins are involved with Na/Ca exchange across cardiac sarcolemma. Furthermore, immunological cross-reactivity is consistent with the hypothesis that the 75, 85 and 120 kDa proteins are proteolytic products of the 140 kDa protein. In bovine, porcine and rat heart microsomes, the polyclonal antibodies reacted with proteins that appear to be comparable to the 140 and 120 kDa proteins in canine cardiac sarcolemma. However, the intensity of reaction in the 75 kDa region was much reduced. Interestingly, the major band upon immunoblotting of canine whole kidney microsomes was 100 kDa (concluded to be a contaminant of the exchanger preparation purified from canine heart). Supported by NIH HL 42040.

M-Pos347

ENERGY TRANSDUCTION IN PHOTOSYNTHESIS.
Roger E. Clapp, The Mitre Corporation, Bedford, Massachusetts 01730.

Evidence from optical spectra and from magnetic circular dichroism [Clapp, Theoret. Chim. Acta 61, 105 (1982)] suggests that the energy in a primary step of green plant photosynthesis is stored in the motion of electrons circulating in a chlorophyll molecule, accompanying and coupled to the "high-energy electron." The associated magnetic field then participates directly in the energy transfer from molecule to molecule in the photosynthetic chain. In particular, the kinetic energy carried by nine electrons circulating in a 19-bond orbit in chlorophyll is about the same as the kinetic energy of one electron in the 6-bond orbit in quinone. In this view the "high-energy electron" need not hop across a spatial gap carrying the main store of energy. Instead the energy is passed magnetically from circulating currents on a donor molecule to circulating currents on an acceptor molecule. Eventually a positive charge migrates back along a molecular chain to neutralize the donor. For example, in the analogous bacterial reaction center [Deisenhofer and Michel, Science 245, 1463 (1989)] the magnetic energy can pass from the special pair of bacteriochlorophyll (BC) molecules to the accessory BC and then to the bacteriopheophytin (BP); the positive charge can return along a phytyl chain that nests in a cleft adjacent to these molecules. A further transfer of magnetic energy to a plastoquinone can be followed by migration of a positive charge back along the plastoquinone's isoprenoid tail to the BP. The result is that the energy travels forward along with the negative charge, losing just enough by dissipation to generate a disposable modicum of entropy, whose creation then ensures that the steps are generally irreversible.

M-Pos348

THE g=4.1 EPR SIGNAL OF THE S_2 STATE OF THE PHOTOSYNTHETIC OXYGEN EVOLVING COMPLEX ARISES FROM A MULTINUCLEAR MANGANESE CLUSTER

Dennis H. Kim,[†,§] R. David Britt,[‡] Melvin P. Klein,[†] and Kenneth Sauer[†,§]

[†]*Laboratory of Chemical Biodynamics, Lawrence Berkeley Laboratory*
[§]*Department of Chemistry, University of California, Berkeley, CA 94720*
[‡]*Department of Chemistry, University of California, Davis, CA 95616*

We have recently reported the first observation of resolved Mn hyperfine structure on the g=4.1 EPR signal arising from the S_2 state of the oxygen evolving complex of Photosystem II (Kim, Britt, Klein and Sauer; *J. Am. Chem. Soc., in press*). In oriented ammonia-treated membranes, we observe the g=4.1 EPR signal with at least 16 Mn hyperfine lines with a regular spacing of approximately 36 G. The signal is highly anisotropic, with maximum resolution of Mn hyperfine structure observed when the membrane normal is oriented parallel to the applied magnetic field. The resolution of hyperfine structure allows us to conclusively assign the g=4.1 EPR signal to a Mn center. Furthermore, the number and spacing of hyperfine lines allow us to rule out an isolated Mn(IV) origin for the g=4.1 EPR signal. The results are strongly suggestive of a model where under conditions of ammonia inhibition of oxygen evolution, both the g=4.1 and g=2 "multiline" EPR signals of the S_2 state arise from a single mixed-valence Mn cluster, probably consisting of four Mn atoms, which can present either an S=1/2 or an S=3/2 ground state depending on slight configurational differences.

Acknowledgment This work was supported by a grant from the National Science Foundation (DMB-8804526) and by the Director, Office of Energy Research, Office of Basic Energy Sciences, Division of Energy Biosciences of the U. S. Department of Energy under contract DE-AC0376SF00098. D. H. K. gratefully acknowledges the receipt of a University of California President's Undergraduate Fellowship (1989-90). R. D. B. gratefully acknowledges support from the Camille and Henry Dreyfus Foundation.

M-Pos349

^{13}C MAGIC ANGLE SPINNING NMR STUDIES OF BATHORHODOPSIN.
S.O. Smith[1], J. Courtin[2], H. de Groot[2], R. Gebhard[2] and J. Lugtenburg[2]. [1]Dept. of Molecular Biophysics and Biochemistry, Yale University, New Haven, CT; [2]Dept. of Chemistry, Rijksuniversiteit te Leiden, Leiden The Netherlands.

Magic angle spinning NMR spectra have been obtained of the bathorhodopsin photointermediate trapped at low temperature (<130 K) using isorhodopsin samples regenerated with retinal specifically ^{13}C-labeled at positions 8, 10, 11, 12, 13, 14, and 15. Comparison of the chemical shifts of the bathorhodopsin resonances with those of an all-*trans* retinal protonated Schiff base (PSB) chloride salt show the largest difference (6.2 ppm) at position 13 of the protein-bound retinal. Small differences in chemical shift between bathorhodopsin and the all-*trans* PSB model compound are also observed at positions 10, 11 and 12. The effects are almost equal in magnitude to those previously observed in rhodopsin and isorhodopsin [Smith et al., **Biochemistry** 29, 8158]. Consequently, the energy stored in the primary photoproduct bathorhodopsin does not give rise to any substantial change in the average electron density at the labeled positions. The data indicate that the electronic and structural properties of the protein environment are similar to those in rhodopsin and isorhodopsin. In particular a previously proposed protein perturbation near position 13 of the retinal appears not to change its position significantly with respect to the chromophore upon isomerization. The data effectively exclude charge separation between the chromophore and a protein residue as a mechanism for energy storage in the primary photoproduct and argue that the light-energy is stored in the form of distortions of the bathorhodopsin chromophore.

M-Pos350

STARK EFFECT SPECTROSCOPY OF PHOTOSYNTHETIC REACTION CENTERS AT 1.5 K.
Laura T. Mazzola, Thomas R. Middendorf, Steven G. Boxer, Dept. of Chemistry, Stanford University, Stanford, CA 94305. Dale Gaul, Craig C. Schenck, Dept. of Biochemistry, Colorado State University, Fort Collins, CO 80523.

The effect of an applied electric field on the absorption spectrum of wild type (WT) and the Tyr M210→ Phe mutant [(M)Y210F] of *Rb. Sphaeroides* RC's has been measured at 1.5 K in glycerol/water glasses. In previous experiments at 77 K, it was found that the lineshape of the Stark spectrum in the region of the lovest energy electronic transition of the primary electron donor P is closely approximated by the second derivative of the absorption spectrum. This result indicates that the effect due to the change in permanent dipole moment between the ground and excited states of P, $\Delta\mu$, dominates effects due to polarizability changes or field-induced changes in oscillator strength, which give different lineshapes. We report here our observation of a striking change in the Stark lineshape of P when the temperature is lowered to 1.5 K. The figure shows the Stark effect spectrum for (M)Y210F RC's in a 50% v/v glycerol glass at 1.5 K in an applied field of 1.23×10^5 V/cm (dashed line) and the corresponding absorption second derivative (solid line, scaled to same magnitude as Stark). The 1.5 K Stark and second derivative spectra differ significantly in the region of the negative features at ~10,900 and ~11,100 cm^{-1}. Similar deviations were observed in WT RC's at both temperatures. At 1.5 K, but not 77 K, a shoulder is seen on the low energy side of the P absorption band, leading to the highly structured second derivative. A variation in $\Delta\mu$ across the P absorption band may lead to the observed deviation from a pure second derivative Stark lineshape at 1.5 K. The extreme limit of such a variation would be the presence of two or more absorption bands in this region, with different linewidths and different values of $\Delta\mu$.

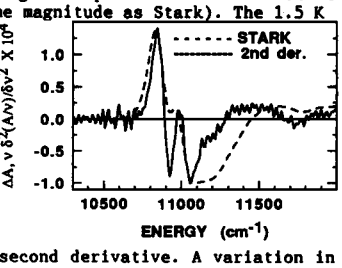

M-Pos351

STARK EFFECT SPECTROSCOPY OF CAROTENOIDS IN PHOTOSYNTHETIC ANTENNA AND REACTION CENTER COMPLEXES. Martin A. Steffen, David S. Gottfried, and Steven G. Boxer. Dept. of Chemistry, Stanford University, Stanford, CA 94305

The effects of electric fields on the absorption spectra of the carotenoids spheroidene and spheroidenone in antenna and reaction center complexes are compared with those for the isolated pigments in organic glasses. The field effects are surprisingly large in spheroidene, and even larger for spheroidenone. In general, the effects for both carotenoids are largest in the B800-850 antenna complex, slightly less in wild-type and mutant reaction centers from *Rb. sphaeroides* and *Rb. capsulatus*, and significantly smaller in the organic glasses. Furthermore, the electrochromic effects for carotenoids are also much larger than those for the Q_X transitions of the bacteriochlorophyll and bacteriopheophytin pigments which absorb in the 450 - 700 nm spectral region.

The Stark spectra of carotenoids in the protein complexes are dominated by changes in the permanent dipole moment between the ground and excited states. This contrasts with isolated spheroidene in a frozen 3-methylpentane glass, in which the change in the dipole moment is considerably smaller, revealing a significant change in the polarizability upon photoexcitation. These results are consistent with a large perturbation on the electronic structure of the carotenoids induced by the structured environments of the protein complexes. The derived values of the change in dipole moment can be used to quantitatively measure transmembrane potentials using carotenoid bandshifts. Furthermore, these results provide an explanation for the linear dependence of the carotenoid bandshift on transmembrane potential in uniaxially oriented systems [Jackson, J., and Crofts, A., *FEBS Lett.* 4, 185 (1969)].

M-Pos352

ABSORPTION AND LINEAR DICHROISM SPECTROSCOPY AT LOW TEMPERATURE OF SINGLE CRYSTALS OF THE REACTION CENTER FROM *Rhodobacter sphaeroides* WILD TYPE STRAIN 2.4.1

Harry A. Frank, Mila A. Aldema, Carol A. Violette and Pierre H. Parot. Department of Chemistry, University of Connecticut, Storrs, Connecticut 06269-3060 USA.

The absorbance, polarized absorbance and linear dichroism spectra of single crystals of the reaction center isolated from *Rhodobacter sphaeroides* wild type strain 2.4.1 have been observed at 85K. The crystals were obtained by the vapor diffusion technique. 50µl droplets containing 30µM reaction centers, 0.8% β-octylglucoside, 10% (w/v) PEG 4000, 1% 1,2,3-heptanetriol, 0.12M NaCl, 10mM Tris buffer at pH, 8.0, 1mM EDTA and 0.1% NaN_3 were equilibrated against 22% (w/v) PEG 4000, 0.25M NaCl, 10mM Tris buffer at pH 8.0, 1mM EDTA and 0.1% NaN_3. After several weeks at 22°C, needle-like, prismatic crystals could be observed. The spectroscopic experiments on these crystals were performed using an optical microspectrometer featuring a custom-built, liquid N_2-flowing cold stage. The crystals were mounted in the cold stage onto optical windows which were fixed in the center of a hollow ring made from O_2-free copper through which the liquid nitrogen was flowed. These data demonstrate the feasibility of conducting optical spectroscopic experiments at cryogenic temperatures on single crystals of photosynthetic reaction center pigment-protein complexes. Several of the spectral changes observed upon cooling the crystal to low temperature are also observed for purified reaction center solutions. This finding and the high degree of linear dichroism observed in the crystals indicate that the integrity and structure of the crystalline complex remain high upon lowering the temperature. This work is supported by grants from the USDA (88-37130-3938) and NIH (GM-30353).

M-Pos353

PROBING THE Q_A ENVIRONMENT IN PHOTOSYNTHETIC BACTERIAL REACTION CENTERS BY LIGHT-INDUCED FTIR DIFFERENCE SPECTROSCOPY.

J. Breton[1], D.L. Thibodeau[1], C. Berthomieu[1], W. Mäntele[2], A. Verméglio[3] & E. Nabedryk[1].
[1]DBCM, C.E.N. Saclay, 91191 Gif-sur-Yvette Cedex, France. [2]Institut für Biophysik und Strahlenbiologie, Universität Freiburg, 7800 Freiburg, FRG. [3]DPVE, C.E.N. Cadarache, B.P. n°1, 13108 St Paul lez Durance Cedex, France.

The photoreduction of the primary electron acceptor, Q_A, has been characterized by light-induced FTIR difference spectroscopy for *Rb. sphaeroides* reaction centers (a) and for *Rsp. rubrum* and *Rp. viridis* (b) chromatophores in the presence of redox compounds which rapidly reduce the photooxidized primary electron donor P^+, and of inhibitors of Q_A^- to Q_B electron transfer. This approach yields FTIR spectra free from P and P^+ contributions. Evidence for Q_A^- formation is demonstrated by the light-induced difference spectrum in the near-IR (see inset for *Rb. sphaeroides* RC). The Q_A^-/Q_A spectrum of *Rb. sphaeroides* compares strikingly well with that of *Rsp. rubrum* chromatophores (not shown), which also contain ubiquinone-10 at the Q_A site. However, large differences in the Q_A^-/Q_A spectra of *Rb. sphaeroides* and *Rp. viridis* are observed in the 1500-1380 cm^{-1} region of the semiquinone anion and can be attributed to the different chemical nature of Q_A in the two species (menaquinone in *Rp. viridis*). On the other hand, the signals in the 1750-1640-cm^{-1} C=O region are very similar in *Rb. sphaeroides*, *Rsp. rubrum* and *Rp. viridis*, suggesting that contributions from aminoacid C=O predominate over that of C=O from the neutral quinone, especially for the bands at ≈1650 cm^{-1} and ≈1670 cm^{-1}.

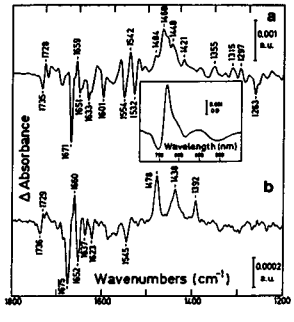

M-Pos354

CHARACTERIZATION OF "P" OXIDATION AND "Q" REDUCTION IN BACTERIAL REACTION CENTERS BY REDOX-TRIGGERED IR DIFFERENCE SPECTROSCOPY

W. Mäntele, M. Bauscher, M. Leonhard, E. Nabedryk*, J. Breton*, D. Moss; Institut für Biophysik, Albertstraße 23, 7800 Freiburg FRG; *Service de Biophysique, CEN Saclay, 91191 Gif-s-Yvette France

Electrochemically-triggered redox reactions have been used to obtain IR difference spectra of P/P^+ and Q/Q^- formation in *Rb. sphaeroides* R26 RC, with FeCy and BV as mediators. Controls for P/P^+ formation and for Q/Q^- formation were performed by simultaneously monitoring the VIS-NIR signals characteristic for these states as well as by probing flash-induced electron transfer. The redox-induced IR difference spectra can be precisely triggered by the selection of the potential range and are completely reversible. The P^+/P FTIR difference spectrum (A: 0.4 V/0 V; *vs.* Ag/AgCl) closely resembles the light-induced P^+Q^-/PQ difference spectrum generated from the same RC sample at 0 V (data not shown). Subtraction (P^+Q^-/PQ minus P^+/P) yields a "constructed" Q^-/Q spectrum, which agrees well with the electrochemically generated Q^-/Q difference spectrum (B: -0.5 V/0 V). The P^+/P spectrum largely represents alterations of bond energies of the dimeric BChl, with only little influence from protein vibrations. In the Q^-/Q spectrum, contributions from protein amide I and side chain group vibrations prevail in addition to quinone C=O and C=C vibrations.

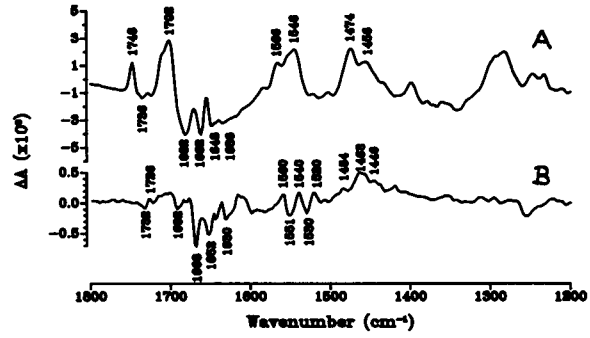

M-Pos355

PHOTOCHEMICAL HOLEBURNING IN A PHOTOSYNTHETIC REACTION CENTER MUTANT WITH ALTERED CHARGE SEPARATION KINETICS. Thomas R. Middendorf, Laura T. Mazzola, Steven G. Boxer, Dept. of Chemistry, Stanford University, Stanford, CA 94305. Dale Gaul, Craig C. Schenck, Dept. of Biochemistry, Colorado State University, Fort Collins, CO 80523.

Photochemical holeburning spectroscopy has been used to study excited-state dynamics and vibronic coupling in the Tyr M210→ Phe mutant [(M)Y210F] of *Rb. Sphaeroides* RC's. The figure is a high resolution difference spectrum showing narrow zero-phonon holes burned with a multiline cw diode laser on the extreme red side of the absorption band of the primary electron donor P in (M)Y210F and wild-type (WT) RC's in a glycerol/buffer glass at 1.5 K. Zero-phonon holes corresponding to each of the individual burn laser lines are observed in (M)Y210F while the holes in WT are clearly broader than the spacing between the laser lines. Analysis of the spectra indicates that the zero-phonon holewidth is ~6 times narrower in (M)Y210F than in WT RC's. Transient absorption measurements performed at 80 K by Parson *et al.* (in press) indicate that the excited-state lifetime of P is ~6 times longer in (M)Y210F than in WT. The agreement between the two experiments indicates that the overall decay rate of *P is the same as the decay rate of the lowest vibrational and phonon level of that state. These results have important implications for the excited-state dynamics of the RC, for they suggest that rapid vibrational relaxation in *P occurs prior to electron transfer. In addition to the narrow holes at the burn wavelength, a much more intense, broad (~400 cm^{-1}) background bleach is observed in (M)Y210F and WT RC's. We have analyzed the overall holeshapes using a vibronic coupling model to obtain quantitative estimates of the inhomogeneous linewidth and the Huang-Rhys factors for the coupled modes.

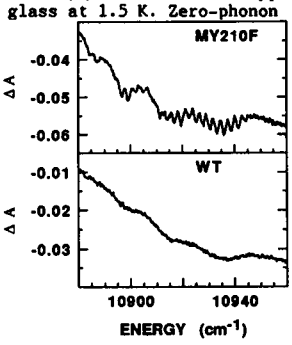

M-Pos356

ESTIMATION OF THE PLASTOQUINONE LATERAL DIFFUSION COEFFICIENT IN SPINACH THYLAKOIDS AND SUBTHYLAKOIDS BY THE PYRENE FLUORESCENCE QUENCHING TECHNIQUE. Scott Gygax, Debbie Czarniecki, Wendy Hill, and Mary Blackwell. Department of Chemistry, Lawrence University, Appleton WI 54911.

Pyrene fluorescence quenching techniques were used to explore the diffusional mobility of plastoquinone in spinach chloroplasts. Nonintegral membrane proteins that most likely do not affect lateral mobility were removed from spinach chloroplasts in order to assess their intrinsic membrane protein composition. Washing with high salt concentrations (0.15 M NaCl or 2 M NaBr) reduces the protein/chlorophyll ratio by about a factor of two, resulting in 36 weight % protein for thylakoids and 30 or 42 weight % for stromal or granal subthylakoids, respectively. Plastoquinone was removed by solvent extraction of lyophilized thylakoids or subthylakoids and reincorporated by several different procedures, including reconstitution with known amounts of pyrene and plastoquinone in aqueous buffers containing detergents. Membranes were reformed by dilution of the detergent incubation mixture to a concentration below the detergent critical micellar concentration. The extent of plastoquinone and pyrene incorporation was quantitated by spectrophotometric analysis of fractions from sucrose density gradients. Only partial incorporation was observed, with the degree of incorporation dependent upon the procedure used. Several pyrene fluorescence quenching measurements in whole thylakoids and subthylakoid fractions have failed to show significant quenching, despite evidence indicating significant incorporation. This suggests that the plastoquinone diffusion coefficient is too small to be measured by the fluorescence quenching method, i.e. less than about $10^{-8}cm^2sec^{-1}$. In order to verify that the observed lack of quenching corresponds to a decrease in plastoquinone lateral mobility, quenching measurements were carried out in thylakoids and subthylakoids diluted with soybean phosphatidylcholine. Preliminary results suggest that the plastoquinone diffusion coefficient correlates positively with the amount of lipid present in diluted membranes. Thus it seems likely that the plastoquinone diffusion coefficient may well be signficantly less than $O(10^{-8}cm^2sec^{-1})$.

M-Pos357

A QUANTITATIVE DESCRIPTION OF FLUORESCENCE EXCITATION SPECTRA IN INTACT BEAN LEAVES GREENED UNDER INTERMITTENT LIGHT

Erhard Pfündel[1] & Ellen Baake[2](Intro. by Richard A.Dilley)

[1]Purdue University, Dept. of Biological Sciences, Lilly Hall of Life Sciences, West Lafayette, IN 47907; [2]Inst. of Mathematics, Universitätsstr. 2, D-8900 Augsburg, FRG.

We present a simple approach for the calculation of in vivo fluorescence excitation spectra from measured absorbance spectra of the isolated pigments involved. Taking into account shading of the leaf pigments by each other, energy transfer from carotene to chlorophyll a, and light scattering by the leaf tissue, we arrive at a model function with 6 free parameters. Fitting them to the measured fluorescence excitation spectrum yields good correspondence between theory and experiment, and parameter estimates which agree with independent measurements. The results are discussed with respect to the origin and the interpretation of in vivo excitation spectra.

M-Pos358

ELECTRIC FIELD INDUCED REVERSE ELECTRON TRANSFER IN CAPACITOR FILMS OF CHROMATOPHORES OF PHOTOSYNTHETIC BACTERIA.

G. Alegria, C. Moser and P.L. Dutton Department of Biochemistry and Biophysics, University of Pennsylvania, Philadelphia, PA. 19104.

Chromatophores of the photosynthetic bacteria *C. vinosum* and *Rps. viridis* were oriented by electrodeposition on conductive substrates, dehydrated and formed into capacitors by evaporation of polyethylene and platinum. In these systems the transmembrane charge separation catalyzed by the reaction center (RC) is decoupled from the in vivo charge recombining reactions mediated by the bc1 complex. Under these conditions the light induced charge separation can be stable on the hour time scale. Application of a voltage across the capacitor plates creates electric fields on the order of 10^6 V/cm and significantly alters the free energy of electron transfer between redox centers. For RC in which $BChl_2$ and one c heme are reduced, the meta-stable light induced charge separation can be collapsed with a voltage pulse. Remarkably, in RC in which $BChl_2$ is reduced and all the c hemes oxidized, field induced electron transfer from $BChl_2$ to a ferri cyt c in the tetra-heme subunit can be observed (see figure).

This work supported by PHS GM41048-02.

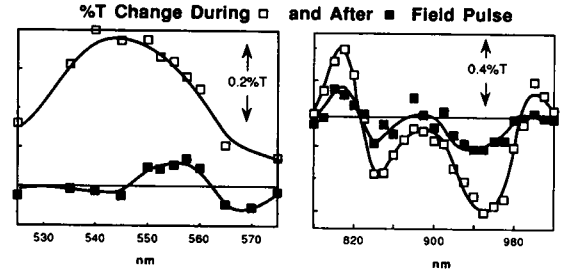

M-Pos359

EFFECTS OF IRON LIGAND SUBSTITUTIONS IN REACTION CENTERS FROM *RHODOBACTER SPHAEROIDES*

J. C. Williams[1], M. L. Paddock[2], G. Feher[2], and J. P. Allen[1]
[1]Department of Chemistry and Center for the Study of Early Events in Photosynthesis, Arizona State University, Tempe, AZ 85287-1604
[2]Department of Physics 0319, University of California, San Diego, La Jolla, CA 92093.

Bacterial reaction centers (RCs) contain a single non-heme Fe^{2+} that is located between the two quinone electron acceptors. In *Rhodobacter sphaeroides*, the iron is coordinated to four nitrogen atoms contributed by the histidine residues M219, M266, L190, and L230, and to two oxygen atoms contributed by the glutamic acid residue M234. A series of changes to the ligands of the iron atom were made to test the contribution of the ligands to the electronic structure of the iron and their effect on the kinetics of electron transfer in the RC. Each of the four histidine ligands was changed independently to Glu, Gln, and Cys, and the glutamic acid ligand was changed to His, Gln, Cys, and Asp. These changes were incorporated into the RC by site-directed mutagenesis of the structural genes. Most of the mutants were capable of photosynthetic growth, and RCs could be isolated from all of the mutants. The metal content of the mutant RCs was measured by atomic absorption and 35 GHz electron paramagnetic resonance spectroscopy (see table). The mutations alter the forward electron transfer rate k_{AB} ($D^+Q_A^-Q_B \rightarrow D^+Q_AQ_B^-$), and the charge recombination rates k_{AD} ($D^+Q_A^- \rightarrow DQ_A$) and k_{BD} ($D^+Q_AQ_B^- \rightarrow DQ_AQ_B$). For example, RCs with the mutation M219 His→Gln show values of 400 and 0.3 sec^{-1} for k_{AD} and k_{BD}, respectively, compared to 10 and 1 sec^{-1} for k_{AD} and k_{BD} in the native RCs. The three dimensional structures of selected mutant RCs are being determined by protein crystallography. Work supported by grants from the NIH.

	Metal Content by atomic absorption (mole fraction)*			RCs not containing Fe or Mn by EPR
	Fe	Zn	Mn	(mole fraction)
native	1.02	0.05	0.07	≤ 0.05
M219 His→Cys	0.12	0.11	≤ 0.05	0.73
M219 His→Gln	0.04	0.07	≤ 0.04	0.85
L190 His→Gln	0.35	0.13	0.06	0.24
M266 His→Cys	0.06	0.41	≤ 0.06	0.98
M234 Glu→His	0.68	0.14	≤ 0.07	0.17

*estimated statistical error is ± 0.07.

M-Pos360

PATHWAY OF PROTON TRANSFER IN BACTERIAL RCs FROM *Rb. SPHAEROIDES*: REPLACEMENT OF ASP-L213 WITH ASN INHIBITS ELECTRON AND PROTON TRANSFER TO THE SECONDARY QUINONE.*

S.H. Rongey, M.L. Paddock, A.L. Juth, P.H. McPherson, G. Feher and M.Y. Okamura; UCSD, Physics Dept. 0319, La Jolla, CA 92093-0319.

Light-induced electron transfer in the bacterial reaction center (RC) is coupled to protonation of the doubly reduced secondary quinone acceptor Q_B (1). Previous studies demonstrated that Ser-L223 is a component of a proton transfer pathway leading to Q_B (1). To further identify components of this pathway, we have replaced Asp-L213, which is in the vicinity of Ser-L223, with Asn [DN(L213) RCs]. The observed forward electron transfer rate constant $k_{AB}^{(2)}$, $Q_A^-Q_B^-+2H^+ \rightarrow Q_A(H^+Q_B^{2-}H^+)$, decreases dramatically, ~ 1000 fold to ~ 1 s^{-1}, at pH 7.5 in the mutant RCs (See Fig.). Proton uptake from solution (at pH 7.5) by isolated RCs was measured with the pH indicator dye phenol red. Following two electron reduction of the quinones, a slow phase with a rate constant comparable to $k_{AB}^{(2)}$ was observed. In contrast, native RCs show only a rapid uptake (<10 ms) of protons. In the presence of cyt c and continuous illumination (at pH 7.5), the mutant RCs show a photocycle rate of ~ 1 s^{-1}, which is ~ 600 fold slower than in native RCs, consistent with a rate limiting $k_{AB}^{(2)}$ of ~ 1 s^{-1} in the mutant. The characteristic slow rate of electron transfer and proton uptake, similar to that observed when Ala replaced Ser-L223 (1), suggests that loss of Asp-L213 blocks proton transfer from Ser-L223 to Q_B. Thus, these results suggest that Asp-L213 is a proton donor to Ser-L223, which protonates Q_B.

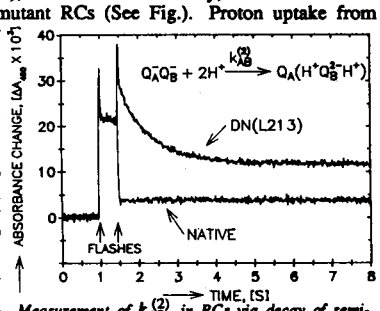

Measurement of $k_{AB}^{(2)}$ in RCs via decay of semiquinone absorbance at 450 nm after a second flash.

(1) Paddock, *et al.* (1990) *Proc. Natl. Acad. Sci.* USA 87, 6803-6807.

*Supported by NIH & NSF.

M-Pos361

THE RATE OF ELECTRON TRANSFER $Q_A^-Q_B \rightarrow Q_AQ_B^-$ in RCs FROM *Rb. SPHAEROIDES* IN WHICH ASP-L213 IS REPLACED WITH ASN.*

P.H. McPherson, S.H. Rongey, M.L. Paddock, G. Feher, and M.Y. Okamura, UCSD, La Jolla, CA 92093.

The replacement of Asp–L213 with Asn (DN(L213) mutant) slows the rate of transfer of the second electron to Q_B by three orders of magnitude at pH 7.5 (1), implicating Asp–L213 as a proton donor to Ser–L223 in a proton pathway that connects reduced Q_B to the aqueous solution. In this work, we have measured the rate $k_{AB}^{(1)}$ of transfer of the *first* electron $Q_A^-Q_B \rightarrow Q_AQ_B^-$ (optically at 750 nm) in the DN(L213) mutant RCs. In both native and DN(L213) mutant RCs, the kinetics are biphasic. The origin of the two phases is not understood. The slower phase (plotted in Fig.) dominates in both native and DN(L213) mutant RCs at pH ≥ 6.5. The decrease in $k_{AB}^{(1)}$ in native RCs at pH ≥ 9 has been attributed to the ionization of Glu–L212 (2). In the DN(L213) mutant RCs, $k_{AB}^{(1)}$ is smaller than in native RCs by factors of ~10 and ~100 at pH 7 and 9, respectively. The smaller $k_{AB}^{(1)}$ in the mutant may be due to a lowering of the pK of Glu–L212 (3), which would shift the curve in the Fig. to lower pH. An alternate explanation is that the replacement of Asp–L213 with Asn slows the rate of protonation of a group (e.g., Glu–L212) in the vicinity of Q_B^- necessary for electron transfer. This explanation would implicate Asp–L213 as a proton donor to Glu–L212, in addition to being a donor to Ser-L223 as discussed in ref. (1).

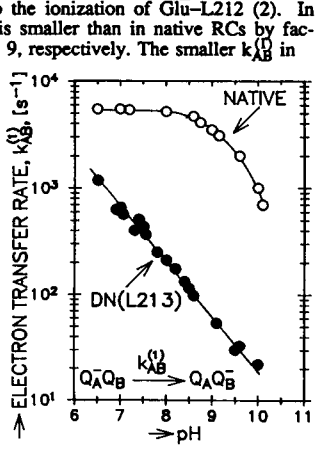

pH-dependence of the rate of transfer of the first electron to Q_B in native and DN(L213) mutant RCs.

(1) Abstract by Rongey et al., these proceedings.
(2) Paddock et al. (1989) PNAS 86, 6602-6606.
(3) Abstract by Paddock et al., these proceedings.

*Supported by NSF and NIH.

M-Pos362

THE pH DEPENDENCE OF CHARGE RECOMBINATION IN RCs FROM *RB. SPHAEROIDES* IN WHICH ASP-L213 IS REPLACED BY ASN.*

M.L. Paddock, S.H. Rongey, P.H. McPherson, G. Feher and M.Y. Okamura; UCSD, Physics Dept. 0319, La Jolla, CA., 92093-0319, USA.

Bacterial reaction centers (RCs) couple proton transfer to the reduction of the secondary quinone Q_B. Several amino acid residues of the L subunit have been implicated in this process : Glu-L212 (1), Ser-L223 (2) and recently Asp-L213 (3). The pH dependence of the charge recombination rate, k_{BD} ($D^+Q_AQ_B^- \rightarrow DQ_AQ_B$), was measured to identify the effective pK of Asp-L213. In native RCs, k_{BD} increased in the pH range from ~ 5 to ~ 7 and again above pH ≅ 9.5 (see Fig.). The increase above pH ≅ 9.5 was attributed to the deprotonation of Glu-L212 (1). In RCs where Asp-L213 was replaced by Asn [DN(L213) mutant RCs], no increase in k_{BD} in the pH range ~ 5 to ~ 7 was observed (Fig.). Consequently, we attribute the increase observed in this pH range in native RCs to the deprotonation of Asp-L213.

The pH dependence of k_{BD} in native RCs can be explained by a model in which the pK of two titratable residues (i.e. Asp-L213 and Glu-L212) is shifted upon formation of Q_B^- from pK_Q to pK_{Q^-}. This model suggests that $pK_Q \cong 5$ and $pK_{Q^-} \cong 7$ for Asp-L213. This results in an uptake of a fraction of a proton from solution at $5 \lesssim pH \lesssim 7$, in good agreement with the observed proton uptake (4,5). Similarly the increase in k_{BD} above pH ≅ 8 in the DN(L213) mutant RCs suggests that the effective pK_Q of Glu-L212 is ~ 8 in the mutant, compared to ~ 9.5 in native RCs. In conclusion, the observed pH dependence in the recombination rate k_{BD} is due to the titration of Asp-L213 and Glu-L212.

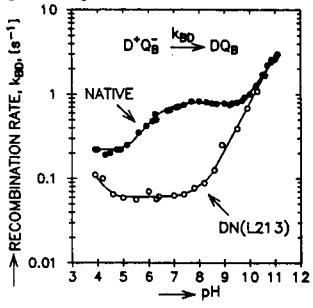

pH dependence of k_{BD} for native and DN(L213) [Asp-L213 → Asn] RCs.

(1) Paddock *et al.* (1989) Proc. Natl. Acad. Sci. USA 86, 6602-6606. (2) Paddock *et al.* (1990) Proc. Natl. Acad. Sci. USA 87, 6803-6807. (3) see abstract by Rongey *et al.*, this meeting. (4) McPherson *et al.* (1988) Biochim. Biophys. Acta 934, 348-368. (5) see abstract by Brzezinski *et al.*, this meeting. *Supported by NSF & NIH.

M-Pos363

ELECTROGENICITY ASSOCIATED WITH PROTON UPTAKE BY Q_B^{2-} IN BACTERIAL RCs.*

P. Brzezinski, M.L. Paddock, M.Y. Okamura and G. Feher; Dept. of Physics, 0319, UCSD, La Jolla, CA 92093, USA.

Flash-induced electrogenic events in reaction centers (RCs) from the photosynthetic bacterium *Rb. sphaeroides* have been measured electrically using a partially oriented Teflon-bound layer of RCs (1). The voltage change associated with the reaction $Q_A^-Q_B^- + 2H^+ \rightarrow Q_A(H^+Q_B^{2-}H^+)$ in native RCs is shown in the Figure. In the EQ(L212) mutant in which the protonable residue Glu-L212, close to the Q_B binding site, was replaced with its non-protonable analog, Gln, the electrogenicity associated with the second electron transfer was approximately one half of that observed in the native species. In the mutant the *electron* transfer kinetics is essentially unaffected whereas the uptake of one of the protons from solution is impaired (2). This suggests that the electrogenic event associated with the formation of Q_B^{2-} is due to proton uptake and not to electron transfer. Moreover, the smaller electrogenicity observed in the EQ(L212) mutant implies that only one proton is transferred to Q_B^{2-} with the same rate as in the wild type. This supports the suggestion that Glu-L212 is a proton donor to Q_B^{2-} (2).

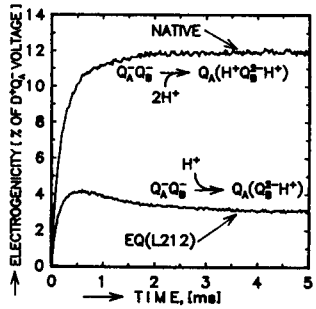

Voltage induced across the interfacial layer of RCs attributed to the reactions shown (pH 7).

(1) Blatt *et al.*, Biophys. J. (abstr.) 41 (1983) 121a.
(2) McPherson *et al.*, Biophys. J. (abstr.) 57 (1990) 404a.

*Supported by NSF, NIH and a research scholarship to PB from the Swedish Natural Science Research Council.

M-Pos364

ELECTROGENICITY ASSOCIATED WITH PROTON UPTAKE BY GLU-L212 AND ASP-L213 UPON FORMING Q_B^- IN BACTERIAL RCs.*

P. Brzezinski, M.L. Paddock, S.H. Rongey, M.Y. Okamura and G. Feher; Dept. of Physics 0319, UCSD, La Jolla, CA 92093, USA.

The electrogenic events associated with the reaction $Q_A^-Q_B \rightarrow Q_AQ_B^-$ have been measured as a function of pH in reaction centers (RCs) from *Rb. sphaeroides* (see preceding abstract). The voltage change was consistent with a positive charge moving into the RCs from the cytoplasmic side. In native RCs this voltage change had two peaks (Fig.), in agreement with the observed proton uptake when the state $D^+Q_AQ_B^-$ is formed (1). The replacement of the protonable residue Glu-L212, close to Q_B, with its non-protonable analog, Gln (EQ(L212) mutant), resulted in the disappearance of the high-pH peak (see Fig.). The replacement of the protonable residue Asp-L213, close to Q_B, with the non-protonable residue Asn (DN(L213) mutant) resulted in the disappearance of the low-pH peak and a shift of the high-pH peak from pH ≅10 to ≅8.5 (Fig.). The observed electrogenicity can be explained in terms of pK shifts of Glu-L212 and Asp-L213 as a consequence of the introduction of a negative charge on Q_B (2). Such shifts result in a partial proton uptake in the range $pK_{Q^-} \geq pH \geq pK_Q$ (see ref. (2)). Since in the EQ(L212) mutant Glu-L212 is absent there is no proton uptake at pH ≅10. The absence of proton uptake at pH ≅4 by the DN(L213) mutant RCs suggests that Asp-L213 is responsible for the proton uptake in this pH region. The negatively charged Asp-L213 (above pH 7) in native RCs is replaced with a neutral Asn in the DN(L213) mutant RCs. Consequently, the apparent pK of Glu-L212 is shifted to lower pH by ≅2 pH units. In conclusion, the observed proton uptake by native RCs upon forming Q_B^- is associated with the pK shifts of Glu-L212 and Asp-L213. (1) McPherson *et al.*, Biochim. Biophys. Acta 934 (1988) 348 (2) See Paddock *et al.* in these proceedings. *Supported by NSF, NIH and a research scholarship to PB from the Swedish Natural Science Research Council.

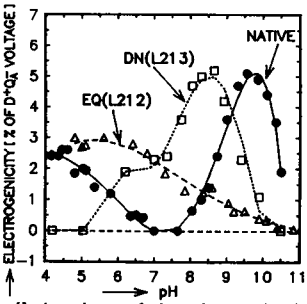

pH dependence of the voltage induced across the interfacial layer of RCs attributed to H^+ uptake associated with the formation of Q_B^-.

M-Pos365

CHLOROPHYLL FE PROTEINS: A NEW CLASS OF ENZYMES WITH A [4FE4S]-BINDING MOTIF RELATED TO NITROGENASE FE PROTEIN

Donald Burke-Agüero, Mel Klein, John Hearst Department of Chemistry, University of California, Berkeley 94720 USA

A new class of [4Fe4S] binding proteins is described. These proteins are involved in the reductive steps in the biosynthesis of chlorophyll (Chl) and bacteriochlorophyll (Bchl), and are therefore known as the Chl/Bchl Fe proteins. Conservation of key amino acid sequences between the Chl/Bchl Fe proteins and nitrogenase Fe protein strongly suggests that they are dimers that bind [4Fe4S] clusters and hydrolyze (Mg)ATP as part of their enzymatic mechanism in a manner similar to that of nitrogenase Fe protein. To continue the analogy, it appears that the Chl/Bchl Fe proteins channel electrons from a donor such as ferredoxin into the substrate- and cofactor-binding subunits of multienzyme complexes. Evidence is presented that the light-independent protochlorophyllide reductase observed in nearly all photosynthetic organisms includes a Chl Fe protein as the entry point for reducing electons.

The Chl/Bchl Fe proteins were originally identified in the *bchL* and *bchX* genes of the purple bacterium *Rhodobacter capsulatus*. These proteins are being overexpressed in *E. coli* and their FeS-binding properties are being investigated using ESR. Polymerase chain reaction primers based on conserved residues between *bchL* and the *chlL* (formerly *frxC*) gene of a nonvascular plant (*Marchantia*) chloroplast were used to amplify nearly identical sequences from a fern (*Polystichum*) chloroplast and a cyanobacterium (*Synechococcus* sp 7002). Thus the Chl/Bchl Fe proteins are probably universal components of Chl and Bchl synthesis. The strong conservation of their functional motifs across several billion years of evolution probably represents powerful structural constraints within the protein structure.

M-Pos366

IDENTIFICATION OF MANGANESE OR CALCIUM LIGANDS IN PHOTOSYSTEM II BY SITE-DIRECTED MUTAGENESIS*.

R.J. Debus, A.P. Nguyen, A.B. Conway, & H.-A. Chu, Dept. of Biochemistry, U.C. Riverside, Riverside CA 92521

The water-splitting apparatus of PS II contains four Mn and 2-3 Ca ions. These ions are believed to be coordinated primarily by carboxyl residues [1,2] located in the lumenal regions of two proteins, known as D1 and D2, that together comprise the reaction center core of PSII [3,4]. To rapidly identify which of the many lumenal carboxyl residues of the D1 polypeptide are most likely to serve as ligands, we have constructed a pair of mutations at each. Based on the criteria that a nonconservative mutation (Asp→Asn or Glu→Gln) inhibits photosynthetic growth, while a conservative mutation (Asp→Glu or Glu→Asp) does not, we have concluded that Asp-61, Glu-65, Asp-170, and Asp-342 are potential Mn or Ca ligands. Characterization of PSII particles having mutations at these positions is being carried out in collaboration with B.A. Barry and coworkers (see abstract by Boerner *et al.*). Redox-active aromatic residues have been proposed to function in oxygen evolution (*e.g.* [5]). To determine whether aromatic residues from D1 are involved, we have constructed mutations at each lumenal Tyr and His residue. We have concluded that Tyr-73, Tyr-94, Tyr-107 and His-92 are unlikely to function in oxygen evolution, since Tyr→Phe or His→Leu mutations at these positions do not inhibit photosynthetic growth. All mutations have been constructed in a strain of the unicellular cyanobacterium *Synechocystis* sp. PCC 6803 that lacks all three of its *psbA* genes.

[1] Pecoraro, V.L. (1988) *Photochem. Photobiol.* 48, 249-264, [2] Brudvig, G.W. & Crabtree, R.H. (1989) *Prog. Inorg. Chem.* 37, 99-142, [3] Babcock, G.T., Barry, B.A., Debus, R.J., Hoganson, C.W., Atamian, M., McIntosh, L., Sithole, I. & Yocum, C.F. (1989) *Biochemistry* 28, 9557-9565, [4] Rutherford, A.W. (1989) *Trends Biochem. Sci.* 14, 227-232, [5], Boussac, A., Zimmermann, J.-L, Rutherford, A.W. & Lavergne, J. (1990) *Nature* 347, 303-306.

*Work supported by the NIH (GM-43496).

M-Pos367

NOVEL REACTION CENTER MUTANTS GENERATED VIA CHIMERIC RESCUE IN RHODOBACTER CAPSULATUS.

Aileen K. Taguchi[1], Jonathan W. Stocker[2], Steven G. Boxer[2], and Neal W. Woodbury[1]. [1]Center for the Study of Early Events in Photosynthesis and the Department of Chemistry, Arizona State University, Tempe, AZ 85287-1604. [2]Department of Chemistry, Stanford University, Stanford, CA 94305.

The core of the photosynthetic reaction center from Rhodobacter capsulatus is encoded on the puf operon by two genes, pufL and pufM. Very homologous genes encode the core of the reaction centers from a variety of other purple nonsulfur bacteria including R. sphaeroides. We have utilized homologous recombination between the puf operons of these two species to form chimeric reaction centers. A 48 bp R. capsulatus deletion mutant (M673 through M720) was constructed which lacked photosynthetic activity. Repair of this deletion occurred when photosynthetic selection was imposed in the presence of a nonexpressing Rhodobacter sphaeroides puf operon. Forty-four chimeric revertants were isolated which fell into four classes: 1) nonreciprocal conversion of R. capsulatus pufM coding sequence (including the deletion) to R. sphaeroides sequence 2) single inversion events resulting in reciprocal exchange between the R. capsulatus and R. sphaeroides puf operons 3) events resulting in expression of the entire R. sphaeroides operon that do not require sequences from the R. capsulatus operon 4) events that do not result in repair of the deletion in the R. capsulatus operon, but require sequences from both operons to be photosynthetically viable. In addition, there were two uncharacterized mutants which did not fall into any class. Phenotypically, the mutants fell into two classes: 1) those in which the decay of the emission from the antenna occurred in about 50 ps, as it does in wild type organisms, and those in which the decay was slower and heterogeneous indicating a change in the energy trapping efficiency of the photosynthetic apparatus. DNA sequencing has shown that the changes that gave rise to the high fluorescence phenotype are 3' of pufM, probably in pufX. This indicates a role for the pufX gene product in energy transfer or trapping. No phenotypic changes were observed for replacement of R. capsulatus by R. sphaeroides sequence anywhere between M445 and M889 which includes essentially all of the M sequence which comes in close contact with the reaction center chromophores.

M-Pos368

SITE-DIRECTED MUTANTS OF PROTONATABLE GROUPS IN THE Q_B-BINDING POCKET OF REACTION CENTERS FROM *RHODOBACTER SPHAEROIDES*

Eiji Takahashi and Colin A. Wraight
Department of Plant Biology and Department of Physiology and Biophysics
University of Illinois, Urbana, IL 61801, USA

The glutamic acid at position 212 (Glu^{L212}) and aspartic acid at position 213 (Asp^{L213}) of the L-subunit of reaction centers from *Rhodobacter sphaeroides* are protonatable residues in the binding site of the secondary quinone (Q_B). The effects of single and double site-directed mutations of these ionizable residues were investigated. Mutation of Asp^{L213} to asparagine drastically affected the light induced proton and electron transfer functions leading to the formation of quinol (Q_BH_2). The first electron transfer from $Q_A^-Q_B$ to $Q_AQ_B^-$ was slowed, to a half time in the millisecond time range, but the equilibrium was substantially increased in favor of in favor of Q_B^- and the pH dependence of the equilibrium was altered, especially below pH 7. The stabilization of Q_B^- is suggested to result from the uncharged nature of the substitution, with the implication that Asp^{L213} is normally ionized (pK < 5) and presents an electrostatic restriction to the first electron transfer. A similar mutation of Glu^{L212} to glutamine showed altered pH dependence of the first electron transfer at high pH, and 25-fold slower release of Q_BH_2, in agreement with the work of Paddock *et al.* [1]. A double mutation of Glu^{L212} and Asp^{L213} to the non-protonatable residues Gln and Asn, respectively, exhibited drastically altered Q_B properties, consistent with the two single mutations. The decay of $P^+Q_AQ_B^-$ for the double mutant is almost pH independent over a wide pH range, as expected for the absence of any ionizable residues in the Q_B pocket. The second electron transfer for the L213 and L212/L213 double mutants were even more severely inhibited by a factor $>10^4$. These results imply a crucial role for Asp^{L213} in the transfer pathway for the first proton to reach Q_B^- or Q_B^{2-} after the second flash. This proton is essential for effective transfer of the second electron. The second proton, leading to formation of Q_BH_2, may be provided by Glu^{L212}.

1. Paddock, M.L., *et al.* (1989) PNAS 86, 6602-6606.

Supported by NSF and the McKnight Foundation.

M-Pos369

CHARACTERIZATION OF PHOTOSYNTHETICALLY DEFECTIVE MUTANTS IN *RHODOPSEUDOMONAS VIRIDIS*

Edward J. Bylina and Erick S. Cooke (Intro. by I. Cooke), Biotechnology Program, University of Hawaii at Manoa, Honolulu, HI 96822.

Tetracycline and ampicillin suicide enrichments were performed to isolate photosynthetically defective spontaneous mutants from *Rhodopseudomonas viridis*. Colonies of survivors formed in 10-12 days under dark aerobic conditions. These mutations affect pigment biosynthesis, reaction center function, and assembly of the photosynthetic apparatus. The absorption spectra, pigment composition, and enhanced fluorescence properties of these mutants will be discussed.

M-Pos370

EXTRACTION AND RECONSTITUTION OF THE Q_a SITE IN *Rhodopseudomonas viridis*: EVIDENCE FOR Q_a SITE SIMILIARITIES BETWEEN *Rhodopseudomonas viridis* AND *Rhodobacter sphaeorides.*

Jonathan M. Keske and P. Leslie Dutton, Dept. of Biochem. and Biophysics, Univ. of Pennsylvania, Philadelphia, PA 19104.

Given the extensive body of data on the temperature and free energy dependence of electron transfer in Q_a substituted reaction centers of *Rhodobacter sphaeroides* (1-3), comparison with similarly substituted reaction centers of *Rhodopseudomonas viridis*, given the intrinsic Bph-Q_a free energy differences between the two species, affords the opportunity to evaluate the role of free energy and reorganization energy in controlling the rate and efficiency of electron transfer. We have found that extraction of menaquinone from the Qa site of *R. viridis* can be achieved under milder conditions, than those recently published by Hoff et al. utilizing a modified version of the methodolgy of Okamura (4). Measurements of the binding affinities; quantum yields; Cyt $C_{556}Q_a$, Cyt $C_{559}Q_a$, and PQ_a recombination rates have been determined for a number of quinone substitutions. The data reveals that the rate of electron transfer from bacteriopheophytin to Qa in *R.. viridis* and *Rb. sphaeroides* exhibit similar free energy and reorganization energy dependence:

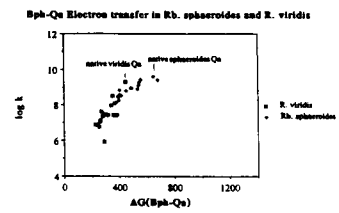

This work was supported by grants from the Public Health Service (GM 27309) and the National Science Foundation (DMB 88 77240).

M-Pos371

THE USE OF SITE-DIRECTED MUTAGENESIS IN SYNECHOCYSTIS TO IDENTIFY MANGANESE LIGANDS IN PHOTOSYSTEM II+. R.J.Boerner, A.P. Nguyen*, A.B. Conway*, K.A. Bixby, R.J. Debus* and B.A.Barry, Dept. of Biochem., Univ. of MN, St. Paul, MN 55108; *Dept.of Biochem.,Univ.of CA,Riverside,CA 92521.

There are four Mn atoms found in the water-splitting complex of PS II that are capable of stabilizing the four oxidizing equivalents necessary for the oxidation of water. The structure of the Mn complex and the ligands that bind the four Mn atoms are not known.

We have generated site-directed mutations in the oxygen-evolving cyanobacteria, Synechocystis 6803, in an attempt to identify protein ligands to Mn. Mutations were made in lumenal hydrophilic loops of the membrane spanning protein, D1. Indirect evidence suggests that this protein is most likely involved in Mn ligation (1). The available evidence concerning Mn chemistry suggests that carboxylic acids are the best candidates to be Mn ligands (2,3,4). Thus, mutations were generated at asp and glu residues. Three sets of mutations have been selected for further analysis based on the criterion that a conservative mutation (asp to glu, or glu to asp) allows the organism to grow photosynthetically, while a nonconservative mutation (asp to asn, or glu to gln) inhibits photosynthetic growth. All of the mutants that we have examined, DE170D1, DN170D1, DE61D1, ED65D1 and EQ65D1, display slight or substantial (<100 μmoles O_2/mg chl.-hr.) inhibition of activity.

To analyze these mutations, we are using an O_2-evolving PS II prep. from Synechocystis in which we can observe Mn multiline spectra (5). We are also quantitating Mn content in purified PS II particles from these mutants and using room temp. EPR spectroscopy to look for alterations in donor-side tyrosine redox behavior. We will present our progress in spectroscopic and biochemical characterization of these mutants. [+Work supported by NIH GM43496 to RJD and NIH GM43273 to BAB.]

1) Babcock, et al. (1989) Biochemistry 28, 9557. 2) Brudvig, et al. (1989) Annu. Rev. Biophys. Biophys. Chem. 18, 25. 3) Brudvig (1987) J. Bioenerg. Biomemb. 19, 91. 4) Pecararo (1988) Photochem. Photobiol. 48, 249. 5) Noren, et al. Biochemistry (in press).

M-Pos372

CHARACTERIZATION OF AN O_2-EVOLVING PHOTOSYSTEM II PREPARATION FROM THE CYANOBACTERIUM SYNECHOCYSTIS 6803+. G.H. Noren, R.J. Boerner, K.A. Bixby and B.A. Barry, Dept. of Biochem., Univ. of Minnesota, St. Paul, MN 55108.

Site-directed mutagenesis in Synechocystis 6803 has been very useful in elucidating the role of the Z+ and D+ tyrosine radicals in Photosystem II (PS II) (1-4) and may help in the identification of protein ligands to the manganese cluster. Isotopic labeling, which is of utility in the identification of spectroscopic intermediates, can also be done in this organism (5).

We have devised a simple method of purifying PS II from Synechocystis that yields O_2 evolving particles suitable for room temperature and cryogenic EPR spectroscopy; this preparation can be used with either photoautotropically or photoheterotropically grown cells (6). The protocol consists of mechanical breakage of the cells, detergent solubilization of the thylakoid membranes, and two rounds of ion-exchange chromatography. These PS II particles show activities of 2600 μmmoles O_2/mg chl-hr, a reaction center size of 60 chlorophylls, and a low PSI content of 930 chlorophylls per P700+. This prep. yields highly resolved tyrosine radical EPR spectra and the first multiline, S_2 signal observed from Synechocystis.

Site-specific mutagenesis of tyrosine-160 (tyr-phe) of the D2 polypeptide has been used to show that this residue gives rise to the stable tyrosine radical, D+ (1,2). We have used the PSII preparation described above to further characterize this D+ mutant. Our results show that Z+ is more sensitive to photodamage in mutant than in wild type particles. Furthermore, the binding of the 33kD protein is destabilized, and there is a loss of bound manganese in the mutant. These data suggest that the D+ mutant is more sensitive to photoinhibition than the wild type and that the D2 protein may be part of the binding site for the 33kD protein. [+Work supported by USDA 89-37130-4887 and NIH GM 43273]. 1) Debus et al. (1988) PNAS 85, 427. 2) Vermaas et al. (1988) PNAS 85, 8477. 3) Debus et al. (1988) Biochemistry 27, 9071. 4) Metz et al. (1989) Biochemistry 28, 6960. 5) Barry and Babcock (1987) PNAS 84, 7099. 6) Noren et al., Biochemistry, in press.

M-Pos373

SPECTRAL AND THERMODYNAMIC CHARACTERIZATION OF CYTOCHROMES b IN STROMA VESICLES FROM SPINACH CHLOROPLASTS

Irene Baroli, Javier Fernandez-Velasco and Antony R. Crofts. Biophysics Division, University of Illinois , 156 Davenport Hall, 607 S.Mathews, Urbana IL 61801.

PS I enriched vesicles prepared by digitonin treatment of spinach chloroplasts have been critically studied in terms of their content of cytochrome b. In contrast with previous results (Peters et al.,BBA 722:460-470,1983), cytochrome b6 showed both a spectral and thermodynamic heterogeneity (b-564, $E_{m,7}$=-170±10mV and b-563, $E_{m,7}$=-50±10 mV) and on the other hand we found that the cytochrome described as b-559 ($E_{m,7}$=32 mV) has actually its alpha peak at 560 nm and an $E_{m,7}$=50±10 mV. No considerable amounts of either low ($E_{m,7}$=120 mV) or high potential ($E_{m,7}$=350 mV) cytochrome b-559 could be detected. The stoichiometry b-564:b-563:b-560:b-559_L:b-559_H in PS I enriched vesicles was 1:1:1.4:<0.1:<0.1. This is to be compared with that of 1:1:0.6:0.4:0.6 found in the PS II enriched membranes ("grana" recovered after digitonin treatment). These results are in agreement with the thermodynamic heterogeneity of the b-type cytochromes in the purified b6f complex (Hurt and Hauska, FEBS Lett. 153:413-419, 1983) and both the spectral heterogeneity of cytochrome b6 at room temperature (alpha peaks at 564 and 563 nm) and the presence of a cytochrome b-560 reported by Kramer and Crofts in intact chloroplasts (Kramer and Crofts in Balscheffsky ed. Cur. Res. Photosynth. 3,pp 381-384, Kluwer; Kramer, DM., Ph. D. Thesis UIUC,1990).

We conclude that cyt b-564 and b-563 are uniformely distributed in the thylakoid system, cyt b-560 is enriched in the stroma vesicles and cyt b-559 (low and high potential forms) is enriched in the "grana" fraction.

M-Pos374

REVERSED ASYMMETRY IN THE REACTION CENTER OF THE PHOTOSYNTHETIC BACTERIUM *RHODOBACTER SPHAEROIDES*

Kevin A. Gray and Dieter Oesterhelt.
Department of Membrane Biochemistry, Max-Planck-Institut für Biochemie, D-8033 Martinsried, FRG.

Tyrosine M210 (YM210) and phenylalanine L181 (FL181) comprise a pair of symmetry breaking residues in the photochemical reaction center of *Rhodobacter sphaeroides*. We have shown previously (1,2) that the site directed exchanges YM210 -> F and L result in slower initial electron transfer from P as well as an increased lifetime of the singlet excited state P*. This is in agreement with electrostatic interaction calculations (3) which suggest that the energy level $P^+B_L^-$ lies either isoenergetic or slightly below that of P* due partly to the interaction with the hydroxyl group of YM210. Since FL181 occupies the symmetry related position on the inactive (B) branch the combination of the two may be a reason for the observed unidirectionality of electron transfer in the reaction center. To continue the characterization of this pair FL181 has been changed to Y, resulting in a pair of tyrosines at L181 and M210. Furthermore the double mutation FL181/YM210 -> YL181/FM210 has been constructed. This mutation causes a reversal of the natural asymmetry. The goal is to determine if the energy level of $P^+B_M^-$ can be altered and if the combined increased level of $P^+B_L^-$ and decreased level of $P^+B_M^-$ could result in partial electron transfer to the B branch. Both the single site mutant (FL181 -> Y) and the double site mutant express photobleachable RC and grow photoheterotrophically. Spectral changes in the positions of the transitions assigned to the monomer bacteriochlorophylls are observed consistent with the changes described for the M210 mutants (1). Biophysical characterization of the mutants RCs is currently underway (e.g. quantum yield measurements; FTIR, in collaboration with J. Breton, E. Nabedryk and W. Mäntele; linear dichroism, with J.B. and; femtosecond kinetic analysis, with W. Zinth).

1. K.A. Gray, J.W. Farchaus, J. Wachtveitl, J. Breton and D. Oesterhelt (1990) *EMBO J.* 9, 2061 - 2070.
2. U. Finkele, C. Lauterwasser,, W. Zinth, K.A.Gray, and D. Oesterhelt (1990) *Biochem.* (in press).
3. W.W. Parson, Z.T. Chu and A. Warshel (1990) *Biochim. Biophys. Acta* **1017**, 251 - 272.

M-Pos375

FUNCTION OF EXOTIC PRIMARY ELECTRON ACCEPTORS IN THE REACTION CENTER PROTEIN. K. Warncke and P.L. Dutton, Department of Biochemistry and Biophysics, University of Pennsylvania, Philadelphia, Pennsylvania, 19104.

The native Q_A site quinone cofactor has been extracted from reaction center protein (RC) isolated from *Rhodobacter sphaeroides* R26 and primary electron acceptor activity reconstituted in aqueous medium with a variety of exotic cofactor structures. Criteria for exotic cofactor function at the native, Q_A primary acceptor site are: a) support of light-induced charge separation at cryogenic temperatures, an established property of quinone cofactors[1], and b) competitive inhibition of activity by tight-binding Q_A site inhibitors. Three exotic cofactors, tetrafluoro- and trinitro-fluorenone and 1,3-dinitrobenzene, meet these criteria. The rate constants for electron transfer from reduced bacteriopheophytin (BPh^-), and charge recombination with oxidized primary donor ($[BChl]_2^+$), mediated by these exotic Q_A site cofactors exhibit reaction free energy (ΔG^o_{et}) dependences that are comparable with those described for a family of quinones[1], from 295 to 14 K. These results demonstrate that the *in situ* electrochemical potential of the cofactor, and not specific structural elements, dominates determination of electron transfer rates at the Q_A site, through establishment of ΔG^o_{et}. In contrast, charge separation at 295 K supported by twenty-three halo-, CH_3-, CF_3-, and CN-substituted nitro- and dinitro-benzenes fails to meet the Q_A site cofactor criteria. The reduction of duroquinone bound at the Q_A site in the presence of these exotic cofactors indicates that their reductant is BPh^-. For seven dinitrobenzenes, values for the quantum yield (Φ) of charge separation vary from 0.57 to 0.86 at 295 K. Absence of observable charge separation at T<240 K (Φ<0.02) places a limit on the activation energy for electron transfer from BPh^- of >10 Kcal/mole. Thus, although control of electron transfer rates at the Q_A site does not depend strongly on cofactor structure, the structure of the protein environment surrounding the Q_A site is essential for promotion of efficient, near temperature-independent electron transfer performance in the native RC. 1. Gunner, M.R., Dutton, P.L. 1989. *J. Am. Chem. Soc.* 111, 3400. Supported by NSF grant DMB 88-17240

M-Pos376

IS BICARBONATE IN PHOTOSYSTEM II THE EQUIVALENT OF THE GLUTAMATE (M234) LIGAND OF THE IRON ATOM IN BACTERIAL REACTION CENTERS?

Xutong Wang, Jiancheng Cao, Peter Maróti, Hans U. Stilz*, Dieter Oesterhelt*, Govindjee, and Colin A. Wraight
Department of Physiology and Biophysics, University of Illinois, Urbana, IL 61801, USA
*Max-Plank Institute fur Biochemie, Martinsried, Germany.

Photosystem II of oxygen-evolving organisms exhibits a bicarbonate-reversible formate effect on electron transfer between Q_A and Q_B. This effect, however, is absent in the similar electron acceptor complex of purple bacteria, e.g., *Rhodobacter sphaeroides*. Amino acid sequence differences in the polypeptides of PS II and bacterial reaction centers (RCs) suggested a possible reason for these different responses [1]: namely that the iron atom of the acceptor quinone complex in PS II might lack the fifth and sixth ligands provided in bacterial RCs by a glutamate (M234) residue of the M subunit (analogous to D2 in PS II). In PS II this role might be filled by bicarbonate. By site-directed mutagenesis we have altered Glu^{M234} in RCs from *Rb. sphaeroides* replacing it with valine, glutamine and glycine to form mutants M234EV, M234EQ and M234EG, respectively. These mutants grew quite competently under phototrophic conditions and were tested for the formate-bicarbonate effect. In chromatophores there were no detectable effects of bicarbonate depletion (by incubation with formate) on cytochrome b_{561} or cytochrome c_2 reduction, and in isolated RCs no formate-bicarbonate effect was observed on: (a) the fast or slow phases of recovery of the oxidized primary donor (P^+) in the absence of exogenous donor, i.e., the recombination of $P^+Q_A^-$ or $P^+Q_B^-$, respectively, (b) the kinetics of electron transfer from Q_A^- to Q_B, or (c) the flash dependent oscillation of semiquinone formation in the presence of exogenous donor to P^+ (Q_B turnover). The absence of a formate-bicarbonate effect in these mutants suggests that Glu^{M234} is not responsible for the absence of the formate-bicarbonate effect in bacterial RCs, or at least that other factors must be taken into account.

1. Michel, H. and Deisenhofer, J. (1988) Biochemistry 27, 1-7.

Supported by NSF and USDA

M-Pos377

STRUCTURE-ACTIVITY RELATIONSHIPS OF SUBSTITUTED COUMARINS AS PHOTOSYNTHETIC ELECTRON TRANSPORT INHIBITORS. Kerry K. Karukstis, David P. Nash, Elisabeth A. Davis, and Roy K. Hom, Department of Chemistry, Harvey Mudd College, Claremont, CA 91711

We have monitored the action of substituted coumarins as inhibitors of Photosystem II (PSII) electron transport in spinach chloroplasts using spectroscopic measurements of photoreduction rates and chlorophyll fluorescence intensities. As analogs of the native PSII electron acceptor Q_B, coumarins compete with Q_B for a common binding region on the D-1 protein and thereby interfere with electron transport. From direct measurements of PSII electron transport rates using the exogenous acceptor dichlorophenolindophenol (DCIP), we note that the lipophilic character of substituents at specific positions on the coumarin structure correlates with inhibitory activity. In particular, hydrophobic substituents at positions 4 and/or 6 and hydrophilic substituents at positions 7 and/or 8 lead to decreased electron transport rates. Strong electron transport inhibitors are also observed to quench room-temperature PSII chlorophyll fluorescence emission at 684 nm, although the degree of fluorescence quenching is not as marked as the decrease in photoreduction rates. Stern-Volmer analyses of the fluorescence data support the DCIP investigations with two major structure-activity relationships: (1) Hydrophobic substituents at position 4 and a general lack of substitution at position 3 substantially increase the coumarin's ability to reach the Q_B binding niche (as evidenced by a value of 1 for the f_a parameter). (2) Hydrophilic substituents at positions 7 and 8 maximize the intrinsic inhibitory activity of the coumarin at its binding site (as evidenced by maximal K_{sv} values). These results permit the design of new and novel members of the coumarin family which are likely to function as effective electron transport inhibitors.

M-Pos378

ANALYSIS OF METAL METHYL BACTERIOPHEOPHORBIDE D AS MODELS FOR PIGMENT ORGANIZATION IN CHLOROSOMES

Peiling Cheng, Paul Liddell and Robert E. Blankenship
Department of Chemistry
ASU Center for the Study of Early Events in Photosynthesis
Tempe, Arizona 85287-1604

The green photosynthetic bacteria that contain bacteriochlorophylls *c*, *d* or *e* as antenna pigments are characterized by unique antenna structures known as chlorosomes. Chlorosomes contain large oligomers of pigments *in vivo* with little protein and thus represent a different mode of pigment organization than that found in chlorophyll-protein complexes. Bacteriochlorophyll *d* analogs, Zn(II) and Mg(II) methyl bacteriopheophorbide *d* (Zn MBPd and Mg MBPd), were synthesized and studied to characterize their properties in their oligomeric forms as models for pigment organization in chlorosomes.

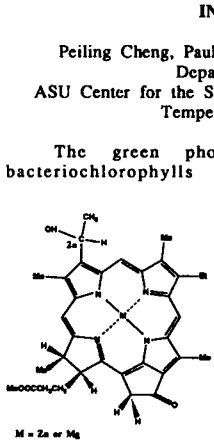

The monomeric Zn analog has Qy absorption maximum at 650 nm in methanol, and a fluorescence emission maximum at 659 nm. The fluorescence lifetime of the monomer is 5 ns. When aggregation of the Zn analog occurred in a nonpolar solvent (200:1, hexane:CH_2Cl_2), the Qy absorption and fluorescence emission maxima were red-shifted to 728 nm and 760 nm respectively. The fluorescence lifetime of Zn MBPd oligomers is ~15 ps.

Characterization of the Mg analog is underway. Model system studies should provide insight into the interactions among the aggregated photosynthetic pigments, and may give ideas about the molecular organization of aggregated pigments in chlorosomes.

M-Pos379

SPECTROSCOPIC STUDIES OF PHYCOBILISOMES LACKING THE β^{18} CORE POLYPEPTIDE

Yvonne M. Gindt, Jianhui Zhou*, Donald A. Bryant*, and Kenneth Sauer, Chemical Biodynamics Division, Lawrence Berkeley Laboratory, University of California, Berkeley, CA. *Department of Molecular and Cell Biology, Penn State University, University Park, PA.

The β^{18} core polypeptide is a chromophore containing protein with spectral properties similar to allophycocyanin. We are studying the function of this peptide by creating a mutant of *Synechococcus* sp. PCC 7002 (*Agmenellum quadruplicatum* PR6) which does not contain the β^{18} subunit and examining its spectroscopic properties. The mutant was created by interrupting the apcF gene which encodes for the β^{18} subunit with an antibiotic resistance cartridge. The apcF- mutant, which grew 20% slower than wild type, assembled phycobilisomes which lacked the β^{18} peptide. The mutant phycobilisomes had slightly different absorption properties with 15% less absorption at 652nm, in the allophycocyanin absorbing part of the spectrum. The steady state fluorescence of the mutant phycobilisomes was blue-shifted, with F_{max} of 662nm compared with 680nm for the wild type, but the quantum yield was unchanged. Time-resolved fluorescence spectroscopy did not show any significant differences in the efficiency of energy transfer. We conclude that the β^{18} core polypeptide is not absolutely essential to the function of the phycobilisome, but it acts to fine-tune energy transfer in the complex.

[This work was supported by the Director, Office of Energy Research, Office of Basic Energy Sciences, Biological Energy Research Division, of the U.S. Department of Energy under Contract No. DE-AC03-76SF00098 (Y.G. and K.S.), and USPHS grant GM-31625 (J.Z. and D.B.).]